Effect of Climate Type and Temporal Variability in Meteorological Input Data in Modeling of Salt Transport in Unsaturated Soils

ERIC MAURICIO PASTORA CHEVEZ

A THESIS SUBMITTED TO THE FACULTY OF GRADUATE STUDIES IN PARTIAL FULFILLMENT OF THE REQUIREMENTS FOR THE DEGREE OF MASTER OF APPLIED SCIENCES

Graduate Program in CIVIL ENGINEERING
York University
Toronto, Ontario
September, 2017

ABSTRACT

Oilfield produced brine is a major source of salt contamination in soil and groundwater. Salt transport in the upper soil layers is controlled by the atmospheric interactions via infiltration of meteoritic water. In lower layers, it is controlled by fluctuations in groundwater table, which are also linked to atmospheric interactions via groundwater recharge. Therefore, climate is an important factor in the movement of contaminants in the unsaturated zone. A one-dimensional variably saturated flow and transport model with soil atmospheric boundary condition was used to estimate the effect of climate type and soil texture on soil water and salt dynamics in variably saturated soils. Numerical simulations were run with Hydrus-1D, using daily and sub-daily climate. Simulations were run for nine-year climate datasets for ten different ecoclimatic locations in Alberta, Canada. Results show that flow and transport are function of climate type. Results also indicated that higher temporal resolutions of precipitation data resulted in higher net infiltration values. Higher net infiltration values resulted in faster solute displacement, especially, if the precipitation events were assumed to occur outside the evaporation hours. Minimal to no interaction was observed between groundwater table and atmosphere in coarse-grained soil material, especially in wetter climatic conditions.

Keywords: Variably saturated soils, climate, soil-atmosphere boundary, water and salt dynamics, groundwater table

Dedication

To my Heavenly Father who dwells secretly within me…

AUTHOR'S DECLARATION

I hereby declare that I am the sole author of this thesis. This is a true copy of the thesis, including any required final revisions, as accepted by my examiners.

I understand that my thesis may be made electronically available to the public.

Acknowledgements

Table of Content

List of Tables

List of Figures

Chapter 1

Introduction

1.1 Problem Formulation

Groundwater resources play an important role in the development of the modern society. On a global scale, the growing groundwater demand has become crucial for the livelihood and food security, especially, in areas with arid and semi-arid climates (Zekser and Everett, 2004). In Canada, approximately 30% of the population depends on groundwater resources for domestic use (Ruttherford, 2004). Therefore, aquifer protection plans from increasing hazards of subsurface contaminant sources must be developed in accordance with the natural attenuation process of the corresponding geological setting (Donado, 2009).

Over the past few decades, the study of the unsaturated zone has received a lot of attention in relation to understanding the effect of water dynamics and solute transport in the unsaturated zone (Šimůnek, J. 2005). The unsaturated zone or vadose zone is the portion of subsurface that lies above the water table, and acts as a natural filter by attenuating pollutants that might migrate from near or at the ground surface before reaching and polluting surface and groundwater resources (Fig. 1.1).

Anthropogenic activities are responsible for release of chemical substances that may affect adversely the quality of surface and groundwater resources (Šimunek, and van Genuchten, 2006). Water movement and solute displacement can be in any direction depending upon the prevailing atmospheric conditions at the ground surface. For instance, lateral salt transport towards a surface water body may endanger

livestock, aquatic life, wildlife, and human health via direct or incidental ingestion or dermal contact ([Alberta Environment, 2014](#)). Downward salt displacement through variably saturated soils increases the risk of aquifer contamination. Upward salt migration from deep soil layers may affect the soil biota within the root zone.
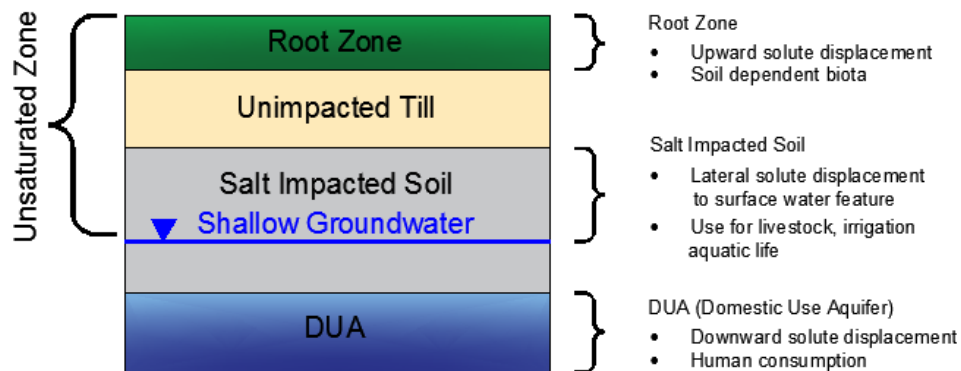
Fig. 1.1: Unsaturated zone showing subsurface salt transport with unacceptable risk. Modified from Alberta Government, 2014

The unsaturated zone plays a key role in the hydrological cycle (Fig. 1.2). The upper boundary of the unsaturated zone is the ground surface, while its lower boundary is the groundwater table. When precipitation (P), in the form of rain or snow falls on the ground surface, a part of it infiltrates into the ground (net infiltration, NI), overcoming the evaporation (AE). Some of this infiltrating water is transmitted through the unsaturated zone all the way to the groundwater table and is termed groundwater recharge. If the precipitation intensity is more than the infiltration capacity of the soil, water either ponds on the surface or flows over the land. The water flowing over the land is termed as Runoff (RO). Transpiration (T) is the process associated with the vegetated system that

takes place via water loss from the stomata (the gas exchange organs found on the leaves of the plants). A part of the infiltrating water can be taken up by the plant roots and it is transpired through the leaves.
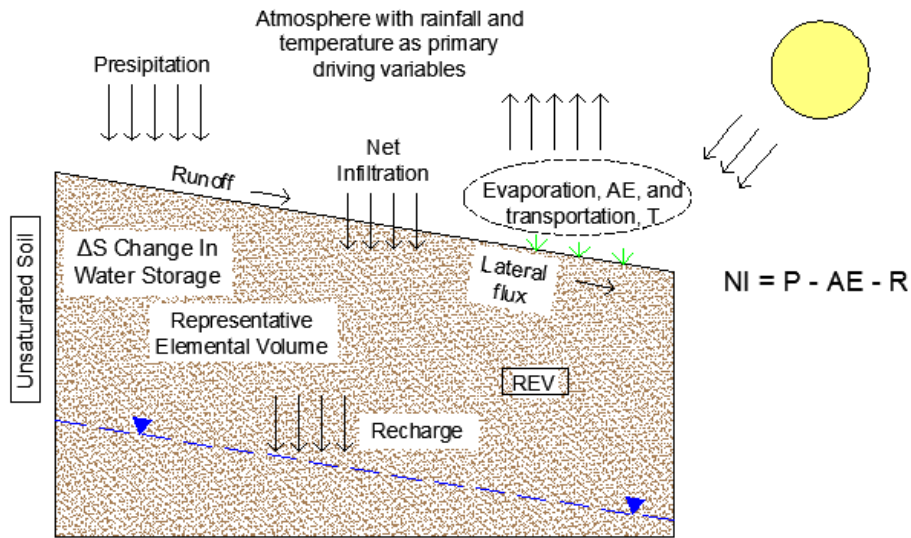
Fig. 1.2: Soil water movement in the unsaturated zone

Large oil and gas operation have existed in the Great Plains area of Canada since the mid-20th century (Robertson et al., 2015). The extraction and processing of these natural resources, sometimes results in spills of highly concentrated drilling fluids and co-produced saline water released at the ground surface or in the subsurface. The spill of salts poses much adverse effect on the near-subsurface environments. The transport of these highly concentrated produced saline waters in the unsaturated zone leads to contamination of groundwater resources and degradation of soil chemical and physical properties caused by excess of sodium and chloride concentrations (Alberta Environment, 2001). The transport becomes more complex due to the heterogeneity of the soil profile. Soil texture and soil layering configurations impact salt migration during

3

the infiltration (*I*) and evaporation (*E*) processes, which in turn increase the risk of salinization and sodification into the root zone (Li et al. 2013). According to Anderson and Woessner (1992), the infiltration and evaporation are controlled by many variables, such as: soil hydraulic properties, depth to groundwater table, interconnectivity between unsaturated zone and groundwater systems, presence of diurnal or nocturnal phreatophytes, root water uptake distribution, and seasonal climatic conditions.

In order to meet the water demand of the growing population and increased agro-industry activities, groundwater resources have to be protected from contamination. In the province of Alberta, environmental guidelines for the protection and management of contaminated sites rely on two key acts. The first is the Environmental Protection and Enhancement Act (EPEA). The act includes prohibitions related to substances released on the ground surface that can pose an adverse effect to the environment and human health (Government of Alberta, GOA, 2006). The Water Act, regulated and implemented by the Government of Alberta, supports and promotes the protection, conservation, and management of water resources including: surface water (AENV, 2014) and groundwater quality guidelines (ESRD, 2007; updated May 21, 2014).

The current applied methods of risk assessment and site-specific remediation controls, regulated by the Alberta's Environmental policy framework in terms of sustainable soil and groundwater contamination management practices, rely on the use of the subsoil salinity tool (SST; Alberta Government, 2014). The SST is a software program designed for the development of soil salinity guidelines applicable below the root zone regarding the net vertical and lateral movement of salt transport over time. For the estimation and fate of vertical non-reactive salts transport, the SST software makes

use of pre-run transport simulations run with Hydrus-1D. Hydrus-1D is a computer code which can be used to simulate water flow, heat, carbon dioxide and major ion solute transport in variably saturated porous media. Hydrus-1D is one-dimensional software and can simulate vertical, horizontal, and inclined soil profiles. Hydrus-1D uses finite element method to solve relevant governing differential equations of energy and mass transfer.

The present research uses the numerical model Hydrus-1D (version 4.16.0110) in order to understand the relationship between the effects of soil texture, climate type and temporal variability on water and salt dynamics in the unsaturated zone at different ecoclimatic regions in Alberta.

1.2 Previous Work

In the past few decades, the emergence of numerical solutions has come a long way with several simulation codes developed to predict the fate and transport of contaminants in unsaturated soils. Computer models offer cost-effective means for the evaluation of different processes occurring in unsaturated soil conditions. Most of these models have been applied mainly to agricultural projects (Feddes et al., 1988). For example, a version of the SWATRE- model was used with the purpose of mapping the extension of the actual evaporation as representative of the growing season (Nieuwenhuis, 1986).

Hetrick et al. (1988) evaluated the performance of a modified version of the one-dimensional seasonal soil code SESOIL to simulate the vertical contaminant migration

5

and fate in unsaturated soil profiles. The pollutant transport results obtained by using the SESOIL code were in good agreement with laboratory measurements involving six chemicals (cicamba, 2,4-dichlorophenoxyacetic acid, atrazine, diazinon, pentachlorophenol, and lindane). However, the SESOIL code is not intended for the analysis of solute dilution in saturated soil settings.

Recent studies have given more emphasis on predicting soil water movement and solute transport under the effect of climate type in unsaturated soils. For instance, Liu et at., (2004) evaluated the importance of including the diurnal evapotranspiration cycle on water dynamics in the vadose zone using the Galerkin finite element technique to solve Richards' equation in one-dimension. The diurnal fluctuation of the potential evapotranspiration followed a sinusoidal form with a maximum at solar noon and it was assumed to be zero before sunrise and after sunset. Simulations were run with coarse and fine soil hydraulic properties using both daily average and diurnal cycle of potential evapotranspiration at different water table depths. Results from clayey soils indicated that difference in actual evaporation between measured daily and diurnal evaporation increased with the increasing water table until 250 cm. Contrary, in sandy soils, the atmospheric water demand (*PE*) at bare ground surface was satisfied when the water table depth was 60 cm.

A series of water balances at the ground surface were carried out using Hydrus-1D at a geomorphically reclaimed site in New Mexico to investigate seed germination and plant survival for a range of land slopes and climatic conditions (Rahman, 2011). Daily meteorological data was used in Hydrus-1D over a 2-year period in vegetated soils of 7.5 cm and 20 cm depth. Soil hydraulic properties used in the model were

derived from measured laboratory and field values. Numerical results indicated that cumulative average water contents over the 7.5 cm and 20 cm depth were consistent with well-vegetated measured values at 95% of confidence level.

Gladyeva and Saifadeen (2012) assessed the effect of hysteresis and temporal variability in precipitation on the water and solute movement using Hydrus-1D for different types of soil throughout Sweden. Initial half-hourly precipitation data were converted into 1, 2, 4, and daily input data. Monthly evaporation data was converted into hourly evaporation consistent with diurnal variations assuming no evaporation during the night. The modeled soil column consisted of 250 cm depth multi-layered soil profile. A contaminated source with 100 g of non-volatile and non-reactive was set at the top 5 cm of soil. Numerical results indicated that the downward solute migration increased with increasing the soil hydraulic conductivity and with increasing temporal resolution of precipitation.

There is no evidence in the peer-reviewed literature that a numerical modelling study with soil-atmosphere boundary and representative climate data has been carried out to quantify the water and salt dynamics variably saturated environments. Such a study will be a great value to understand the soil and groundwater contamination in the western Great Plains area of Canada.

1.3 Objectives

1.3.1 General Objective

- To understand water and salt dynamics in the unsaturated zone for various climate and soil types in the province of Alberta, Canada.

1.3.2 Specific Objectives

- To estimate the water balance at the soil-atmosphere interface in sandy and clayey soil profiles for various climate types for the province of Alberta.
- To understand the impact of soil and climate type on salt mobilization in unsaturated soils.

1.4 Thesis Organization

This research has been organized in five chapters. Chapter 2 provides theoretical background information and literature review on various aspects of the thesis such as: soil texture and layering effect on water and salt dynamics, infiltration and evaporation from the unsaturated zone, soil-atmosphere water models, and flow and solute transport in unsaturated soils. Chapter 2 also provides details on governing partial differential equations for water flow and solute transport in the variably saturated zone. It also briefly discusses how soil-atmosphere models estimate actual evaporation using climate data and transient soil moisture conditions.

Chapter 3 reports the details of the meteorological data compilation and processing to estimate the variability and availability of water budget at the ground surface for different climate types in the province of Alberta, Canada. The compilation of climate data across the province of Alberta was available on a daily resolution. Compiled climate variables included: maximum and minimum temperature (°C), mean relative humidity (%), total precipitation (mm), wind speed (Km/h), and total solar net radiation (MJ/m^2 – day). Nine year daily climate data sets (2005-2014) were compiled for 10 different locations in Alberta. Daily values of temperature, relative humidity, wind speed, and net radiation were used to estimate daily potential evaporation using Penman (1948) method as described by Fredlund et al. (2012). Details of the climate classification for the 10 sets are also described in this chapter. As mentioned early that the data was only available at a daily resolution, a set of Matlab codes were written to convert calculated daily precipitation and potential evaporation records to higher time resolution data using recommended procedures. The details of the exercise are also mentioned in this chapter.

Numerical modelling results and discussion are presented in Chapter 4. Numerical simulations were carried out using Hydrus-1D (version 4.16.0110) to estimate the effect of climate type and temporal variability on soil water and solute transport in the unsaturated zone. This chapter is divided in three parts as follows: i) effect of climate type, ii) effect of temporal resolution of climate data, and iii) interaction of groundwater table with climate type. The simulations make use of the compiled daily climate data from ten different natural regions of Alberta. Plotted results from extreme climatic conditions are shown in two different sets of graphs, including: water balances

at the ground surface and vertical solute displacement along the 9 water years in variably saturated soil profiles.

Chapter 5 is the synthesis of the insights derived from this study and it is presented in the form of conclusions. Recommendations for future research are also outlined in this chapter.

Chapter 2

Definition and Review of Basic Concepts

2.1 Theoretical Background Information

In unsaturated soils, the rate of salt movement can be influenced by atmospheric conditions and soil hydraulic properties. After a precipitation event, some of the water available at the ground surface does not evaporate or drain out of the system in the form of runoff. This excess of water infiltrates into the unsaturated zone and may carry down with it salts released near or at the surface into deeper soil layers. When the stored soil water is still enough at the sub-surface the water evaporates and moves water and salt upwards by capillary rise which extends the risk of salinization into the root zone (Li et al., 2014). Similarly, in deeper layers, groundwater table fluctuations affect the salt transport via groundwater recharge (from precipitation) and discharge (due to evaporation process). Over the recent years, the climate factor has received special attention to better understand the fate and transport of saline waters in the unsaturated zone (Delleur, 2007).

The migration, distribution and accumulation of dissolved salts in the soil profile can be closely associated with the volumetric soil water content and consequently the direction of water flow as a function of the soil properties of the unsaturated zone. Changes in volumetric of water content represent the difference between the amount of water gain and the amount of water losses at the same period of analysis. Additionally, changes in the soil water pressure can affect significantly the water content. The variability of water content causes differences in the magnitude of the hydraulic

conductivity for different soil types. Therefore, the analysis of the soil hydraulic properties is of particular importance to the evaluation of salt transport in unsaturated soils.

2.2 Brief notes on soil texture and layering effect on water and salt dynamics

Water and salt dynamics in layered one-dimensional soils can migrate in two directions: downward displacement (recharge) and upward displacement or capillary rise (discharge flux). During infiltration and soil water redistribution processes the downward water movement can be impeded by soils with different textural layering. The fate of upward salt migration to the ground surface is controlled by evapotranspiration process, diffusion due to a salinity gradient with depth, and restricted drainage flow caused by the flow barrier effect (Kessler et al., 2010, as cited by Li et al., 2014). The thickness of the soil layers and their spatial configuration are also factors that affect the upward and downward water movement in unsaturated soils.

Textural layering can form capillary barriers that can potential create a capillary break effect on vertical water movements. The capillary break effect is usually observed on infiltrating water flowing from an overlying fine-textured soil layer into an unsaturated coarse-textured soil layer. The difference between the hydraulic connectivity and high soil water pressure in the capillary barrier layer impedes the infiltrating water to cross the soil layer interface. This effect makes the upper soil layer to hold more water and also reduces the rate of upward water flow. A hydraulic barrier is observed in reverse soil layer configurations when coarse layers overlie fine-textured layers, namely

hydraulic barrier. In this case, evaporation may also be enhanced if the coarse-textured layer is not too thick and the textural layering interface is close to the ground surface. In both flow barriers, if the capillary layer is too thick and the capillary rise is less than the thickness of the layer then it will result in an increased lateral soil water movement due to the low hydraulic connection. In high groundwater table systems, water moves upwards through capillary rise and can enter the atmosphere through plant transpiration or direct evaporation at a relatively high rate. This effect can pose a high risk of salinization at the ground surface by bringing salts up from deeper soil horizons.

2.3 Water flow and solute transport in unsaturated soils

In unsaturated soils, the hydraulic properties considered in the water and solute transport are expressed in the form of non-linear mathematical relationships with the soil pressure or soil water content. The unsaturated flow can be mathematically expressed with Darcy-Buckingham equation (Narasimhan, 2005) as follows:

$$q = -K(h)\frac{\partial h}{\partial z} = -K(h)\left[\frac{\partial h}{\partial z} + 1\right]$$
<div align="right">Eq. (1)</div>

The above expression states that q is the flux density or volumetric water flux flowing through a unit surface area per unit time (L^3/L^2T). In the above equation $K(h)$ is the unsaturated hydraulic conductivity (L/T) and is the function of the soil water pressure head (h), and z is the elevation head or height above a reference level (L).

Richards (1931) defined the one-dimensional uniform water movement equation

for unsaturated flow (when pore voids are filled with water and continuous air phase)

combining the mass balance equation with the Darcy-Buckingham equation:

$$\frac{\partial \theta}{\partial t} = -\frac{\partial q}{\partial z} - S = \frac{\partial}{\partial z}\left[K(h)\left(\frac{\partial h}{\partial z} + 1\right)\right] - S \qquad \text{Eq. (2)}$$

where θ is the volumetric water content (L^3/L^3), t is time (T), and S is the sink term

(L^3/L^3T) that accounts, for example, for root water uptake (transpiration).

In order to solve the above equation, two sets of hydraulic properties are

required. These properties are soil water characteristic curve (SWCC) and the

unsaturated hydraulic conductivity function (K(h)) relationship (Bashir et al., 2015). The

unsaturated soil hydraulic properties are of great importance especially when numerical

models are to be used in the analysis of variably-saturated water flow and salt transport

(Šimůnek and van Genuchten, 1996). van Genuchten (1980) estimated the unsaturated

hydraulic conductivity in terms of SWCC parameters based upon the theory of Maulem

(1976). The van Genuchten function for SWCC is as follows:

$$\theta = \frac{(\theta_s - \theta_r)}{[1 + (|\alpha h|)^n]^m} + \theta_r \qquad \text{Eq. (3)}$$

where θ is the volumetric water content (L^3/L^3), θ_s is the saturated water content (L^3/L^3),

θ_r is the residual water content (L^3/L^3) and α (1/L), n (-), and m (-) are curve fitting

parameters. The parameter α can be related to the inverse of air entry value (also

referred to as the bubbling pressure which is the negative pressure head that must be

exceeded before air recedes into the soil pores (Fredlund and Rahardjo, 1993). The

parameter n is related to the pore size distribution index. Using the assumption that m =

1-1/n, van Genuchten (1980) formulated the following equation for unsaturated hydraulic conductivity function:

$$K(h) = K_s S_e^{\ell} \left[1 - \left(1 - S_e^{1/m} \right)^m \right]^2 \qquad \text{Eq. (4)}$$

In which the effective saturation, S_e, is computed as shown below:

$$S_e = \frac{\theta - \theta_r}{\theta_s - \theta_r} \qquad \text{Eq. (5)}$$

where K_s is the saturated hydraulic conductivity (L/T) while ℓ (-) is an empirical parameter that is normally assumed to be 0.5 (Šimunek et al., 2013) and all the other parameters are as described earlier. It should be noted that in most instances Eq. (3) is fitted to the measured SWCC data and the fitted parameters are used to estimate the unsaturated hydraulic conductivity function.

In unsaturated soils, the driving force controlling the soil water movement is total soil water pressure head (H, in length units when expressed per unit weight). Total head (H) is the sum of the gravitational force (z, vertical coordinate or elevation) and pore water (capillary) pressure head (or soil water matric suction, Ψ; if negative relative to atmospheric pressure, H ≤ 0). It is important to note that soil water upward movement only occurs under certain conditions. Gladyeva and Saifadeen (2012) stated that in unsaturated soils, upward water movement is controlled by capillary surface tension, which depends on pore size and soil structure (arrangement of soil particles into aggregates). According to Deeb et al. (2016), the extension of the upward water

movement can be calculated by using the Jurin-Laplace equation (Eq. 6) when reaching

balance in a certain pore size.

$$\psi = h = \frac{4\sigma \cos \varphi}{d_{eq}}$$
Eq. (6)

where h is the water potential head, σ is water surface tension, φ is liquid-surface

contact angle, and d_{eq} is the equivalent size of the pore resembling the diameter of a

cylindrical capillary. Lehmann et al. (2008, as cited by Li et al., 2014) formulated an

analogous mathematical expression to equation 6 for the calculation of the maximum

capillary height using van Genutchen soil parameters.

$$h_{max} = \frac{1}{\alpha}\left(\frac{n-1}{n}\right)^{(1-2n)/n}$$
Eq. (7)

2.4 Mass Transport in the Unsaturated Zone

This section briefly describes the transport of contaminants in unsaturated soils

which is closely linked with the water flux formulated using a mass balance expression

(Eq. 8) as defined by Šimůnek and van Genuchten (2006):

$$\frac{\partial C}{\partial t} = -\frac{\partial J_{Ti}}{\partial z} - \phi$$
Eq. (8)

where C is the total concentration of chemical in all forms (ML^{-3}), J_{Ti} is the total chemical

mass flux per unit area per unit time (ML^{-2}T^{-1}), and ϕ is the rate of change of mass per

unit volume by reaction or other processes (ML^{-3}T^{-1}). The negative sign indicates that

the movement is from areas of greater concentration to those of lesser concentration.

Two main physical processes control the solute transport in the subsurface. Advection represents the solute movement related to transport by the flowing water, (Freeze and Cherry, 1979). The hydrodynamic dispersion process occurs as a result of mechanical mixing and molecular diffusion. Mechanical dispersion results from uneven distribution of water flow velocities within and between different soil-pore sizes. Diffusion is a result of the random motion of chemical molecules. Equation (9) combines the advection-dispersion equations for one-dimensional transport of inert, non-adsorbing solutes during steady-state water flow in the unsaturated zone:

$$\frac{\partial}{\partial t}(\theta C) = \frac{\partial}{\partial z}\left(D_e \frac{\partial C}{\partial z}\right) - \frac{\partial}{\partial z}(qC) \qquad \text{Eq. (9)}$$

where θ is the volumetric water content (L^3/L^3), q is the volumetric flux density (LT^{-1}), D_e is the hydrodynamic dispersion coefficient (L^2T^{-1}).

2.5 Estimation of soil hydraulic properties for the province of Alberta

In the previous section, mathematical expressions describing the movement of water and salt transport in variably-saturated soils were presented. The salt transport is dependent on the water flow distribution in the soil domain. In order to solve the water flow equation for the unsaturated zone two set of hydraulic properties are required. These are namely SWCC and unsaturated hydraulic function. Both of these properties can be measured in the laboratory and in the field. Field or laboratory measurements for unsaturated soil hydraulic properties are difficult, time consuming and costly (Saxton and Rawls 2006). Therefore, several methods have been proposed to estimate soil

hydraulic properties from easily measured soil properties, e.g., texture, bulk density, and particle size distribution. A recent review of such techniques over the last two decades has been provided by Patil and Singh (2016).

The U.S. Department of Agriculture has developed a soil textural classification system based on three major groups of soil particles: sand, silt, and clay (USDA, 1987). The textural triangle is shown in Fig. 2.1. Based on the percentage of weight of sand, silt, and clay fraction soils can be classified into 12 major textural types namely: sand, silt, clay, loamy sand, sandy loam, sandy clay loam, sandy clay, clay loam, loam, silty clay, silty clay loam, and silt loam. The abundant of soil particle sizes defined 12 major soil texture types often represented in a soil texture triangle (Fig. 2.1).

In contrast to USDA, the Canadian system of soil classification only identifies sand and clay fractions (Agriculture Canada, 1998). Figure 2.2 shows the 13 soil texture classes based on the percentage of sand and clay presented by the Canadian system, namely: heavy clay, HC; Clay, C; silty clay, ScC; silty clay loam, SiCL; clay loam, CL; sandy clay, SC; silt loam, SiL; loam, L; sandy clay loam, SCL; sandy loam, SL; silt, Si; loamy sand, LS; and sand, S. The particle size range for sand and clay are the same for the Canadian and USDA systems.

The continuous red lines shown in Fig. 2.2 represent the two generalized soil lithology groups to categorize soil texture at sites across the province of Alberta for coarse and fine-grained soil materials (Alberta Government, 2014). This range represents the percentage of clay varying from <18% (includes sandy loam, silt, loamy

sand, and sand), clay content between 18% and 60% (clay, silt clay, silty loam), up to 60% (heavy clays).
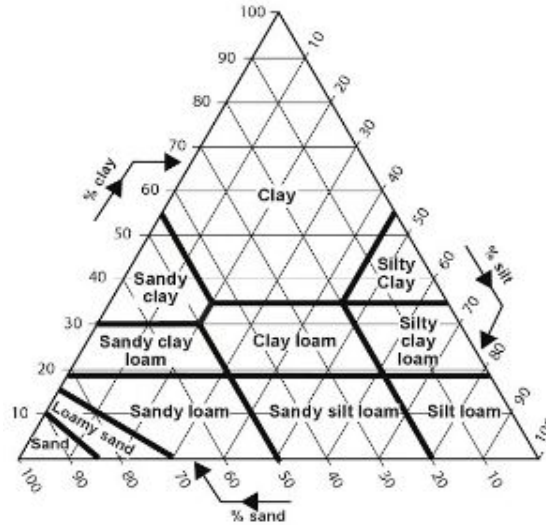
Fig. 2.1: USDA Soil Texture Classification. Modified from Friske et al., 2010
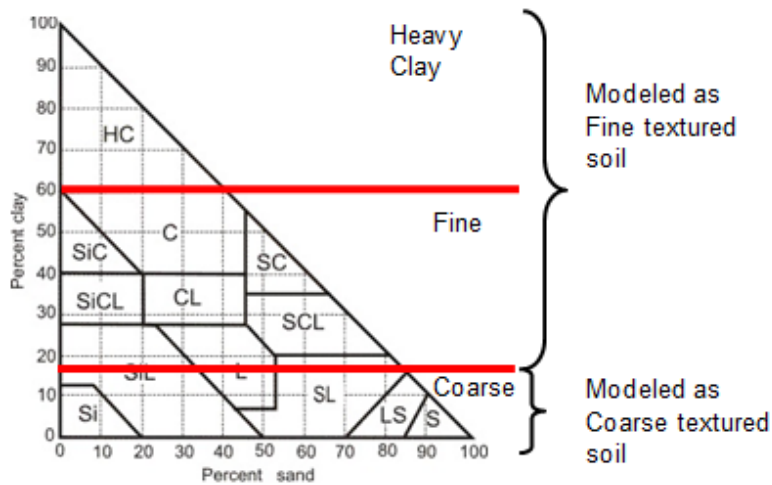
Fig. 2.2: The Canadian Soil Textural Classification. Modified from Alberta Government, 2014

According to Fredlund et al. (2012), the SWCC describes the relationship between soil water content (θ) in the soil and the soil-water pressure (matric potential or negative pressure head). The SWCC is the single most valuable piece of soil information for the analysis the hydraulic conductivity, water storage and field capacity.

These curves also represent the soil hydraulic properties of partially saturated soils (Heshmati and Motahari, 2012). The soil water pressures in the SWCC's are often represented using logarithmic scale; whereas, the volumetric water content range is represented in arithmetic scale. Fig. 2.3 shows a series of SWCCs of different soil types based on the USDA soil texture classification. The dotted black lines shown in Fig. 2.3 represent the soil texture range that is currently being used in salinity assessment for the province of Alberta (Alberta Government, 2014).
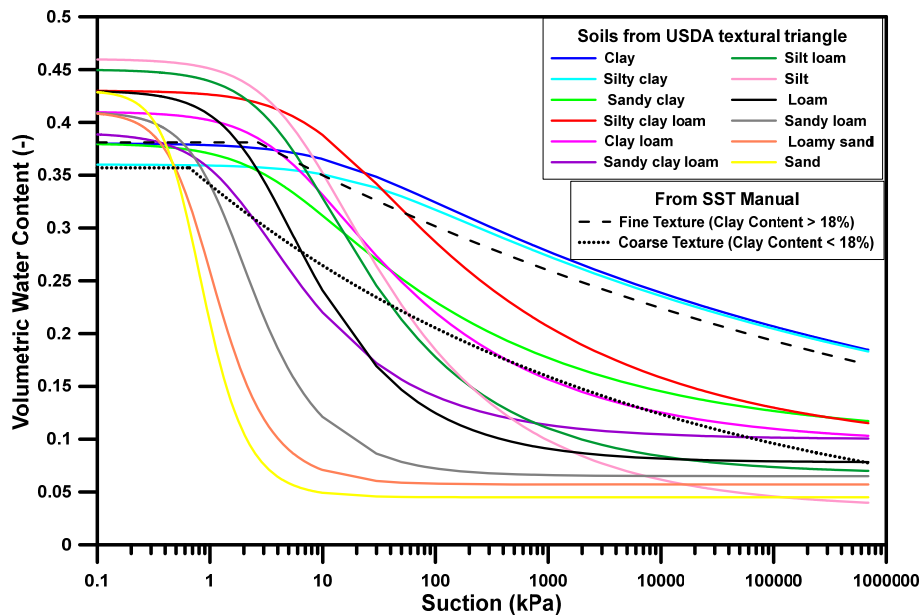
Fig. 2.3: Soil moisture characteristics of different soil materials. Modified from Bashir (2012)

Estimation methods to compute basic relationships of soil hydraulic properties from more easily measurable and available input data are referred as to pedo-transfer functions. These functions act as small modules within the estimation methods base on the soil information system. Pedo-transfer functions have been proposed for various soil types to estimate the van Genuchten (1980) parameters for soil hydraulic functions

([Verrecken et al., 2010](#)). Soil hydraulic parameters play an important role in hydrologic models as they directly control the movement of water and water balance partitioning.

Hydrus-1D offers mainly two options for determining the soil hydraulic properties when users do not have measured soil parameter values. The first option is the catalogue of soil hydraulic properties corresponding to the 12 soil textural classes of the USDA textural triangle. These values are based on the work of [Carsel and Parrish, (1988)](#) and are averages of large number of measured values reported in the literature. As a second option, Hydrus-1D uses an estimation program called Rosetta ([Schaap et al., 2001](#)). The Rosetta program is capable of estimating unsaturated hydraulic properties for soils using a hierarchical sequence of input data. The input data includes: soil textural class, bulk density and percentages of sand, silt, and clay ([Ungurasu et al., 2012](#)). During the course of this research, it was not possible to find the information related to the information related to soil hydraulic properties at any specific site across of the province of Alberta. A decision was made to use the hydraulic properties of sand and clay from the catalogue of Hydrus-1D. This decision was based on two reasons. First, as pointed out earlier that the soil classification used by Alberta is very similar to the USDA system. Therefore, selection of average properties from USDA textural classes provides a perfect analogue for others to provide specific conclusion from this research if required. The bigger objective of this thesis was to compare and contrast the water and salt dynamics for different soil types or textures. Considering that, the hydraulic properties of sands and clays are vastly different in terms of retention and conduction, simulations run with sand and clay hydraulic properties are expected to

provide maximum insight in the effect of soil texture on water flow and solute transport in the unsaturated zone.

2.6 Estimation of Potential Evaporation

Infiltration and evaporation in the unsaturated zone are the driving forces controlling the direction of the water movement. Both of these processes depend on atmospheric conditions but also on soil moisture conditions. Potential evaporation (*PE*) depends on the prevailing atmospheric conditions and limitless supply of water. It is the amount of evaporation that would take place over a water body or a soil profile which always remains saturated. In most instances the soil profile will not always be saturated and actual evaporation (*AE*) will depend on the prevailing atmospheric conditions and transient soil moisture conditions. The rate of evaporation will decrease substantially from *PE* as the soil becomes drier. The net moisture flux or net infiltration (*NI*) is the quantity of water that makes its way into a soil profile overcoming evaporation and runoff process at the soil atmosphere interface. Mathematically, it can be estimated as:

$$NI = P - AE - RO$$ Eq. (10)

where *P* is the precipitation (L), *AE* is the actual evaporation (L), and *RO* is the runoff (L).

The daily potential evaporation at the soil-atmosphere interface can be computed using Penman 1948 equation (Fredlund et al., 2012).

$$PE = \frac{\Gamma Q_n + \eta E_a}{\Gamma + \eta}$$ Eq. (11)

where *PE* is the potential evaporation (mm/day); Γ, slope of saturation vapour pressure versus temperature (kPa/°C); Q_n = 1000R_n/L_v, where Q_n is the net radiation at the water (or saturated ground) surface (mm/day); R_n, net radiation (MJ/m²/day); L_v, volumetric latent heat of vaporization (MJ/m³); η, is the psychrometric constant (kPa°C⁻¹).

The computation of the constant E_a was based on the following expression:

$$E_a = 2.625(1 + 0.146W_w)\left(u_{vo}^{air} - u_v^{air}\right) \qquad \text{Eq. (12)}$$

where: W_w, wind speed (kmh⁻¹); u^{air}_{vo}, vapour pressure in the air above the water (or saturated ground) (kPa); and u^{air}_v, saturated vapour pressure at the mean air temperature (kPa). According to Allen et al. (1998), the computation of daily net radiation values equation is expressed in terms of energy balance of global atmosphere equation:

$$R_n = R_{ns} - R_{nl} \qquad \text{Eq. (13)}$$

where R_n is net radiation (MJ/m²/d), and represents a mass balance of the absorbed, reflected, and emitted energy by the earth's surface. R_{ns} is the incoming net short wave radiation or solar radiation (MJ/m²/d) and R_{nl} represents the outgoing net long-wave radiation or terrestrial radiation (MJ/m²/d). The estimation of the both forms of energy is computed using the following expressions:

$$R_{ns} = (1 - \alpha)R_s \qquad \text{Eq. (14)}$$

$$R_{nl} = \sigma\left[\frac{T_{max,K}^4 + T_{min,K}^4}{2}\right]\left(0.34 - 0.14\sqrt{e_a}\right)\left(1.35\frac{R_s}{R_{so}} - 0.35\right) \qquad \text{Eq. (15)}$$

where α = albedo or canopy reflection coefficient; R_s is the total incoming radiation (MJ/m²/d); σ = Stefan-Boltzman constant (4.903×10-9 MJ/K⁴m²d¹); $T_{max,K}$ = daily maximum absolute temperature (°K = °C+273.16); $T_{min,K}$ = daily minimum absolute temperature (°K = °C+273.16); e_a = actual air vapour pressure (kPa); and R_{so} = calculated clear sky solar radiation (MJm⁻²d⁻¹).

2.7 System-dependent boundary conditions at soil- atmosphere interface

The magnitude and direction of the water flux across the soil-atmosphere interface depends upon the specified initial and atmospheric boundary conditions (Šimůnek, 2008; as cited by Huang. et al., 2012). Initial conditions can be referred as to the initial state of the soil surface system in terms of water content (θ) or pressure head (h). The soil-atmosphere interface is an example of system-dependent boundary, where the flux across this interface (pressure head or gradient) is not known a priori. The potential surface flux across this boundary is controlled exclusively by atmospheric conditions, namely: precipitation; minimum and maximum relative humidity and temperature; wind speed; and net radiation. The actual surface flux depends also on transient soil moisture conditions near or at the ground surface and may change from prescribed flux to prescribed head conditions. For example, in those instances where the precipitation exceeds the infiltration soil capacity, the infiltration rate switches from precipitation rate control to infiltration soil capacity control. On the other hand, in instances where the potential evaporation rate exceeds the capacity of soils to release enough water to the atmosphere, then this is reduced to a value known as actual

evaporation rate (*AE*). Hydrus-1D uses the following methodology by Neuman et al. (1974) to assess the maximum potential rate (E) of infiltration (*I*) or evaporation (*PE*) flux across the interface (LT^{-1}) on the basis of current climate conditions of the study site and prevailing moisture conditions in the soil:

$$\left| -K_{(h)} \left[\frac{\partial h}{\partial z} + 1 \right] \right| \leq E \qquad \text{at } z = L \qquad \text{Eq. (16)}$$

where *h* (L) is the pressure head at the soil ground surface allowed under prevailing soil conditions. This head may vary between the minimum (h_a) and maximum (h_s) pressure heads defined by the following condition: $h_a \leq h \leq h_s$ (at z = L). The value of h_a represents the equilibrium conditions between soil, water, and atmospheric water vapour. The value of h_s represents the pressure head at which the surface runoff has been previously set to begin evacuating the excess of water between infiltration (*I*) and precipitation (*P*) rates. The excess of water (L) may range between zero (no ponding) and a specified layer of water ponded. According to Šimunek et al. (2013), the h_a value can be calculated from the air humidity as follows:

$$h_a = \frac{RT}{Mg} ln(H_r) \qquad \text{Eq. (17)}$$

where H_r is relative humidity of the atmosphere (dimensionless); *R* is the gas constant (8.31 kg m^2 s^{-2} K^{-1} g mol^{-1}); *M* is the molecular weight of water (0.018 kg g mol^{-1}); *g* is the gravitational acceleration (9.81 m s^{-2}); and *T* is the air temperature (K).

Chapter 3

Material and Methods

In chapter 2, the governing equations for water flow and solute transport in the unsaturated zone were discussed together with the soil hydraulic properties that are essential for their solution. It was also mentioned that the numerical model Hydrus-1D (version 4.16.0110) solves these governing equations for a variety of initial and boundary conditions. The soil atmosphere boundary condition requires information on atmospheric conditions to estimate the direction and magnitude of water flux across the soil-surface interface. The atmospheric conditions can be provided to the model in the form of a multi-year climate dataset comprising of a minimum and maximum temperature and relative humidity, total precipitation, wind speed and net radiation. It should be noted that an extensive amount of work is required in compilation and processing of meteorological input data to formulate the soil atmosphere boundary. It should be also noted that temporal resolution of the climate data is also important and influences the prediction of water flow and solute transport in the unsaturated zone.

3.1 Meteorological data compilation, processing, and classification

In the previous chapters, it was explained that climatic conditions and soil type can influence the rate of infiltrating soil water, water content distribution, and solute transport. Therefore, the compilation and processing of the available meteorological

data to formulate the soil-atmosphere boundary is critical for the accuracy of the numerical results in order to meet the established objectives of the study. For this research, in order to assess the effect of climate variability on water and solute transport, climate data was compiled for a number of locations in the province of Alberta. The major climatic characteristics related to the natural regions of Alberta are: Boreal, Grassland and Cordilleran ecoclimatic provinces (Downing and Pettapiece, 2006). Table 3.1 shows a brief summary of the main climatic characteristics of the ecoclimatic provinces in Alberta.

Table 3.1: Climatic characteristics of the ecoclimatic provinces in Alberta

	Ecoclimatic province		
Characteristic	*Grassland*	*Boreal*	*Cardilleran*
Mean Annual Temperature[1]	+3°C	+0.5°C	-0.5°C
Mean Annual Precipitation[1]	410 mm	480 mm	800 mm
Mean Annual Evaporation[2]	800 mm	612 mm	725 mm
Natural Region	Grassland and Parkland	Boreal Forest, Canadian Shield,	Rocky Mountain

[1] Downing and Pettapiece, 2006

[2] Alberta Environment and Sustainable Resource Development, 2013

A graphical illustration of natural regions and subregions of Alberta in terms of summer moisture index (SMI) is shown in Fig. 3.1. Summer moisture index (SMI) is a measure of the precipitation effectiveness during the growing season for the natural regions of Alberta. The SMI indicates that at certain time during the growing season the evaporation demand will be greater than the precipitation demand. This ratio is calculated by dividing the degree-days greater than 5°C by the mean growing season precipitation (April through August). SMI values greater than 4 indicates dry to very dry

climate conditions and includes the Grassland and Canadian Shield regions. Boreal Forests and Parkland natural regions are related to neither dry nor wet climates (SMI values between 3 and 4). SMI values less than 3 represent wet climate conditions with not moisture deficit during the growing season. Natural regions related to the latter climate condition include the Rocky Mountain and Foothills.

For this research, daily continuous climatic datasets were compiled for 10 different locations across Alberta. These dataset consisted of daily values of maximum and minimum temperature, mean relative humidity, total precipitation, wind speed and net radiation. These dataset covered a period from January 2005 to December 2014.
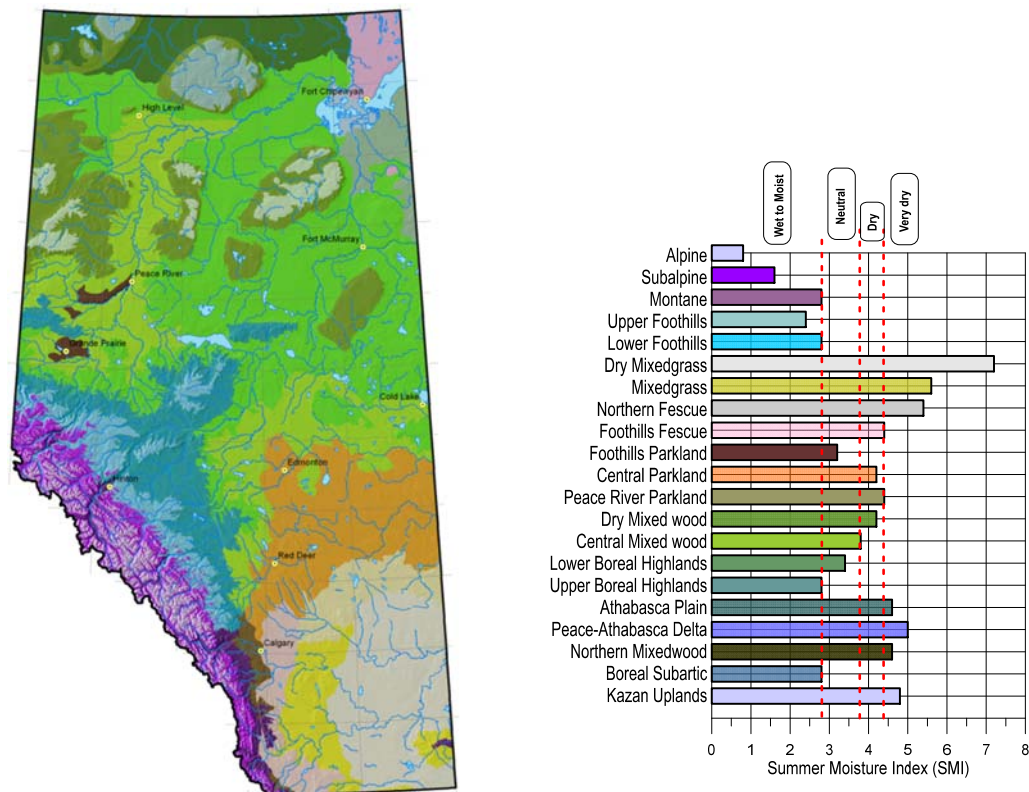
Fig. 3.1: Climate regions of Alberta based on summer moisture index (SMI). Modified from Downing and Pettapiece (2006)

Compiled historic climate data was acquired directly from three weather websites, including: Environment Canada, Alberta Agriculture and Forestry, and Alberta Township Survey (ATS). Available climate data from Environment Canada (EC) and Alberta Agriculture and Forestry (AF) are from weather stations throughout the province of Alberta.

The Alberta Township Survey (ATS) consists of a grid that divides the province in equal six-mile-wide meridians or parcels of land. Between each meridian, there are six-mile wide columns called ranges. Parcels and ranges result in a grid of cells called townships. Each township uses a pre-defined search radius that weighted up the 8 nearest weather stations from which uses interpolated weather data from Alberta Agriculture and Forestry.

The compilation of the available climate variables from selected weather stations (Fig. 3.2) consists of daily continuous records. The compiled information was carefully checked for inconsistencies such as missing data or anomalous maximum and minimum values among the climatological variables. Short gaps in data were infilled using average of the preceding and following records. Climate variables compiled from Environment Canada included: maximum and minimum temperature (°C), mean relative humidity (%), and total precipitation (mm). Mean wind speed records (Km/h) were compiled from Alberta Agriculture and Forestry, and measured global solar radiation records (MJ/m^2/day) were compiled from the Alberta Township Survey.

Table 3.2 summarizes the relevant information of the selected weather stations including station name, latitude, longitude, elevation and associated climate type as described in this study.

Fig. 3.2: Selected weather stations associated with the natural regions of Alberta. Modified from Downing and Pettapiece (2006)

Table 3.2: Selected weather stations in province of Alberta

Station Name	Latitude (N)	Longitude (W)	Elevation (m)	Alberta Natural Region
Beaverlodge	55°11'48.002"	119°23'47.090"	745.0	Parkland
Bighorn Dam	52°19'00.000"	116°20'00.000"	1341.0	Rocky Mountains
Calgary Airport	51°06'50.000"	114°01'13.000"	1084.1	Grassland
Edson	53°35'00.000"	116°25'00.000"	922.6	Foot Hills
Fort Mcmurray	56°39'00.000"	111°13'00.000"	369.1	Boreal Forest
High Level	58°37'17.000"	117°09'53.000"	338.0	Boreal Forest
High Prairie	55°23'44.880"	116°28'46.200"	591.0	Boreal Forest
Lloydminster	53°18'33.000"	110°04'21.000"	668.4	Boreal Forest
Medicine Hat	50°01'08.000"	110°43'15.000"	716.9	Grassland
Neir AEDM	51°21'59.760"	114°05'60.000"	1145.0	Canadian Shield

3.2 Meteorological input data

As an example, the following information describes and illustrates each climate variable of the compiled measured dataset related to the Bighorn area. Daily and cumulative precipitations records are presented in Fig. 3.3. The compiled average annual precipitation for this region was 485 mm. Results indicate a single rainfall event of 72.3 mm measured on June 17th, 2005. Review of data shows that over the 10-year period only 1% of precipitation events exceeded the 20 mm. Review of the data indicates that over the 10 year period only about 2% of the precipitation events were greater than 10 mm/day.

Fig. 3.4 shows the daily maximum and minimum temperatures. Review of the data indicates that over this period a maximum temperature of 31.1 °C was recorded on July 30th, 2014. Generally, July and August are warmest months of the year. The minimum temperature of -37.2 °C was recorded on January 19th, 2012.
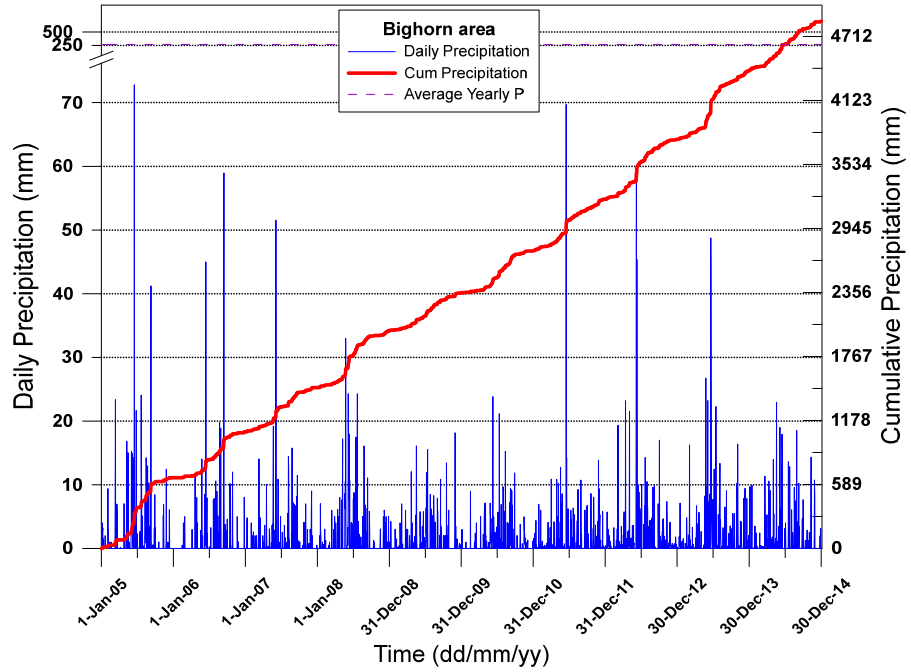
Fig. 3.3: Precipitation data for the Bighorn area, Alberta (2005 - 2014)
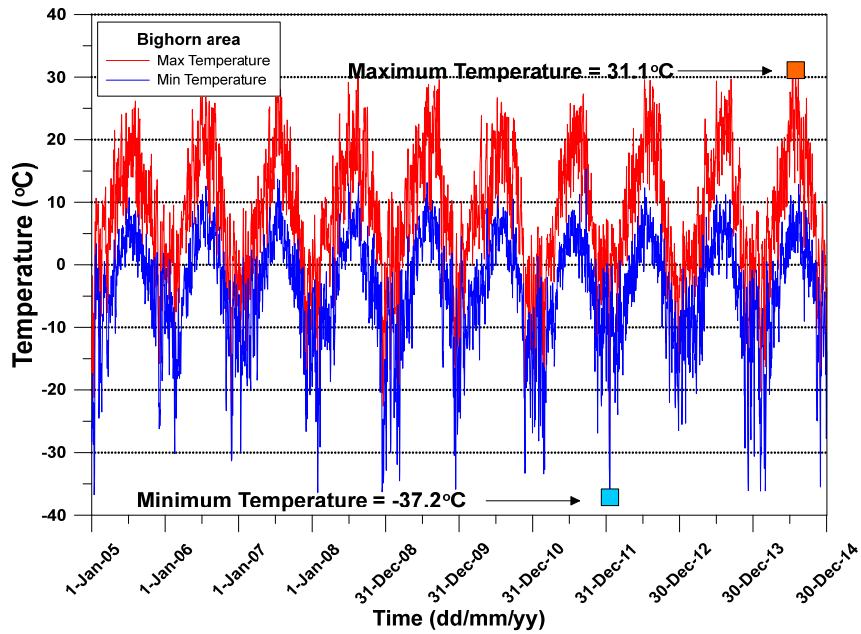
Fig. 3.4: Maximum and minimum temperature data for the Bighorn area (2005 - 2014)

Relative humidity values for Bighorn were only available as mean daily values. The data is plotted in Fig. 3.5 and it can be observed that the mean value varies from a maximum of 98% to a minimum of 29%. The review of records indicated that values higher than 90% were observed for only 5% of the 10-year period. It was also observed that for more than half of the 10-year period considered in this study the mean RH was about 70%.

Data for daily wind speed values is shown in Fig. 3.6. A maximum value of 13.7 Km/h was recorded on November 9th, 2005. Similarly, a minimum wind speed value of 0.7 Km/h was observed on March 19th, 2010. The yearly average value was found to be 5.1 Km/h with a standard deviation of ±2.2 km/h.
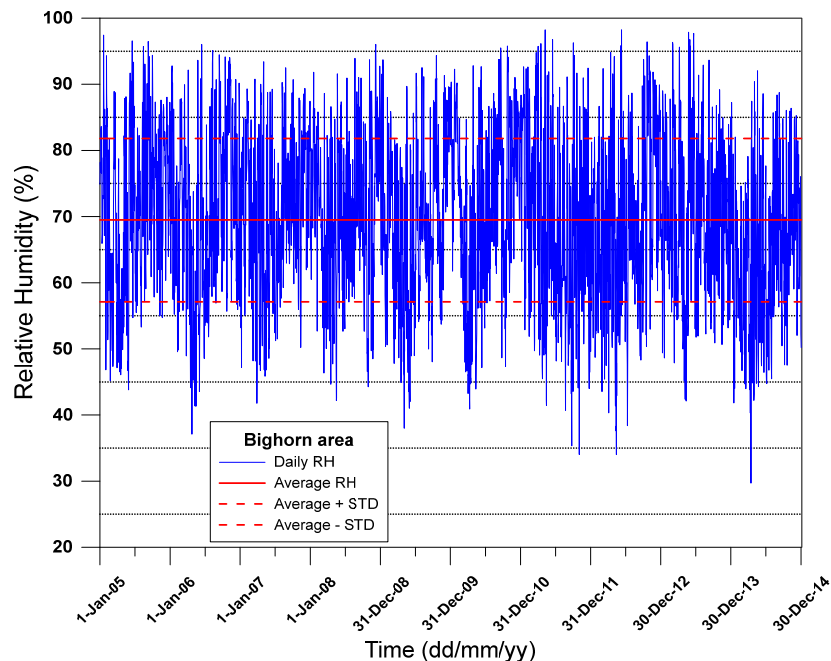
Fig. 3.5: Mean relative humidity data for the Bighorn area (2005 - 2014)
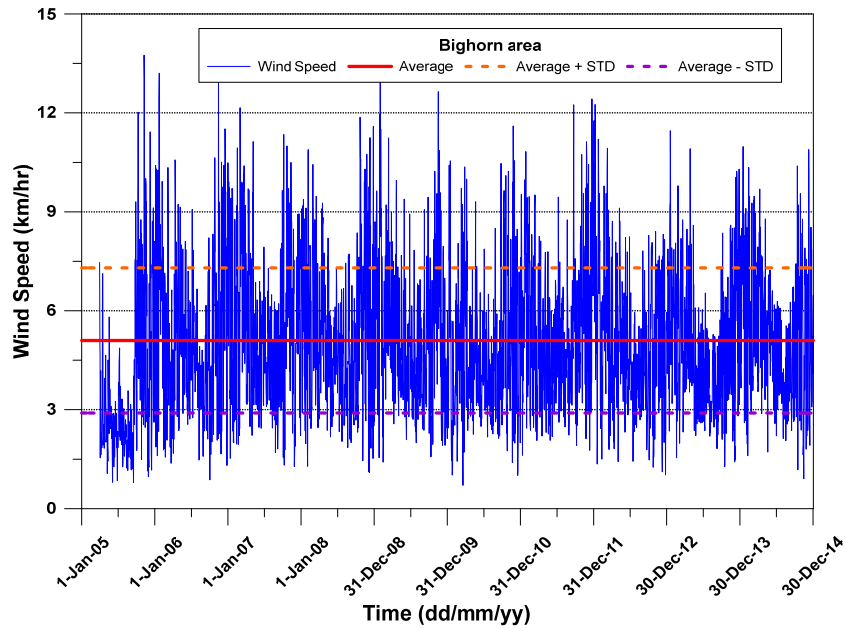
Fig. 3.6: Mean speed wind data for the Bighorn area (2005 - 2014)

Net radiation values for this location were calculated using temperature records, relative humidity, and total solar radiation data using a procedure by Allen et al. (1988) as explained in Fredlund (2012). The net radiation calculations also require an albedo coefficient, station elevation (m ASL) and station latitude (°). The predicted net radiation values are the most sensitive to the selection of an albedo coefficient. The albedo coefficient is used to describe the percentage of total incoming solar radiation that gets reflected at the ground surface. Albedo coefficients can range from 0.06 for dark brown (wet) tailings, 0.23 for grass, to 0.5 to 0.8 for snow.

The net radiation equations were originally developed with the intention of applying one albedo coefficient over a year. However, this assumption is only valid for locations with no snow on the ground are expected. As the albedo coefficient for snow is quite different from that for a vegetated surface. The net radiation equations were

34

modified to permit the application of two different albedo coefficients over a calendar year. One value of albedo coefficient was used when snow is expected to be accumulated on the ground surface, and a second value was used for the remainder of the year. The snow albedo coefficient was set to be 0.75. An albedo coefficient of 0.23 was applied over the remainder of the year, considering that the soil cover will likely support some form of vegetation. Snow was assumed to be accumulated on the ground surface over a certain period of a year, which was identified after reviewing the entire temperature record for the site. Measured solar radiation and estimated net radiation values are shown in Fig. 3.7.
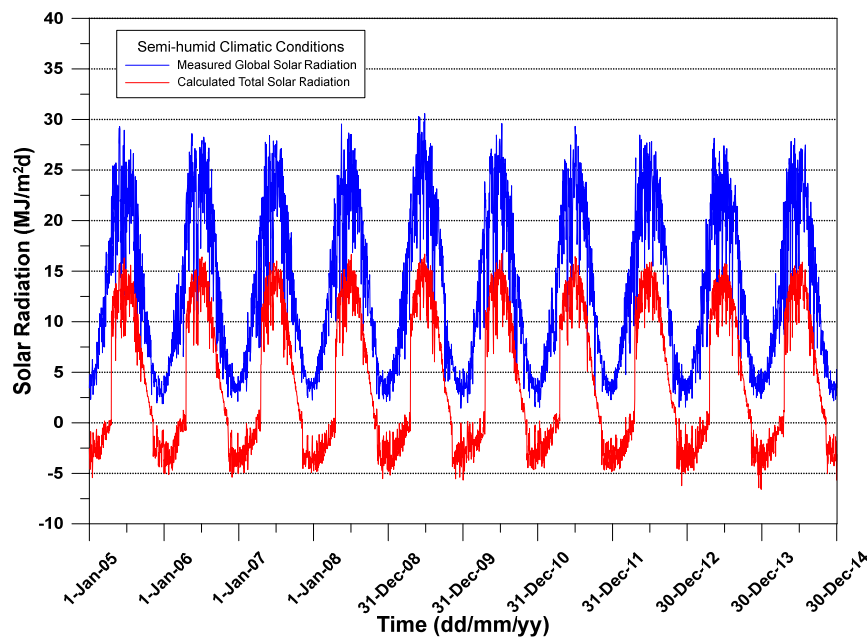
Fig. 3.7: Daily solar and net radiation data for the Bighorn area (2005 - 2014)

Average values from the compiled data were compared with historical climate normals for the period 1981-2010 reported by Environment Canada ([Environment Canada, 2017](#)). This was done to see the correlation between the compiled dataset and reported climate normals. Figure 3.8 shows the comparison of the monthly averages from compiled dataset to climate normals. This figure clearly shows that there is a good correlation between the compiled dataset and the reported climate normals. It should be noted that minor variances between the compiled dataset and reported values are due to the fact that climate normal are 30 year averages while the compiled dataset is only 10 years long. Comparison between the compiled dataset and climate normal for other sites are presented in Appendix A (from A.1 through A.10).

3.3 Seasonal consideration

The ground surface is subjected to extreme changes in weather from being frozen throughout the winter, subjected to thaw and runoff in the spring, to vegetation growth and wetting and drying during the summer. Each calendar year can be divided into active and inactive time periods. The active period represents thawed ground conditions when precipitation can either make its way into the ground as infiltration, or can flow away as runoff. The inactive period represents the period when the ground is frozen and precipitation accumulates on the ground as snow.
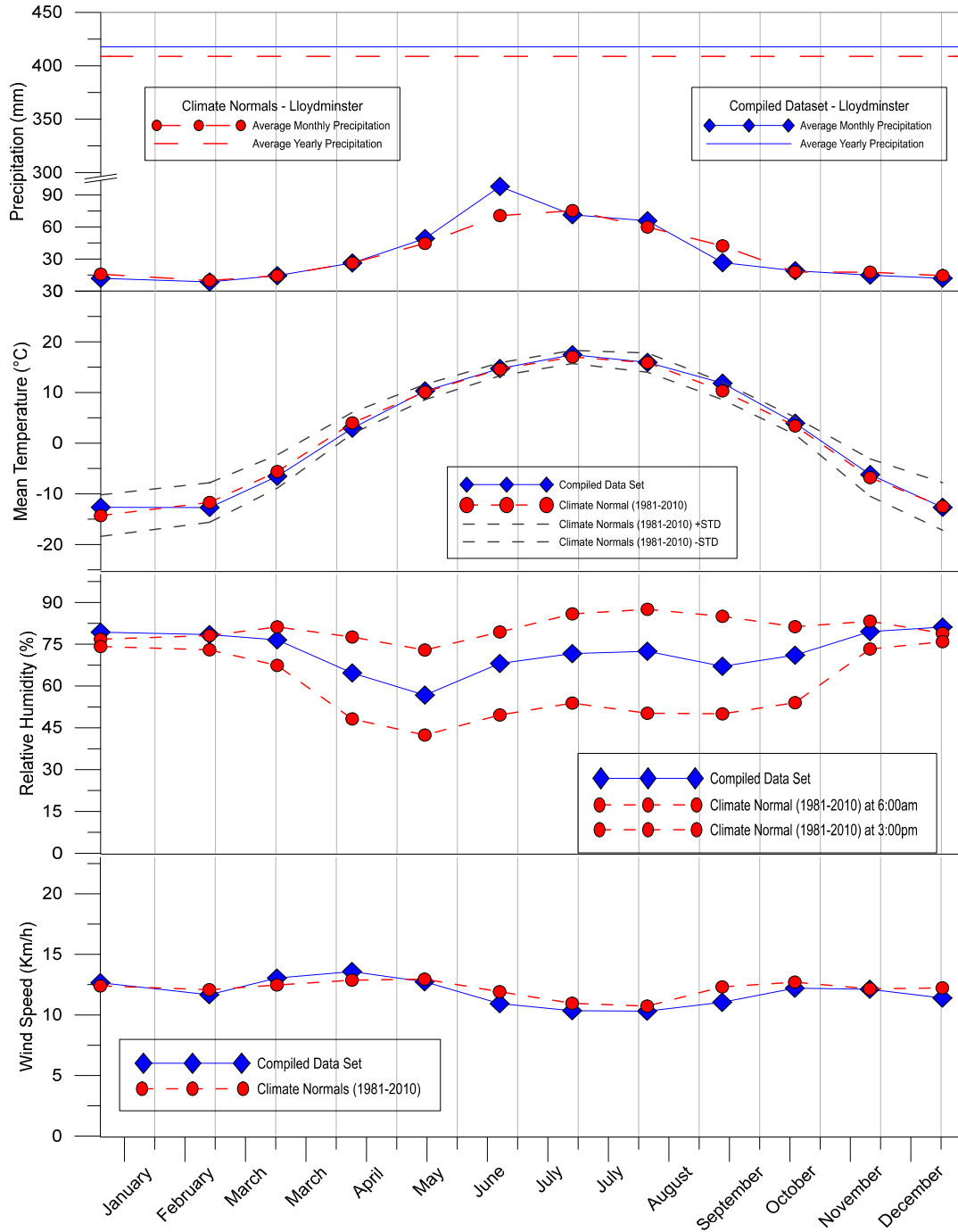
Fig. 3.8: Compiled climate data vs Canadian climate normals of Lloydminster region (2005- 2014)

Assuming a relationship between the air and the ground temperatures, a statistical analysis of the temperature data was carried out for all climate datasets. Temperature data for the Bighorn area indicated that on average active period comprises approximately 213 days. Based on the analysis, the first date of freezing (i.e. start of winter) was selected to be November 15 and the first date of spring was selected to be April 12 (i.e., a date where the soil column could be expected to be thawed). Appendix B (from B.1 through B.10) shows the air temperature graphs corresponding with the first year of analysis (2005) used in the computation of the active season of all climate datasets.

3.4 Climate classification of the province of Alberta

In previous sections, it was mentioned that the climate of the province of Alberta varies from region to region. Understanding the patterns of climate variability is useful for the implementation of sustainable water management practices at a local scale. The climate type of a particular region influences all components of the hydrologic cycle, which in turn define the spatial and temporal water availability.

The Thornthwaite climate classification is an empirical system that was developed from climatic data collected in United State (Thornthwaite, 1948; Thornthwaite and Hare, 1955). It forms an adequate basis for evaluating the climate for engineering purposes. The climate can be classified by computing the moisture index as follows:

$$I_m = 100 \left(\frac{P}{PE} - 1 \right)$$

<div align="right">Eq. (18)</div>

where I_m is the 1955 Thornthwaite's moisture index, P the total annual precipitation (compiled from weather stations), and PE is the annual potential evaporation (Penman, 1948, as cited by Fredlund et al., 2012). From results obtained using Eq. (18), the moisture index may vary from positive values indicating moist/humid climates to negative values indicating dry climates. An I_m value of zero signifies that the annual precipitation and potential evaporation are equal. Table 3.3 summarizes the climate classification criteria.

Table 3.3: Criteria for climate classification based on Eq. (18)

I_m	Category of Climate
> 100	Perhumid
20 - 100	Humid
0 - 20	Moist humid
-33 to 0	Dry subhumid
-67 to -33	Semiarid
-100 to -33	Arid

Based on the computed annual moisture index, the climate classification for various locations in the province of Alberta (Fig.3.9) can be divided in three main climate conditions as follows: dry sub-humid (Bighorn Dam and Edson); semi-arid (High Level, Fort McMurray, Beaverlodge, High Prairie, Lloydminster, Neir AEDM); and arid (Calgary and Medicine Hat).
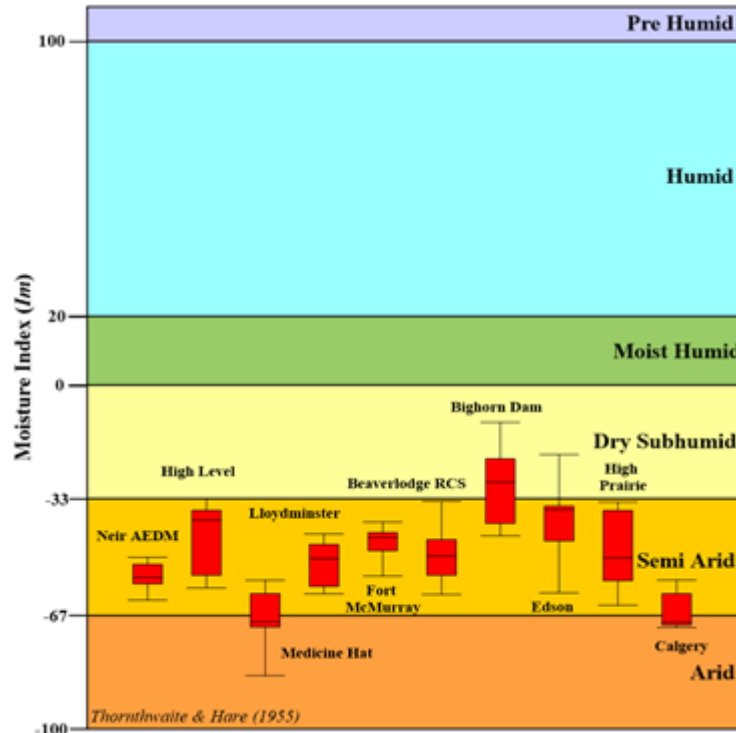
Fig. 3.9: Climate classification for various locations in the province of Alberta

3.5 Numerical Modeling

Numerical simulations were carried out using Hydrus-1D version 4.16 (Šimunek et al., 2013) to estimate the effect of climate type and soil texture on the soil water and solute transport in the unsaturated zone. A one-dimensional unsaturated flow and transport model with soil atmospheric boundary condition (BC) was used for the simulations. The model is capable of estimating the water balance at the ground surface by estimating the actual evaporation (*AE*) based on prevailing climate conditions and transient soil moisture conditions. The model was used to simulate different climate types by using the compiled historical climate datasets.

For the analysis, two different soil types (sand and clay) were considered. The soil hydraulic properties of selected soil types were taken from the soil catalog available in Hydrus-1D. Table 3.4 shows van Genutchen parameters for the hydraulic functions. Root water uptake and freezing-thawing processes were not taken in consideration for this study as the simulations were run for active period only.

Table 3.4: Hydraulic soil properties available in Hydrus-1D

Material	θ_r (-)	θ_s (-)	Alpha (1/mm)	n (-)	K_s (mm/h)	l (-)
Sand	0.045	0.43	0.0145	2.68	297	0.5
Clay	0.068	0.38	0.0008	1.09	2	0.5

The model comprised of a one dimensional (1D) soil column of 3 m depth. This was in line with recommendation by Shah et al. (2007) for shallow-rooted vegetation covers (e.g. shrubs and grasses). The soil column was divided in 300 elements to provide suitable discretization for the analysis. In all simulations, an atmospheric boundary condition with surface runoff was imposed at the top of the column. The top boundary comprised of the 9 year daily climate records. A zero-gradient water flow boundary condition was set at the bottom of the column to simulate free drainage: this is representative of deep groundwater table conditions (Šimunek et al., 2013).

For the simulation of the solute transport a non-reactive solute input source equal to 1 mg/L was assumed to be located between 1.0 m and 1.5 m depth (Fig. 3.10). A concentration flux boundary condition (BC) was used as the upper boundary and zero concentration gradient was assumed as the lower boundary condition. The liquid phase concentration was set as solute transport initial condition. The period of analysis

considered for the salt transport simulation matched with the compiled nine-year continuous climate data.

For coarse materials, the solute migrated through the domain in less than 3 years. However, for fine material, the solute movement was substantially slower than in coarse material. Therefore, simulations were run for 18-year period. In order to achieve this, the simulated concentration through the domain at the end of the nine year period was assumed to be the initial concentration for the next 9-year period. The meteorological input data used in the first set of simulation was repeated for the second set of simulations.
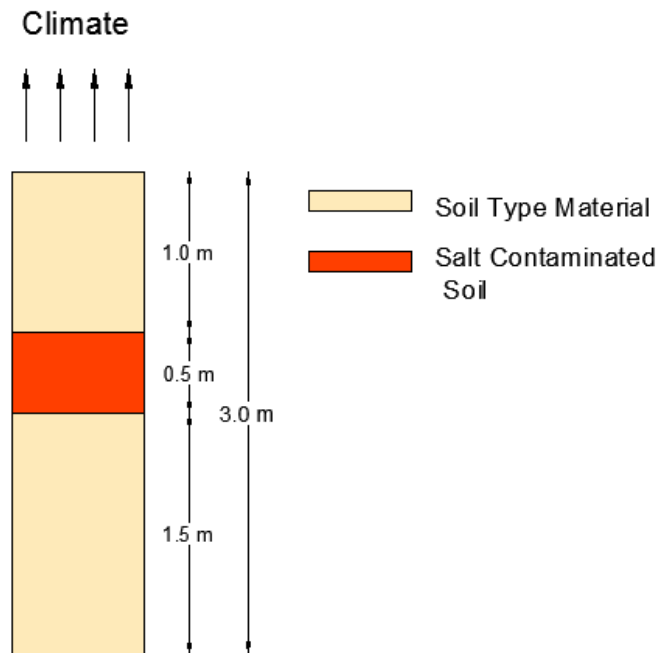
Fig. 3.10: 1D soil column of 3m depth comprised of atmospheric boundary condition with surface layer at the top and free drainage water flow at the bottom

In order to assess the effect of temporal resolution of meteorological data, simulations were run with meteorological data at sub daily resolutions. The measured climate data was only available on a daily resolution. Thus, daily data was converted into sub data based on a methodology adopted by Gladnyeva and Saifadeen (2012). A set of Matlab codes were written to convert calculated daily climate input records to a higher time resolution data (Appendix C1 and C2). Using the above-mentioned approach, daily precipitation values were increased in intensity to occur over 12, 6, 4, 2, and 1 hour periods. Daily potential evaporation records were converted into 12 hour time intervals assuming that there is no ET during the night, 18:00 until 06:00. The analysis of the temporal variability was carried out only on extreme climate conditions. For example, the Bighorn region (located in the Rocky Mountains) was considered as wet climatic conditions; whereas, the Calgary region was considered as dry climatic condition.

A second set of models were simulated to evaluate the effect of temporal variability based on two potential climatological scenarios. In the first set, precipitation records overlap with peak potential evaporation hours; whereas, in the second set, the precipitation does not overlap evaporation (Fig. 3.11). In both dataset, the potential evaporation (*PE*) data was assumed to extend along the diurnal hours (from 6:00 to 18:00). In all cases of precipitation events during peak evaporation hours, the modeling time variable boundary condition was set to begin at 06:00, and it was extended consistently with the temporal resolution of precipitation. Precipitation records set during off evaporation hours begin right after the end of the evaporation process, that is, from 18:00 onward.
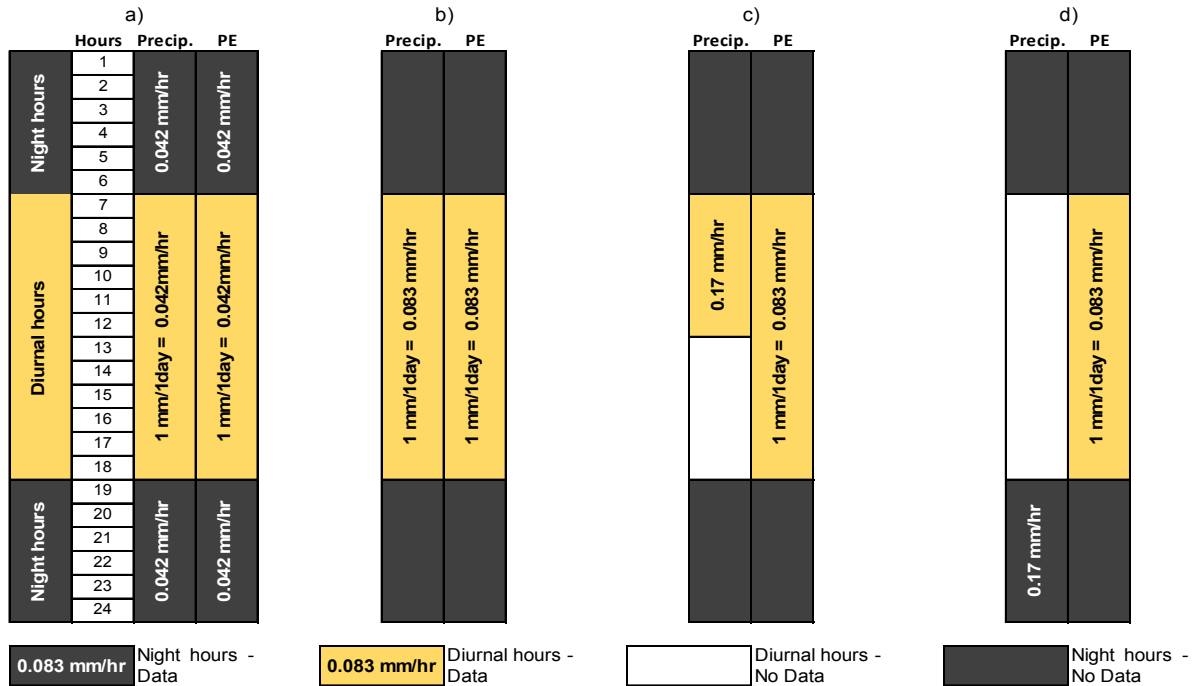
Fig. 3.11: Graphical representation of climate input data used in Hydrus-1D. a) assuming a meteorological event when *P* and *PE* = 1 mm/day or 0.083 mm/hr.; b) Temporal variation for 12-hour resolution; c) Temporal variation for 6-hour resolution; d) Temporal variation for 6-hour resolution during off diurnal evaporation hours.

The effect of shallow groundwater on water and salt dynamics was also investigated using a different set of simulations. Two different water table settings were selected for this analysis (Fig. 3.12). In the first condition, the water table was set at 3-meter depth (lower boundary condition); whereas, in the second modeling conditions the water table was set at 1-meter depth (right at the top of the contaminant source). These sets of simulations were carried out using daily and 1-hour resolution of precipitation data. The simulations were run with coarse and fine-grained soils in arid and sub-humid climatic conditions. In all simulations, an atmospheric boundary condition with surface runoff was imposed at the top of the column. A constant pressure head boundary condition was set at 3 and 1-meter depth to simulate the water table setting.
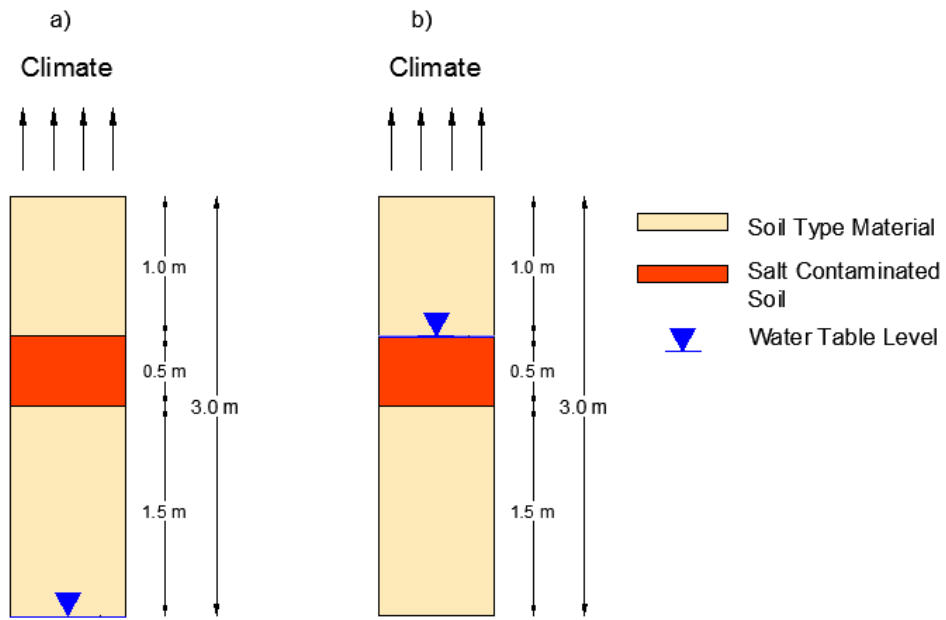
Fig. 3.12: One dimensional soil column of 3m depth consisted of a) water table at the bottom, and b) water table at 1.0 m depth.

Chapter 4

Results and Discussion

In this chapter, important findings from numerical simulation results are presented and discussed. Simulations were run for three different scenarios. These scenarios quantify the effect of climate type and soil texture on water and salt dynamics in variably saturated environments. The first set of simulations focused on the vertical salt migration in coarse and fine-grained soils for different climatological regimes in deep water table settings. For these simulations, the climate data used was of daily resolution.

The second set of simulations quantified the effect of temporal variability of meteorological input data on soil water and salt transport dynamics. Firstly, the intensity of precipitation data given in daily resolution was increased at 1 and 2 hour time intervals. For all of these simulations the distribution of evaporation was assumed to follow the diurnal cycle and precipitation was assumed to occur during the peak evaporation hours. A different set of simulations were then run for the above-mentioned precipitation intensities but with the assumption that precipitation events happen off peak evaporation hours. As before, the distribution of evaporation was assumed to follow diurnal cycle.

The third set of simulations investigated the soil water and salt dynamics in shallow water table settings. The intent of these simulations was to assess the interaction between shallow groundwater table and the atmosphere and its impact on

vertical solute transport. These interactions were investigated using hourly and daily resolution precipitation climate data.

4.1 Effect of climate type on soil water and salt dynamics in variably saturated soils

Compiled meteorological data from different natural regions of Alberta was used in numerical simulations. These simulations were carried out using Hydrus-1D (version 4.16.0110). The simulations were carried out with the purpose of estimating water fluxes at ground surface and solute transport in variably saturated soil profiles. Based on the climate classification of various regions in Alberta as described in previous chapter, the following selections were made. For the study of the dry climatic condition, the climate data from Calgary region was used. The analysis of semi-arid climatic condition (or neutral climatic condition) was carried out using climate data from Lloydminster region. The Bighorn region was chosen for the analysis of the sub-humid climate (or wet climate condition). It should be noted that all compiled climate data was available on a daily resolution.

4.1.1 Arid climatic condition

Calgary lies on the border of two ecoclimatic regions: Canadian Shield and Grassland in southern Alberta (ESRD, 2013). These regions are characterised as having meteorological events of low precipitation values and high evaporation rates.

The climatic data compiled for this region yielded a yearly average value of 293 mm for precipitation, and a yearly potential evaporation average of 795 mm. The reported yearly precipitation average of 326 mm from [Environment Canada (2017)](); based on 30-years period (1981-2010)) was found to be slightly higher than the compiled value. The compiled average yearly PE value correlated well with the reported values between 760 and 850 mm ([ESRD, 2013]()).

The results from the simulations are presented in different ways starting from water balance at ground surface. Figure 4.1 summarizes the water balance at the ground surface for simulations run with fine and coarse soil hydraulic properties. The results presented are cumulative values over 9 water years. The quantities that appear as negative values represent water leaving the system or water loss, while positive values represent water entering the system or water gain conditions. Similarly, a negative value of net infiltration *(NI)* would imply net water loss conditions and vice versa. It should be noted that *NI* is estimated as the difference of *P* and sum of *AE* and *RO*. Review for Fig. 4.1 indicates that for simulations using fine and coarse grained soil hydraulic properties there was no runoff generated. This is an expected result. The maximum intensity precipitation recorded was 0.75 mm/hour which is less than the K_s values of 297 mm/hour and 2 mm/hour for coarse and fine-grained soil materials, respectively.

The *AE* values for coarse and fine grained materials show significant difference. The cumulative *AE* values of fine-grained materials (-2639 mm, dotted purple line) are approximately two times higher than the *AE* of coarse grained materials (-1447 mm,

continuous purple line). This is attributed to fine material's lower hydraulic conductivity value and higher water retention when compared to coarse-grained material.
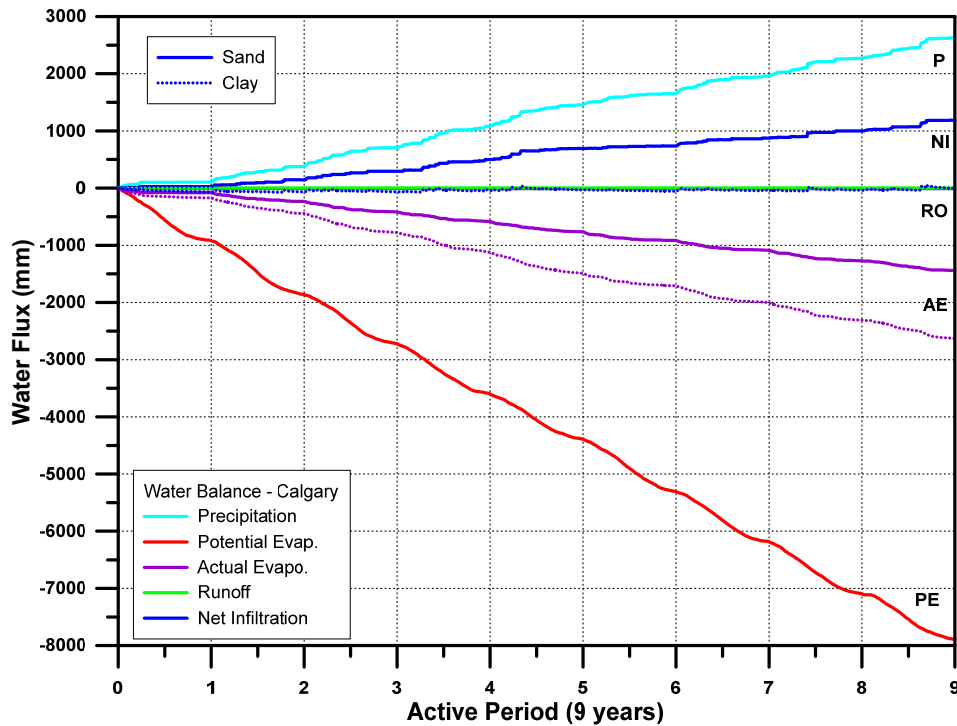
Fig. 4.1: Estimated water balance at the ground surface in arid climatic conditions

The fine material tends to hold more water near the surface soil layer owing to its higher retention capacity and lower hydraulic conductivity resulting in higher *AE*. The difference in *AE* values for fine grained materials and coarse grained materials result in different water balance conditions at the ground surface. From the *NI* plot for coarse material it can be observed that there is water gain of 1187 mm over the 9 year period. This amount is approximately 50% of the average yearly precipitation. These observations lead one to conclude that for coarse material there would be significant amount of downward water movement in the system as 50 percent of the meteoric water makes it way into the soil profile.

On the other hand, the *NI* plot for fine-grained soil materials indicates that there is minimal or no water loss or gain at the ground surface. This indicates that for the fine-grained soil materials most of the meteoric water will be lost by evaporation at the ground surface. This observation, and considering the fact that the system is a representation of deep groundwater table condition, it can be concluded that there probably would be no appreciable downward or upward water movement in the system.

Figure 4.2 shows results of solute displacement in coarse and fine-grained materials over the simulated period. These concentration contours provide vertical distribution of solute over a period of three years for coarse-grained material and 18-year period for the fine-grained material. These different time periods relate to the time taken by the solute to reach any of the model boundaries. The 18-years simulation results for the fine-grained material are from two different nine-year simulations. The 2nd nine-year simulation used the moisture and concentration distribution over the domain at the end of first simulation. Same 9-year climate data set was used for both simulations.

Two horizontal black continuous lines have been drawn on Fig. 4.2 to represent the initial location of the salt. Graphical results indicate that soil texture had a strong effect on the rate and direction of the salt movement. For instance, in homogenous coarse-grained soil material, the direction of the salt displacement is exclusively downwards. The estimated time for the infiltrating water to fully drain the initial solute concentration appears to be slightly less than 2.4 years. The salt movement depicted in this figure is consistent with the water balance results presented previously.
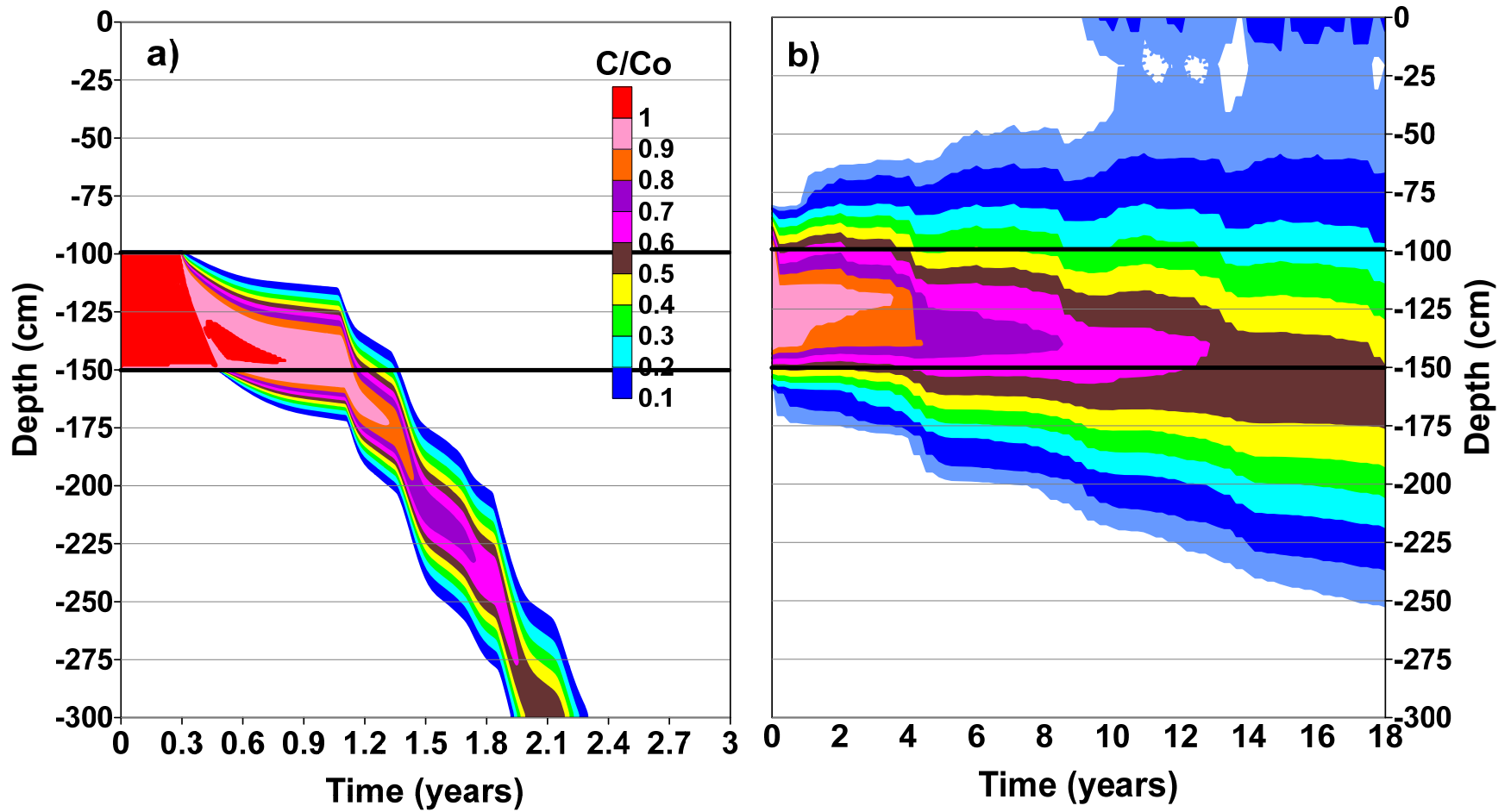
Fig 4.2: Vertical solute displacement over time in arid climatic conditions
a) coarse-grained and *b)* fine-grained soil materials

In Fig. 4.1, it was shown that for coarse-grained soil materials almost half of the meteoric water makes its way into the soil profile overcoming evaporation. In addition, it was concluded that the water movement in the system will be predominantly downwards. Therefore, the salt movement results for coarse-grained material shown in Fig. 4.2a are consistent with anticipated behaviour. The result also clearly indicate that even for dryer climatic conditions there is a potential for the salt to migrate downwards over a short period of time to potentially impact deeper groundwater resources.

Results from simulation run with fine soil hydraulic properties illustrate the spreading of solute in both upward and downward directions (Fig. 4.2b). There appears to slightly higher affinity for the solute to move in downward direction. These observations are consistent with the water balance results for fine-grained soil profile. As mentioned above, little or no water loss or gain was estimated at the ground surface for the fine-grained material. Therefore, the infiltration of meteoric water in the soil domain was expected to be minimal. However, any water movement in the system is expected to be downward. Upward movement, if any would have been attributed to capillary rise from groundwater which in this case is very deep. Therefore, it can be concluded that in fine-grained materials, the vertical solute displacement appears to be a diffusion dominated transport process. The difference in slightly more downward migration could be due to slight downward advection in the system owing to gravity drainage. However, the results for the fine-grained material also clearly indicate that there is a potential for the salt to migrate in to the root zone.

4.1.2 Semi-arid climatic condition

Lloydminster is located in east-central Alberta. Its climate is characterized as humid continental corresponding to Boreal ecoclimatic natural region (Downing and Pettapiece, 2006). Compiled meteorological data for Lloydminster yielded yearly average precipitation and potential evaporation values of 333 mm and 668 mm. These values correlate well with the reported yearly average values of 317 mm for precipitation (Environment Canada, 2017; based on 30-years period (1981-2010)) and 675 to 700 mm for *PE* (ESRD, 2013).

The results for water balance at the ground surface for coarse and fine-grained materials under semi-arid climatic conditions are shown in Fig. 4.3. These results appear to be quite similar to those for arid climatic conditions presented in Fig. 4.1. For instance, results in Fig. 4.3, once again show no runoff for either fine or coarse-grained materials. The maximum precipitation intensity for semi-arid climate was 2.6 mm/hour based on daily average data. This value is two orders of magnitude lower than the K_s of the coarse-grained material and only 0.6 mm/hour higher than the K_s of the fine-grained material. However, there was only 1 precipitation event greater than 2.0 mm/hour during the period of analysis. Therefore, the runoff was expected to be negligible.

The cumulative *AE* value of fine-grained soil material over 9 years for semi-arid climatic conditions (-3286 mm, dotted purple line) was approximately two times higher than the *AE* of coarse-grained materials (-1829 mm, continuous purple line). The difference between the values is due to difference in conductivity and retention

properties of the coarse and fine-grained soil materials as explained in the previous section.

The *NI* values for semi-arid climatic conditions plotted in Fig. 4.3 indicate net water gain conditions for coarse-grained material and near neutral condition for fine-grained materials. These values are higher than those for arid climatic conditions owing to larger precipitation events, and lower potential and actual evaporation. For coarse-grained material approximately 50% of meteoric water makes its way in the soil profile. In comparison with arid conditions, although it is similar percentage of meteoric water, however, it accounts for approximately 25% more water influx at the ground surface ($NI_{semi-arid}/NI_{arid}$ = 1.25). This observation leads one to conclude that the downward movement in coarse-grained material could potentially be higher than that in arid climatic condition.

For fine-grained material only 1.2 percent of the meteoric water made its way into the soil profile. Although it is a quite small number, however, in comparison with arid conditions (NI/P = 0.2%), it can be expected that on a relative basis there could be more downward water movement.

Figure 4.4 shows the migration of solute under semi-arid climatic conditions in coarse and fine-grained soil materials. The results are consistent with the water balance conditions for this region. It can be observed that there is downward migration of salt for both coarse and fine-grained soils, which is result of water gain conditions at the ground surface. In coarse grained material, the higher amount of infiltrating water (NI = 1498 mm) resulted in faster downward solute displacement throughout the soil domain.
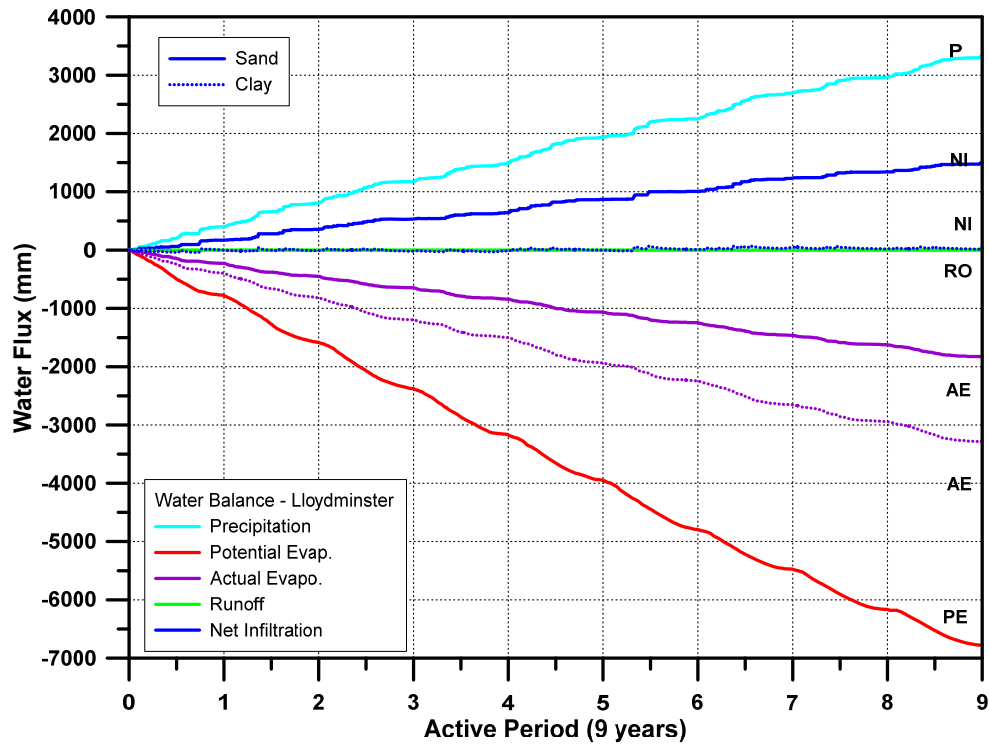
Fig. 4.3: Estimated water balance at the ground surface in semi-arid climatic conditions

In coarse-grained material, the estimated time to drain 50% of the initial concentration out of the domain was less than one year. The downward solute displacement resulted in a seepage rate of 150 cm/year. In comparison to arid conditions, the rate of downward migration in semi-arid conditions is much faster. The total time to flush out all the solute from the soil domain reduces to 1.4 years from 2.4 years. This can partially be explained by the fact that more water flux at the ground surface was making its way into the soil domain, when compared to arid conditions. For semi-arid conditions, the downward solute displacement in fine-grained soils was much slower than that in coarse-grained soils.
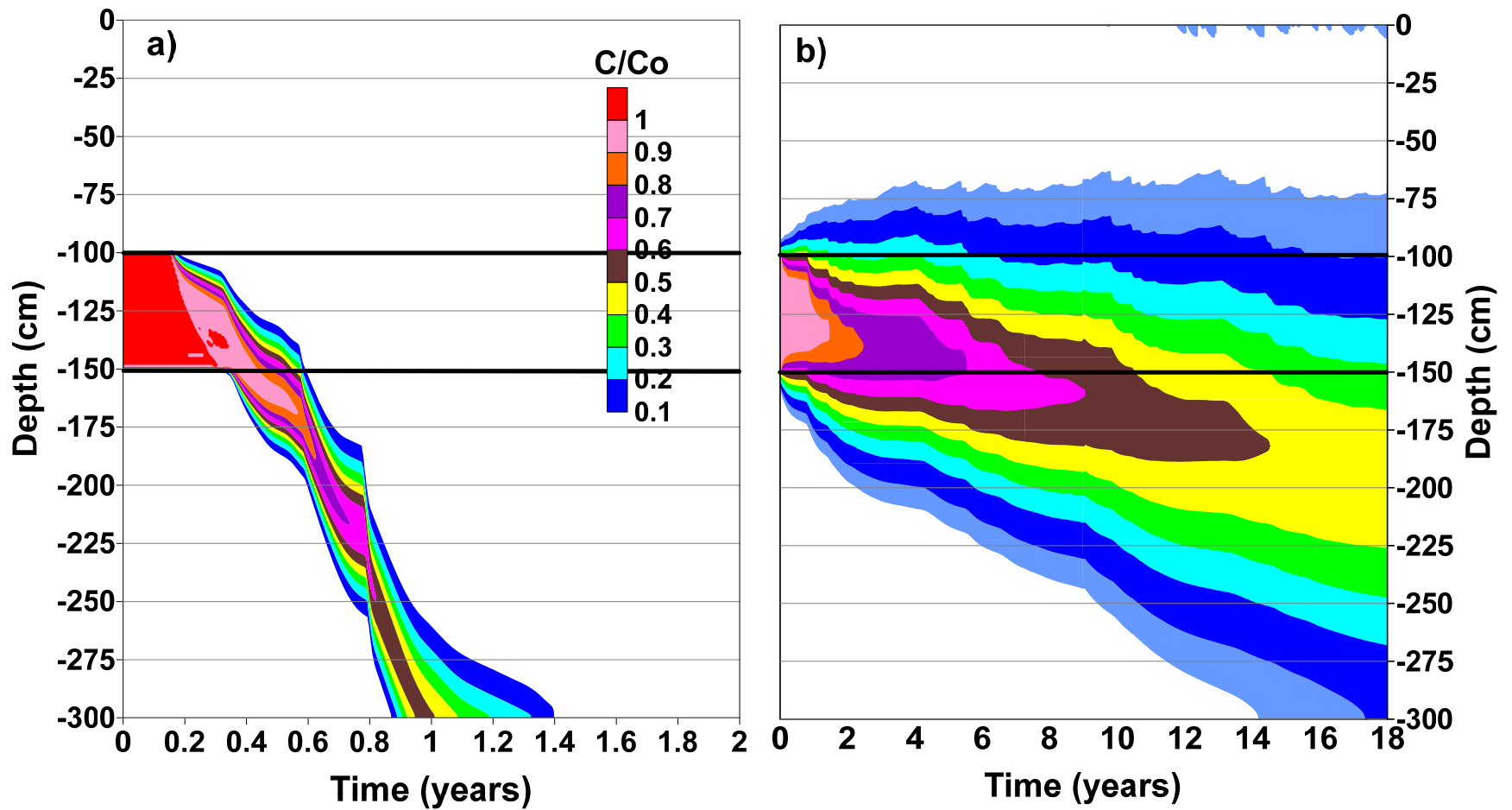
Fig 4.4: Vertical solute displacement over time in semi-arid climatic conditions
a) coarse-grained and *b)* fine-grained soil materials

For instance, it took over 14 years for the 5% contour curve to reach the bottom of the soil column. In terms of solute displacement rate, the 50% of the initial concentration moved from the source to the bottom of the soil column at an approximated seepage rate of 12.9 cm/year. Important to note is that in semi-arid climatic conditions the vertical solute displacement shows a downward trend in comparison with arid climatic conditions where up to 18 years none of the solute reached the bottom boundary.

4.1.3 Dry sub-humid climatic condition

The Bighorn region is located in the Rocky Mountain natural region at the border between the provinces of British Columbia and Alberta, Canada. This region is characterized as having cold winters and very short cool summer (Downing and Pettapiece, 2006). Compiled meteorological data for Bighorn region yielded annual average P and PE values of 408 mm and 588 mm, respectively. The compiled annual average P value is higher with the reported annual precipitation average value of 334 mm (Environment Canada, 2017); based on 30-years period (1981-2010). However, the compiled annual average evaporation value correlate well with the reported evaporation rates varying between 500 mm to 600 mm (Den Hartog and Ferguson, 1978); based on 10-years period (1957-1966).

Fig. 4.5 shows the water balance at ground surface for sub-humid conditions. Review of this figure indicates that similar to arid and semi-arid regions, there is no runoff for either coarse or fine-grained materials. The maximum precipitation intensity

for this region's climate was 2.9 mm/hour based on daily average data. This value is two orders of magnitude lower than the K_s of the coarse-grained material ($K_s = 297$ mm/h) and only 0.9 mm/hour higher than the K_s of the fine-grained material ($K_s = 2.0$ mm/h). However, this event was recorded to occur only once over the 9 year period considered in this study.
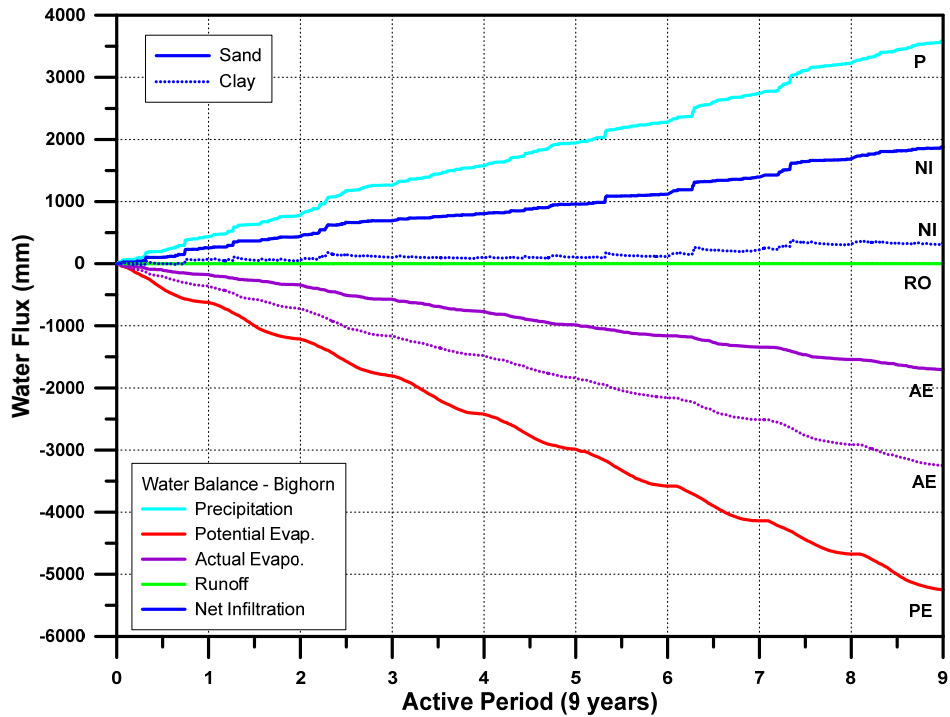
Fig. 4.5: Estimated water balance at the ground surface in dry sub-humid climatic conditions

The *NI* values for dry sub-humid climatic conditions plotted in Fig. 4.5 show the highest net water gain for both coarse and fine-grained materials for the three different climatic conditions considered in this study. For coarse-grained material more than half of meteoric water would enter in the soil domain based on the calculated net infiltration-precipitation ratio (*NI/P = 54%*). This water gain is higher when compared to semi-arid climatic conditions (*NI$_{dry-subhumid}$/NI$_{semi-arid}$* = 1.32) and arid climatic conditions (*NI$_{dry-subhumid}$/NI$_{arid}$* = 1.66). This observation leads one to conclude that the downward solute

displacement could be faster than the semi-arid climatic conditions and much faster than that in arid climatic conditions.

For fine-grained material, the cumulative ratio *NI/P* indicates that approximately 10% of meteoric water would overcome evaporation. This ratio turned out to be greater than that of semi-arid climatic conditions (*NI/P* = 1.2%). This is consistent with results shown in Fig. 4.3 and 4.5, where the total cumulative precipitation value (*P*) for dry sub-humid climatic condition is higher than the semi-arid climatic condition (3,680 mm and 3,326 mm, respectively).

Results from dry sub-humid climatic conditions show similar trend as described in previous climatic conditions. Review of Fig. 4.5 indicates a large difference between the *AE* values for coarse and fine-grained materials. The computed total cumulative *PE* value in dry sub-humid climatic conditions (5,300 mm) is lower than those from Calgary and Lloydminster regions (6,687 mm and 7,953 mm, respectively). The cumulative *AE/PE* ratio from fine-grained soil material (61%) is approximately 100% higher than the *AE/PE* ratio of coarse-grained material (32%). As mentioned in previous sections, the difference can be attributed to fine material's lower hydraulic conductivity value and higher water retention properties compared to the coarse-grained material.

Review of Fig. 4.6 shows the fastest downward salt movement response in both coarse and fine-grained materials among the three different climatic conditions in the province of Alberta, Canada. For instance, in coarse grained material (4.6a), the estimated time for the salt to reach the bottom of the soil column was less than 1 year. The estimated salt movement indicates a seepage rate of 374 cm/year. It is important to

note the rapid downward salt displacement occurred throughout the first water year of analysis which is in line with the meteorological data behaviour as explained before. This can also indicate a higher risk of aquifer contamination for natural areas having higher humid climatic conditions.

Figure 4.6b shows the salt displacement for fine-grained material in dry sub-humid climatic conditions. The results are consistent with the observations discussed in the water balance section. In this figure, it can be observed that the spreading of concentration contours extends beyond the limits of the 18-year of analysis. It is noted that the amount of the infiltrating water was no enough to drain the total mass of the contaminant out of the soil domain. In this graph, the 5% contour curve indicates the threshold of salt displacement located at the bottom of the soil column at the seven year. The estimated salt movement for the 5% concentration contour indicates a seepage rate of 44.7 cm/year.

Graphical results from selected ecoclimatic regions included in this research are shown in Appendices D.1 through D.7. These graphs have been grouped accordingly with the three main climate conditions based on the computed annual moisture index of the province of Alberta: sub-humid (Edson), semi-arid (High Level, Fort McMurray, Beaverlodge, High Prairie, Neir AEDM), and arid (Medicine Hat).
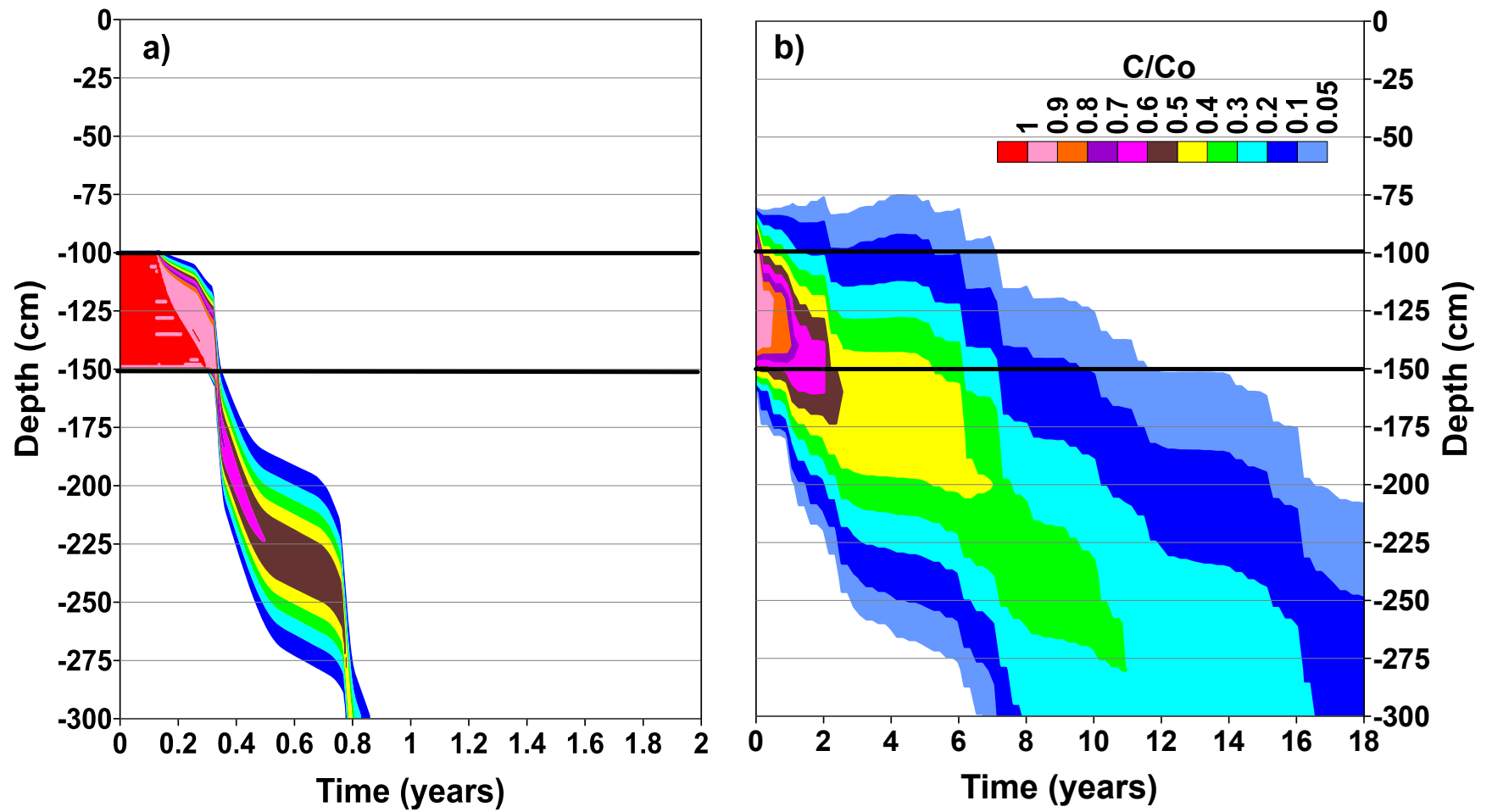
Fig. 4.6: Vertical solute displacement over time in dry sub-humid climatic conditions
a) coarse-grained and **b)** fine-grained soil materials

4.1.4 Detailed water balance assessment

Review of Figs. 4.1, 4.3, and 4.5 indicated a general trend of cumulative amount of water gain (*NI*) in the soil domain over the 9-year period. The water gain was larger for wetter climates, i.e. more precipitation and less evaporation. It was also observed that larger water gain conditions resulted in faster vertical solute transport. The following sections present water balance for the whole domain. First, an analysis of the input to the models in the form of precipitation and potential evaporation intensities is presented, followed by the detailed water balance. These results further enhance our understanding of the system in relation to various climate and soil types.

Figure 4.7 provides a graphical comparison of the precipitation records for the three different climatic conditions used in the analysis. Precipitation records from arid climatic conditions show the lowest precipitation occurred during the first year of analysis, amounting to only 108 mm. For the same first water year, the Lloydminster and Bighorn precipitation records show quite similar precipitation quantities with cumulative yearly values of 397 and 418 mm, respectively. The presentation of the records in this manner indicates that the precipitation intensities appear to be quite similar, at least from a visual perspective. Therefore, it is not possible to observe changes in the precipitation pattern that can potentially affect water and solute dynamics over time. In order to further analyze the precipitation intensities, occurrence of events of specific intensity are presented in the following section.

The occurrence of precipitation events was estimated and is plotted in Fig. 4.8. The plot indicates that the Bighorn region (dry sub-humid) clearly has higher occurrence

of larger precipitation events compared to Calgary (arid) and Lloydminster (semi-arid climatic conditions). It can also be observed that Calgary appears to have the highest occurrence of precipitation events less than 1mm. In general, it can be concluded that for the 9-year period considered in this study Bighorn appears to have higher occurrence of larger precipitation events, followed by Lloydminster and Calgary. It is important to note that for same precipitation quantity, a higher intensity event can result in faster solute transport. This is studied in detail in the section on effect of temporal variability of meteorological data on soil water and salt dynamics in the later sections.
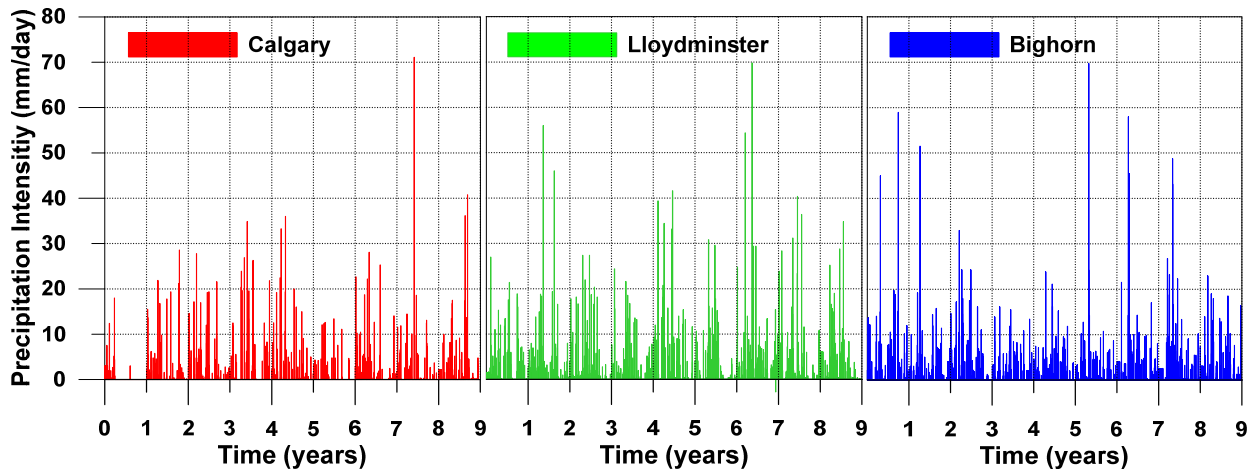
Figure 4.7: Calculated precipitation intensities over the 9-years period for three different climatic conditions in Alberta, Canada
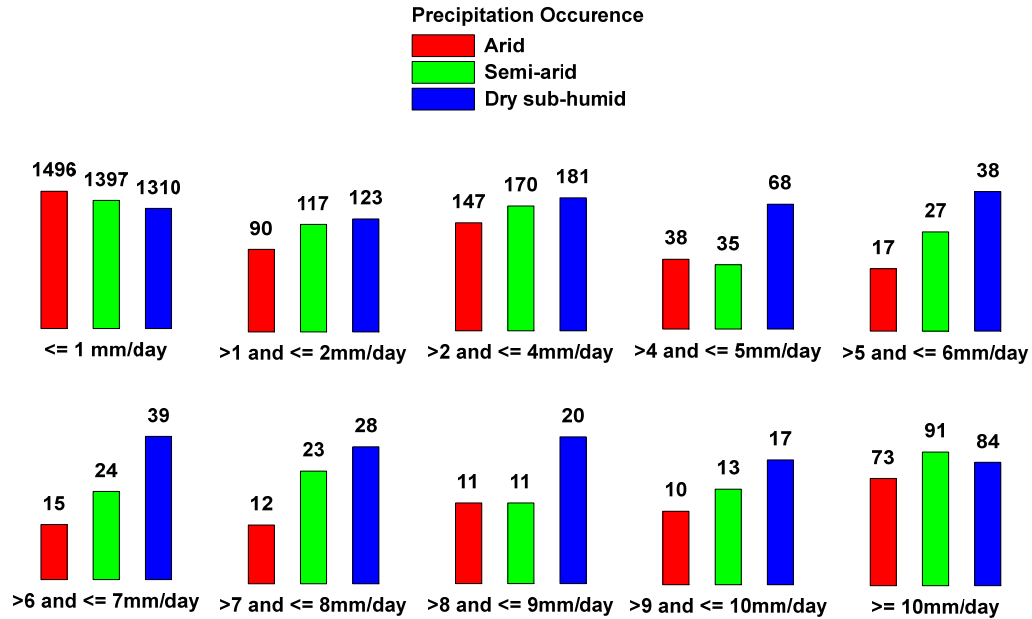
Fig. 4.8: Daily estimated of precipitation occurrence over the 9-year period for three different climatic conditions in Alberta, Canada

Figure 4.9 shows the statistical evaluation of the potential evaporation values for the three different climatic conditions in the form of Box and Whisker plots. Graphical results indicate that the highest median value is for the arid climatic condition (4.4 mm/day, marked by a horizontal line in the red box). Conversely, the Bighorn region (blue box) shows the lowest median value (2.9 mm/day). It can also be observed that for arid climatic conditions, *PE* values show much larger variation in comparison with the semi-arid and dry sub-humid climatic conditions (from 0.6 to 7.9, displayed with vertical lines). Review of this figure clearly indicates that the daily *PE* values for Calgary are highest followed by Lloydminster and Bighorn. This observation implies that over a given time period the water balance and associated water and solute transport could be different as a result of difference in quantity and distribution of *PE*.
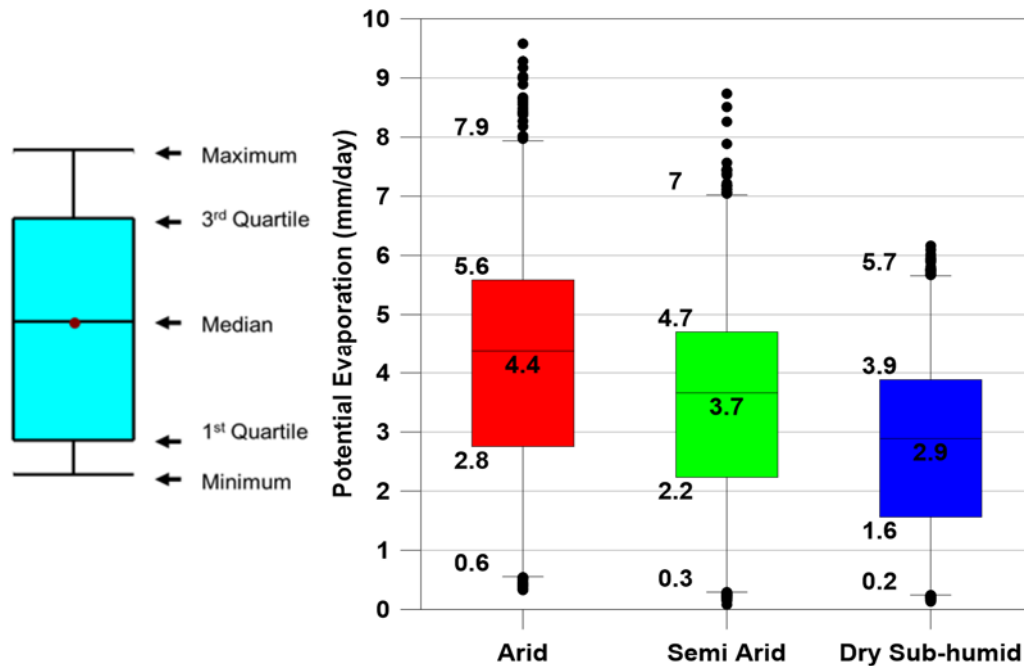
Fig. 4.9: Calculated daily potential evaporation box-whisker plots for three different climatic conditions in Alberta, Canada

Complete water balances for simulations run with coarse and fine soil hydraulic properties is presented in Fig. 4.10 and Fig. 4.11, respectively. Results presented in these figures are cumulative values over 9-year period. Similarly, as mentioned in section 4.1.1, the quantities that appear as negative values represent soil water leaving the system or water loss, while positive values represent water entering the system or water gain conditions. A negative water storage value *(S)* in the soil domain would imply soil water discharge and/or soil water storage decrease. A positive water storage value *(S)* represents soil water recharge. It should be noted that *S* is estimated at each simulated time step by integrating the volumetric water content over the soil domain.

Results from previous water balance at the ground surface for simulations run with coarse soil hydraulic properties indicate water gain (positive *NI* values) in the

following order: Calgary region = 1187 mm, Lloydminster region = 1498 mm, and Bighorn region = 1880 mm. this observation leads one to conclude that most of meteoric water that enters the soil domain exist the bottom boundary of the soil domain. Consistent with the *NI* values, the cumulative bottom flux (*BF*) values are highest for Bighorn followed by Lloydminster and Calgary, hence supporting the observation of fastest solute transport for the Bighorn region. The differences in the *NI* and *BF* values match closely with the change in water storage in the domain. Review of the change in water storage results also reveals that although the cumulative values at the end of 9-year period are quite similar for the three regions, however, the Bighorn region shows much higher saturation during the course of the simulations. Considering that the pore water velocity is also a function of saturation, this observation also supports the observation of faster transport.

Complete water balance results for fine-grained soil materials shown in Fig. 4.11 are in contrast to those for coarse-grained soils. It can be observed that the NI values for Bighorn (336 mm) and Lloydminster (41 mm) show water gain conditions, while for Calgary (-2 mm) water loss conditions. The total cumulative bottom flux values over the simulated period were: Calgary region = -101 mm, Lloydminster region = -146 and Bighorn region = -367 mm. These observations imply that overall for all three-climate types the soil domain goes through water loss. The water loss comes from the initial water storage and can be observed in the plots for change water storage. The difference between the amounts of water coming in and out of the system is consistent with the water storage values. Depletion of water storage implies that the saturation within the soil domain will be lower resulting in less advective transport.
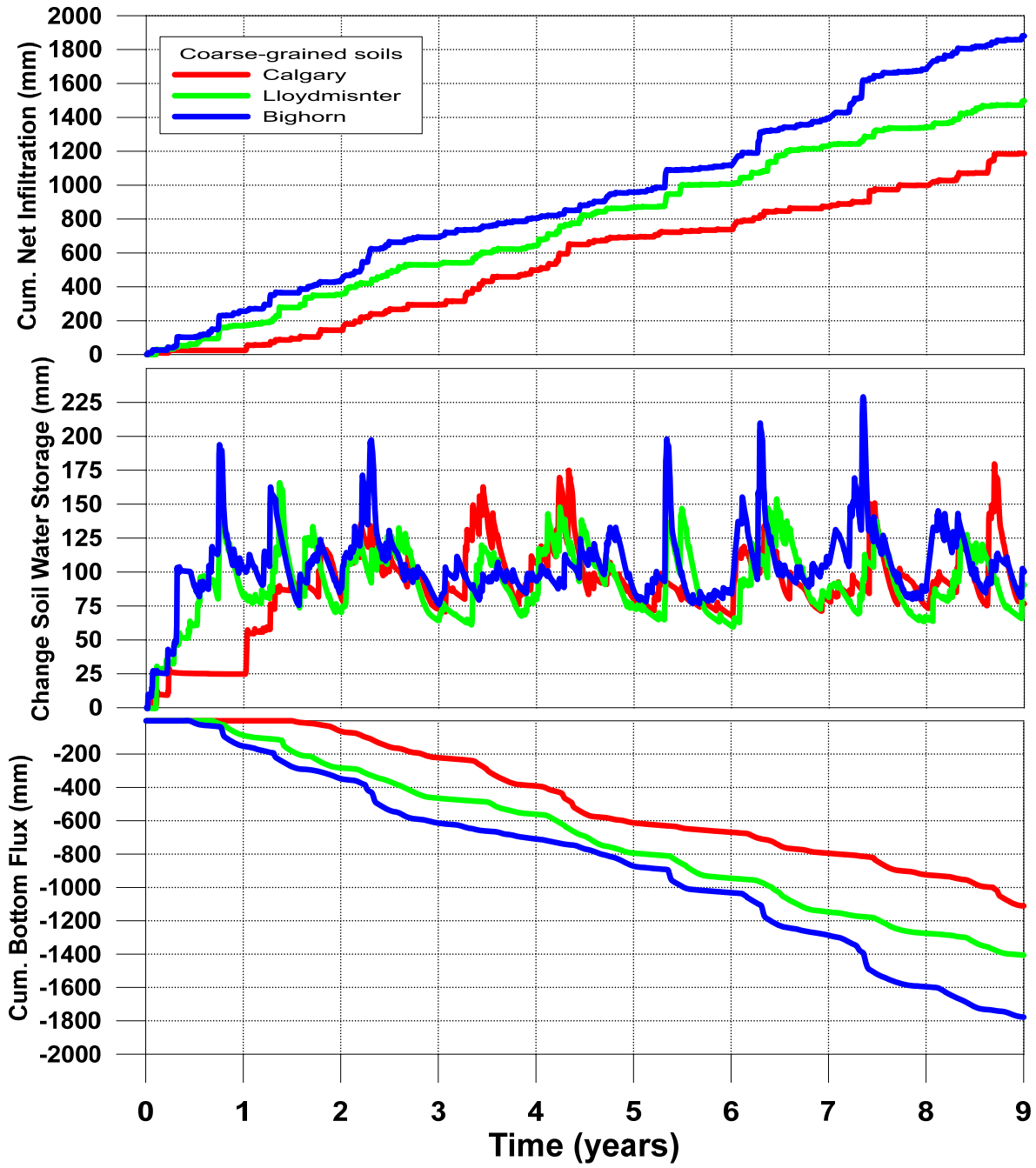
Fig. 4.10: Estimated water balance in the soil domain run with coarse-grained soil materials for three different climatic conditions of Alberta
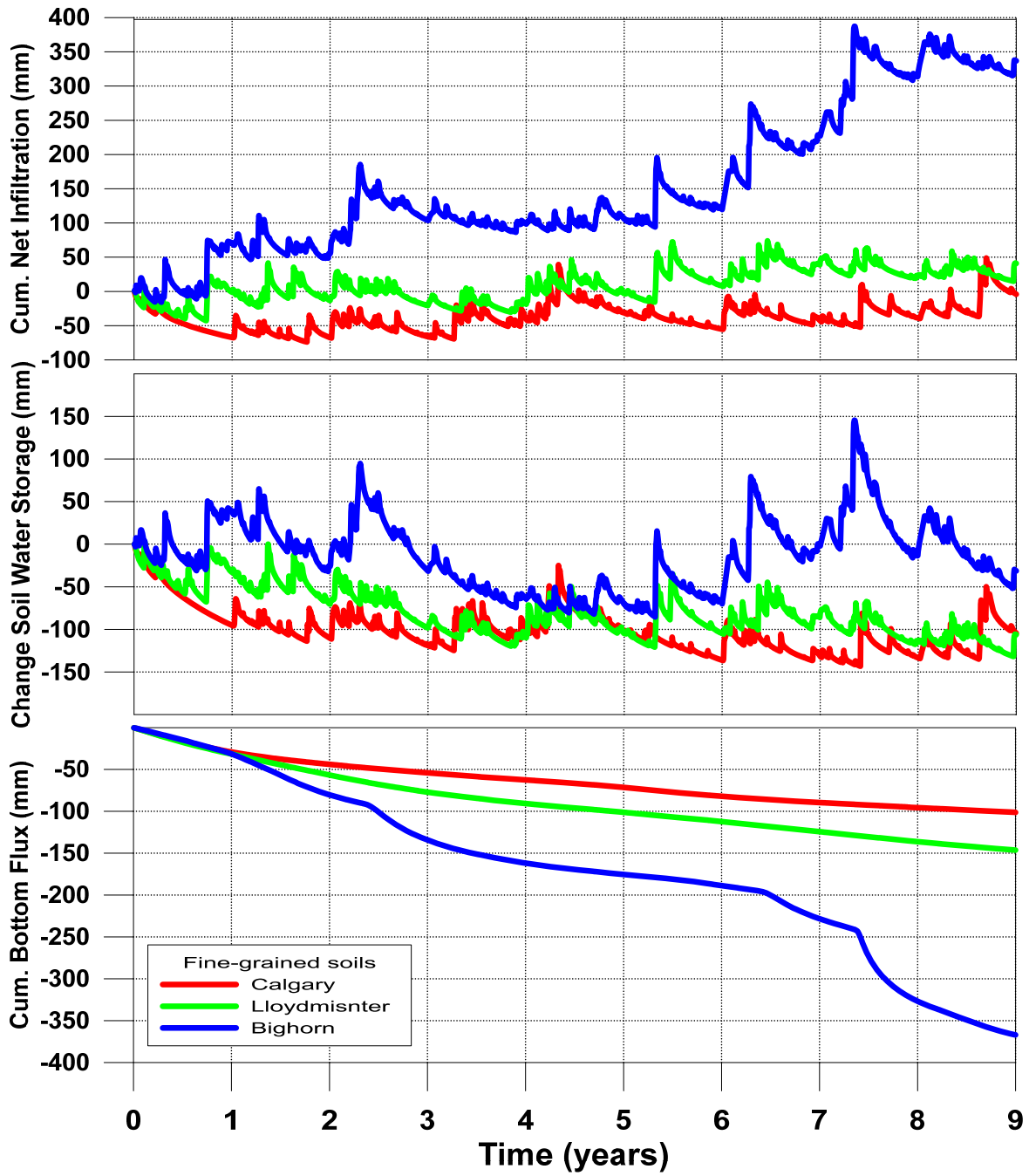
Fig. 4.11: Estimated water balance in the soil domain run with fine-grained soil materials for three different climatic conditions of Alberta

4.2 Effect of temporal variability of meteorological input data on soil water and salt dynamics during peak and off peak *PE* hours

The effect of temporal variability of meteorological input data on soil water and salt dynamics was quantified in variably saturated soil profiles under the influence of arid and dry sub-humid climatic conditions of Alberta. The new set of simulations was run for coarse and fine-grained soil materials in deep water table settings. Compiled daily precipitation data (*P*) was converted into 12, 6, 4, 2 and 1 hour resolution with the assumption that precipitation occurred in peak evaporation hours. Compiled daily *PE* values were converted into 12-hour resolution. For all these simulations the distribution of potential evaporation (PE) was assumed to follow the diurnal cycle (from 6:00am to 6:00pm). For the first set of simulations, the sub-daily precipitation events were assumed to occur during the peak evaporation period. For the second set of simulations, it was assumed that the sub-daily precipitation events occurred outside the peak evaporation period. Similar to daily climate data simulations, the new set of simulations were run using Hydrus-1D (version 4.16.0110). In the following sections, the results from these simulations are described and discussed in the following order: water balances at the ground surface, and vertical solute displacement in the soil domain.

4.2.1 Arid climatic condition - Calgary region

4.2.1.1 Water balance at ground surface for coarse and fine-grained soil materials

Figures 4.12 through 4.15 show estimated water balances at the ground surface from simulation run with coarse and fine soil hydraulic properties. These figures show cumulative *NI* and *AE* curves over the 9-year period as well as the cumulative values for the ninth year. The single year results are presented to provide a greater level of detail

for yearly cumulative totals of the *NI* and *AE*. The results for simulations run with the assumption that precipitation events occurred during peak evaporation hours are presented first (Figs. 4.12 and 4.13). The results from simulations with precipitation events assumed to occur outside the peak evaporation hours are presented next (Figs. 4.14 and 4.15). Following are some general observations from these results. More detailed analysis and comparison is presented in the following sections.

Generally, results from simulation run with coarse soil hydraulic properties indicate that for higher temporal resolution of precipitation data, *NI* values increases. The increase in *NI* values is consistent with the decrease in *AE* values. The review of results also indicates that the increase in *NI* values is higher for simulations run with the assumption that precipitation events happened outside the peak evaporations hours. Based on these observations it is expected that the solute transport is accelerated as the resolution of precipitation data increases. It is also expected, that solute transport could potentially be faster for a particular temporal resolution of precipitation event, if the event occurred outside the peak evaporations hours.

The increase in *NI* values with increasing precipitation intensies can be explained by the corresponding decrease in *AE*. For higher precipitation intensity events, same quantity of water becomes available in a shorter period of time. Evaporation on the other hand follows the diurnal daily cycle and the net result is that for periods where there is more water availability, evaporative demand remains the same. This results in less *AE* and increased *NI*. The same cogency also applies to the results for the simulations where precipitation events occur outside the peak

70

evaporation hours. As it relates to the availability of water during the time of low evaporative demand results in lower *AE* and higher NI values.

The results for simulations for fine-grained soil shown in Figures 4.14 and 4.15 show similar trends as observed for coarse-grained soil. It can be observed that with increase in temporal resolution of precipitation data, there is decrease in *AE* and associated increase in *NI*. It can also be observed that with higher temporal resolution of precipitation data, net water gain conditions at the ground surface are simulated. This is in contrast to the simulation runs with daily precipitation data which estimate net water loss conditions at the ground surface.

It should be noted that for fine grained material, the change in *NI* and *AE* values are less than those observed for coarse grained material. The primary reason for this is the difference in the hydraulic properties of the two materials. In comparison to coarse-grained material, the fine-grained material has higher retention and lower conduction. Therefore, for fine-grained materials the meteoritic water is held in the near surface soil layers longer as compared to coarse-grained materials. This results in higher actual evaporation for fine-grained materials than for coarse-grained material for same precipitation intensities.
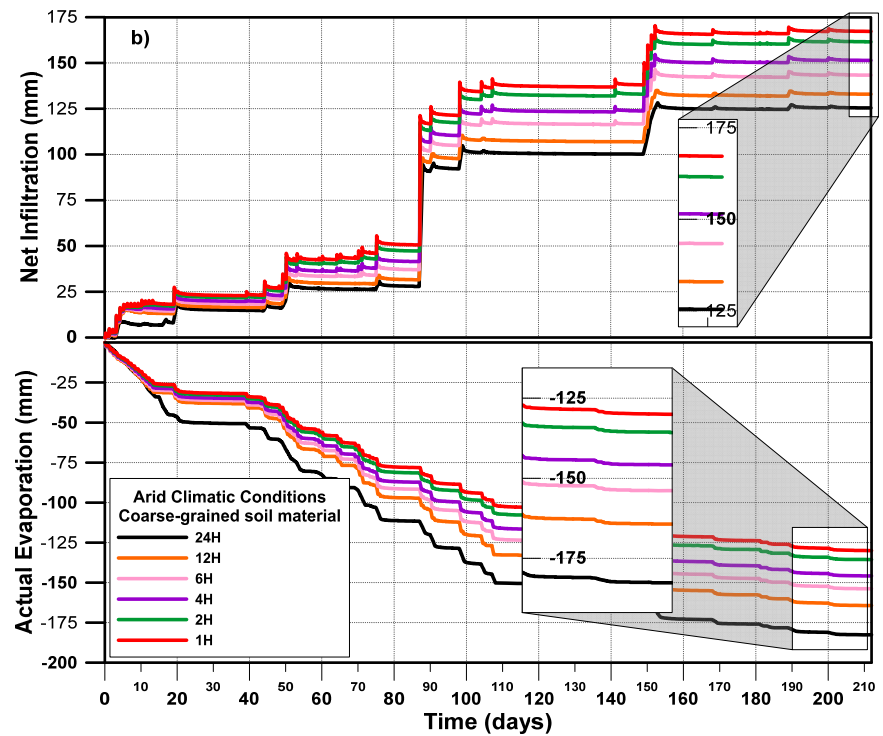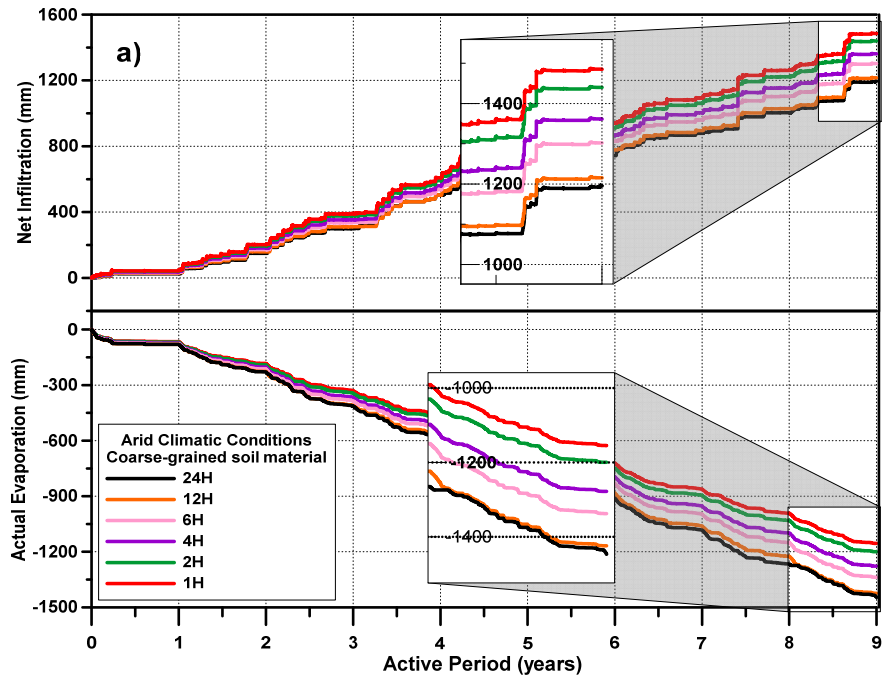
Fig. 4.12: Estimated water balance in arid climatic conditions assuming precipitation occurred during peak evaporation hours in coarse-grained soil materials
a) Cumulative totals over the 9-year period, *b)* cumulative totals over the 9th water year
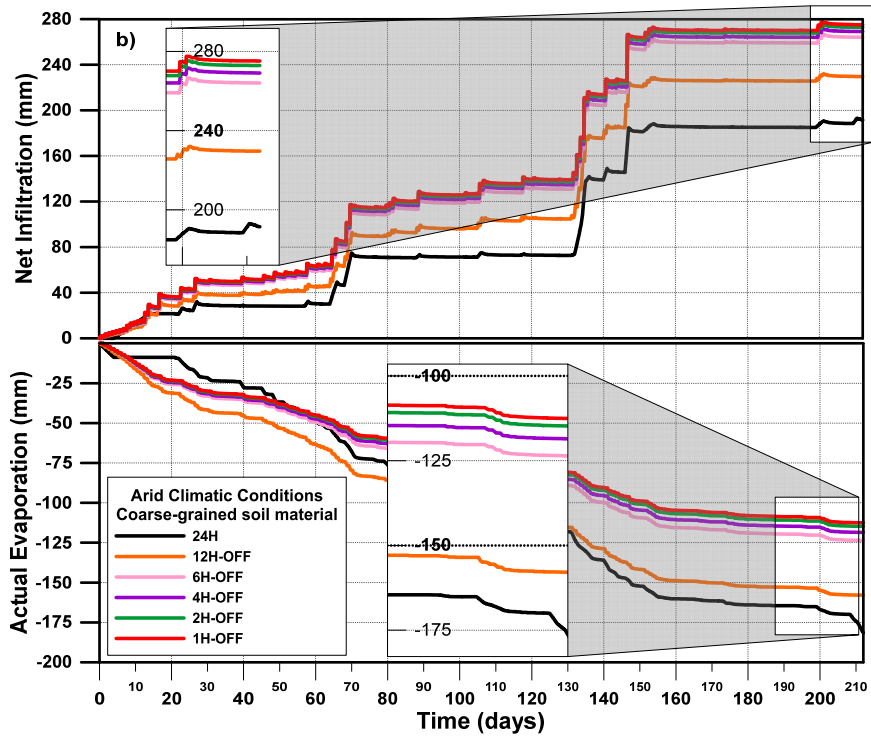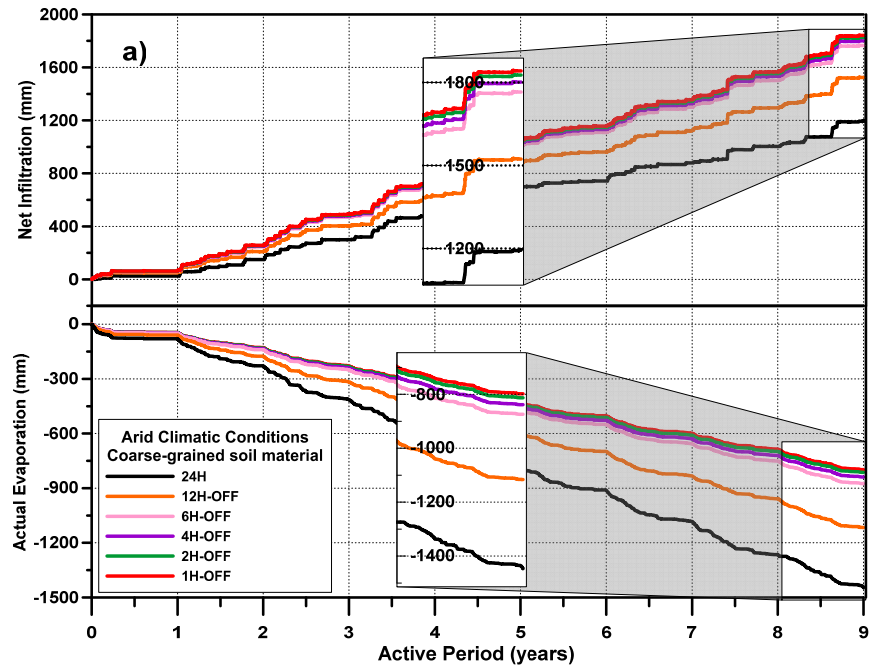
Fig. 4.13: Estimated water balance in arid climatic conditions assuming precipitation occurred during off-peak evaporation hours in coarse-grained soil materials
a) Cumulative totals over the 9-year period, *b)* cumulative totals over the 9th water year
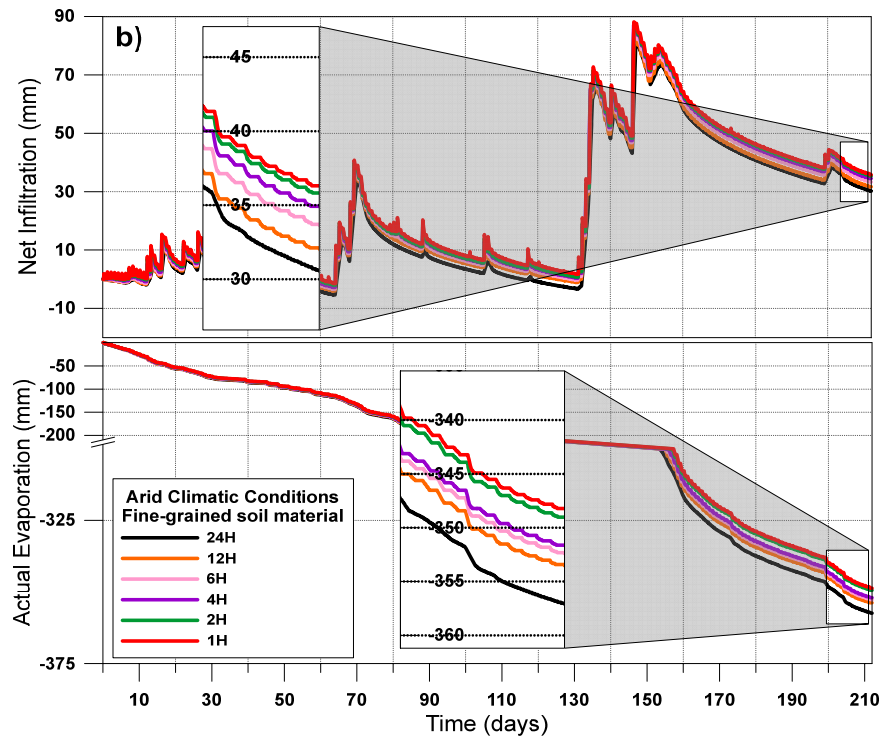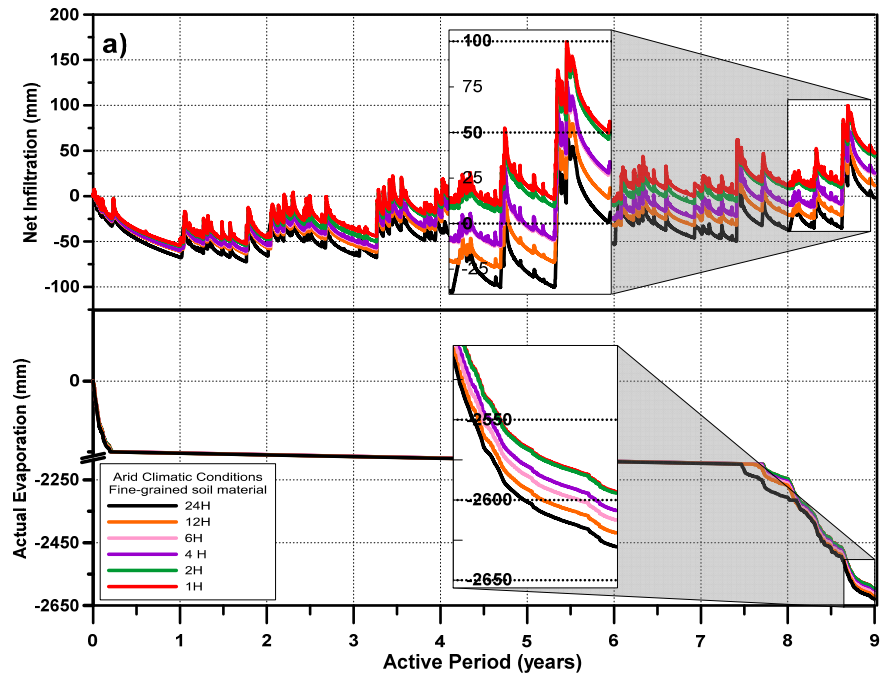
Fig. 4.14: Estimated water balance in arid climatic conditions assuming precipitation occurred during peak evaporation hours in fine-grained soil materials
a) Cumulative totals over the 9-year period, *b)* Cumulative totals over the 9th water year

74
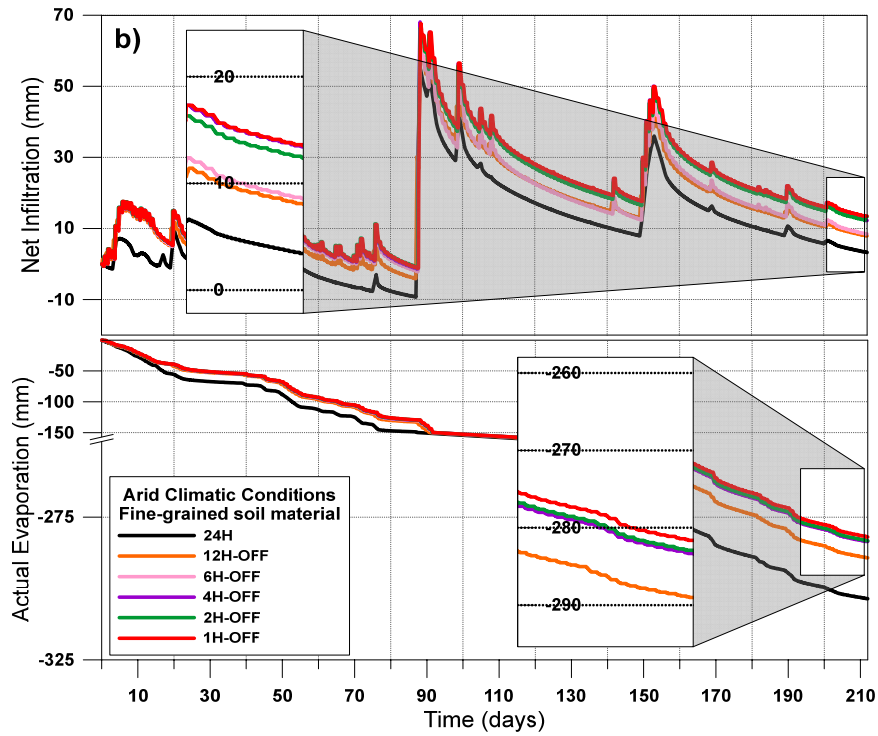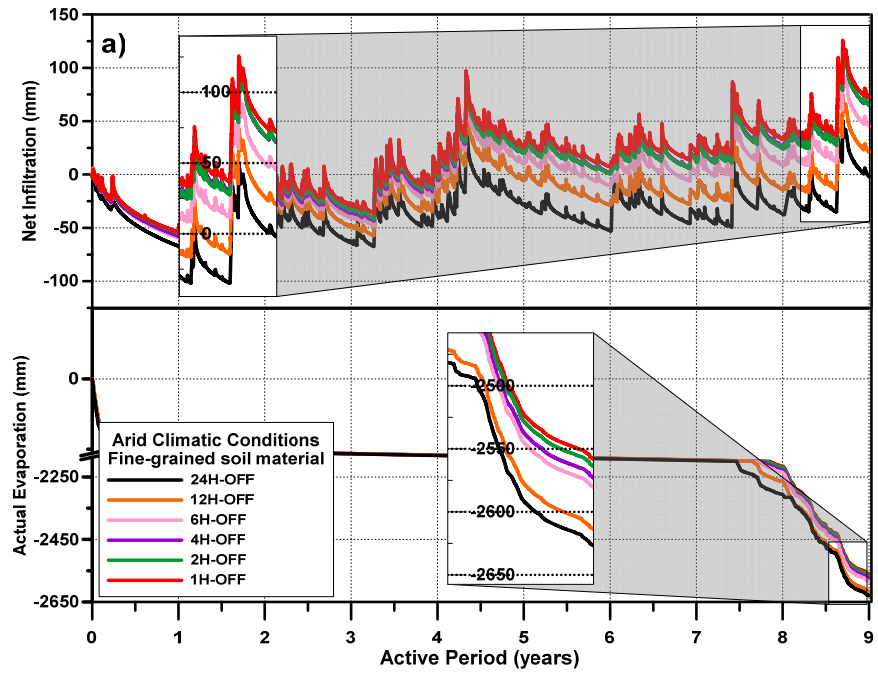
Fig. 4.15: Estimated water balance in arid climatic conditions assuming precipitation occurred during off-peak evaporation hours in fine-grained soil materials
a) Cumulative totals over the 9-year period, *b)* Cumulative totals over the 9th water year

Fig. 4.16 summarizes the cumulative *NI* and *AE* values at the end of the nine year period for both coarse and fine-grained materials. As mentioned previously all these simulations use same set of hourly meteorological input data with the assumption that precipitation occurrences happened either during or outside the peak evaporation hours. Presentation of results in this manner aids in making a comparison between soil types, precipitation intensities and time of occurrence of precipitation. Review of this figure shows that the decrease in *AE* with resulting increase in *NI* is consistent with increasing precipitation intensities. This observation is valid for both soil materials. However, differences in *AE* and *NI* appear to be an order of magnitude higher for coarse-grained material than for fine-grained material.

Review of Fig. 4.16 indicates that most significant increase in *NI* as result of change in resolution of precipitation intensity was 646 mm. This was estimated for 1-hour resolution precipitation events assumed to occur outside the peak hours of evaporation for coarse-grained material. This water gain equates to 25% increase over the calculated daily value and 14% increase in comparison with the 1-hour resolution precipitation events during peak evaporation hours. Similarly, results from simulations for fine-grained material, show that the highest water gain of 74 mm was estimated for 1-hour resolution precipitation events assumed to occur outside the peak hours of evaporation. As explained earlier that the differences in *AE* and *NI* values for coarse-grained material and fine-grained soil materials is mainly due to soil hydraulic properties. Fine-grained material's large water retention capacity and lower conductivity tends to impede the infiltrating water near the ground surface to later be released to the atmosphere by evaporation.
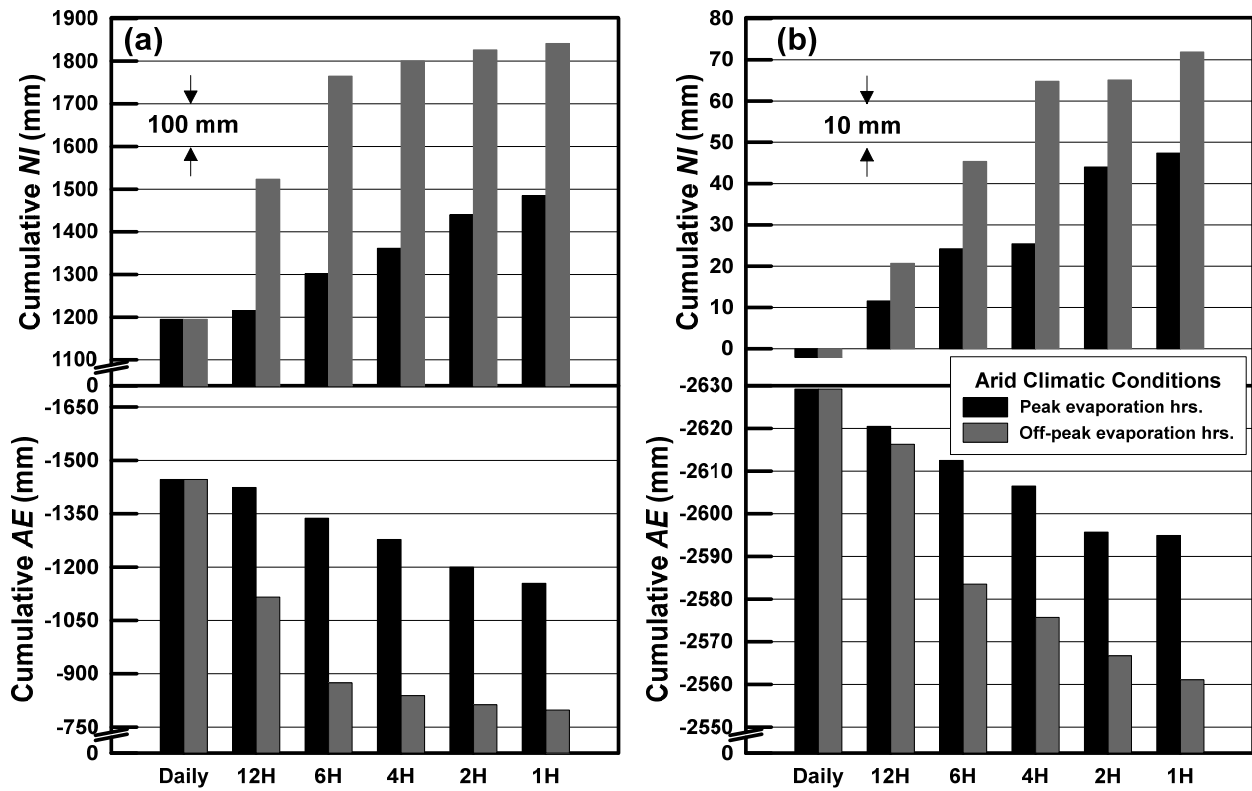
Fig. 4.16: Effect of temporal variability on water balance at the ground surface in arid climatic conditions for simulations run with **a)** coarse and **b)** fine soil hydraulic properties

4.2.1.2 Vertical solute displacement over time in coarse and fine-grained soil materials

Figure 4.17 shows the vertical displacement of the concentration contours along 3-meter homogenous coarse and fine-grained soil profile showing the effect of dry climatic conditions subjected to daily and 1-hour precipitation intensity resolutions. It can be observed that for coarse-grained material, the vertical solute displacement is downward and increases consistently with higher precipitation intensity events. For instance, from daily climate data results, the time for the initial solute concentration to be completely flushed out of the soil domain was approximately 2.3 years. As expected, for higher precipitation intensity (1-hour resolution) the average time to drain the initial

77

solute concentration was approximately 2 years. For simulation where the precipitation events were assumed to occur outside the peak evaporation hours the total time to drain the solute reduced to less than 1.8 years. In general the solute transport results are consistent with the results from the water balance at the ground surface. Therefore, it can be concluded that for the arid climatic condition and coarse grained materials increase in precipitation intensity results in faster transport.

The solute transport results for fine-grained material presented in Fig. 4.17 (d), (e), and (f) indicate more stark changes with increase in precipitation intensity and time of occurrence as compared to coarse-grained material. In section 4.1.1, it was explained that the salt movement in fine-grained soil settings under the effect of daily climate data showed significant upward displacement of solute. This can be observed in Fig. 4.18(d). It can also be observed that some of the solute makes its ways into the root zone and starts to accumulate at the ground surface. Moreover, it is also important to note that the salt movement at daily precipitation intensity never reaches the bottom of the soil column over the 18-year period. The solute transport profile for the hourly precipitation intensity during the peak evaporation hours presented in 4.17 (e) indicates that unlike the daily data simulation there is minimal upward migration of the solute. It can also be observed that downward migration is enhanced with solute reaching the bottom boundary in less than 12 years. These results correlate well with the water balance at the ground surface. For daily precipitation data simulation, groundwater balance indicated net moisture loss conditions. This is indicative of little or downward advection due to meteoric water. In contrast, the hourly precipitation data simulation indicated a net moisture gain of more than 5mm a year on average.

78
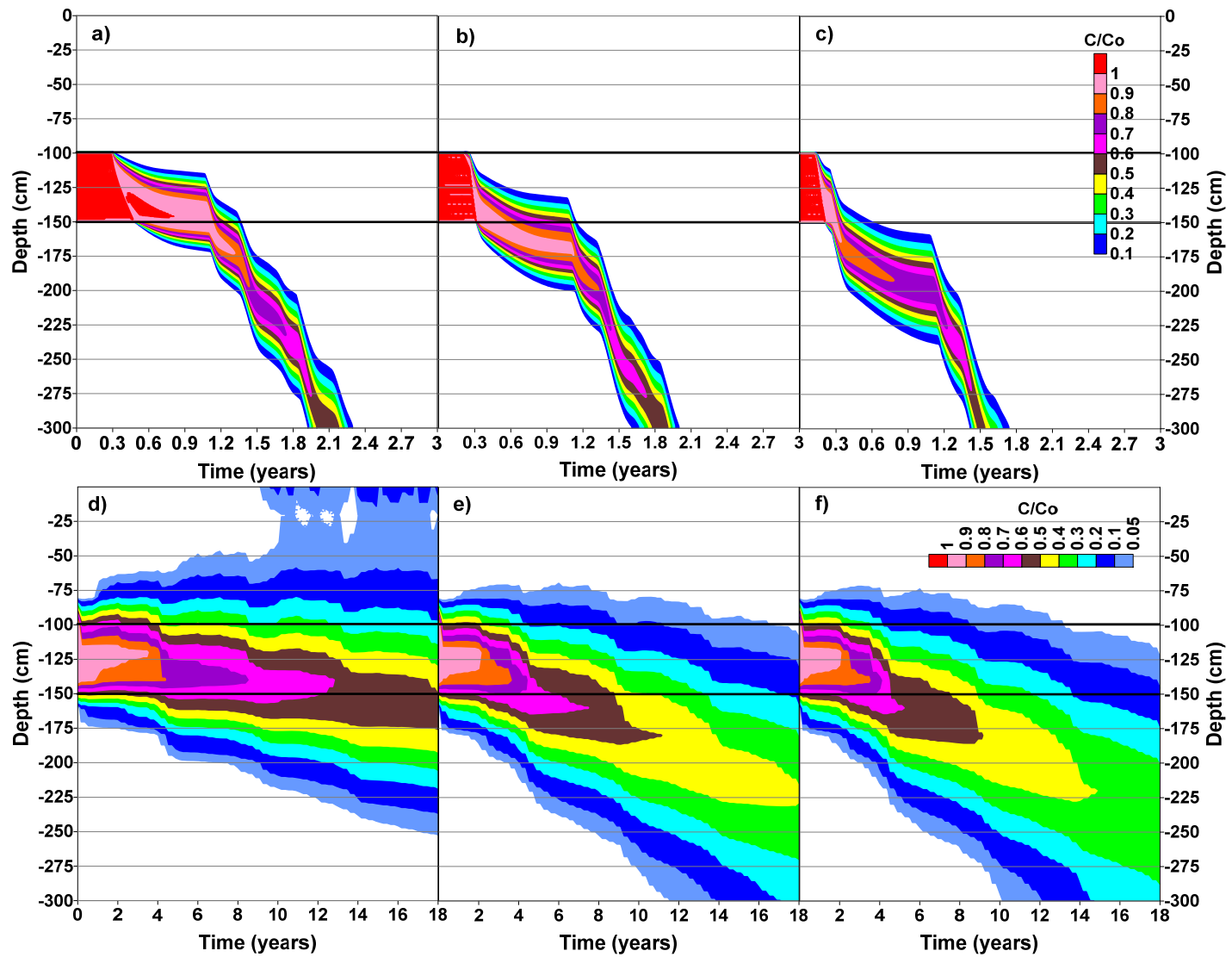
Fig. 4.17: Vertical solute displacement in arid climatic conditions
***Coarse-grained soil materials:* a)** daily resolution, **b)** 1-hour resolution and **c)** 1-hour resolution during off-peak evaporation hours
***Fine-grained soil materials:* d)** daily resolution, **e)** 1-hour resolution and **f)** 1-hour resolution during off-peak evaporation hours

Although this value is quite small, it appears that it changes the vertical transport to be predominantly downwards. This observation is further supported by the results of the simulation run with hourly precipitation data assumed to occur outside the peak evaporation hours. The results presented in Fig. 4.17 (f) indicate that vertical transport becomes faster if the precipitation events occur outside the peak evaporation hours as the time for the solute to reach bottom boundary reduces by approximately 2 years. This reduction in solute transport appears to be the result of an additional 3mm of *NI* per year for hourly precipitation data occurring outside the peak evaporation hours. Based on the observations that the change in resolution of precipitation data results in change of direction of solute transport, it can be concluded that the resolution of precipitation data is more important for simulations for fine-grained materials.

4.2.2 Dry sub-humid climatic conditions - Bighorn region

4.2.2.1 Water balance at ground surface for coarse and fine-grained soil materials

Simulated results for Dry sub-humid climate run with coarse and fine soil hydraulic properties during peak and off-peak evaporation hours show similar trend as was observed for arid climatic conditions. For the sake of brevity, the detailed 9-year water balance results are show in Appendices E.1 and E.2. A summary of the results is presented in the following sections.

Figure 4.18 shows the cumulative *NI* and *AE* values for both coarse and fine-grained materials. Results are presented for precipitation intensity resolutions of 24, 12, 6, 4, 2 and 1 hrs. for occurrences during and outside the peak evaporation hours. It can be observed that similar to the observations for arid climate, higher precipitation resolution results in decreased *AE* and increased *NI*. Also consistent with the results for arid climatic region, the differences for fine grained material are an order for magnitude smaller than for coarse grained soil. As explained earlier, decreased *AE* and increased *NI* is a consequence of availability of more meteoric water in a shorter period of time when the evaporative demand during this period remains the same. This results in reduced evaporation allowing more meteoric water to enter the soil domain.

Moreover, as also explained earlier differences in fine and coarse-grained materials is due to the difference in their hydraulic properties. Less retention and more conduction in coarse materials facilitate the downward movement of water resulting in larger differences in *AE* and *NI* for different precipitation intensities. On the other hand, fine-grained materials impede downward movement of water due to more retention and less conduction, resulting in smaller differences in *AE* and *NI* for different precipitation intensities.
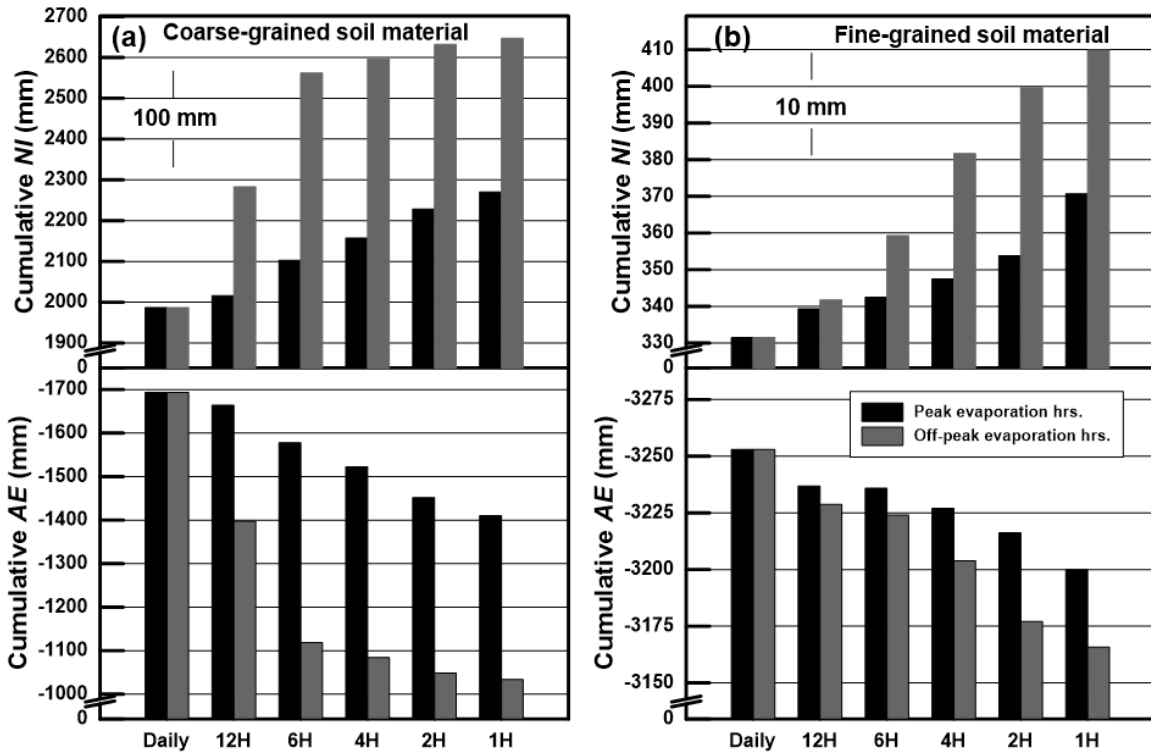
Fig. 4.18: Effect of temporal variability on water balance at the ground surface in dry sub-humid climatic conditions in **a)** coarse and **b)** fine-grained soil materials

A comparison of *NI* values for arid and dry sub-humid climatic conditions is presented in Fig. 4.19. Review of this figure indicates that for coarse-grained material, the changes in NI values for different precipitation intensities are similar for the two climate types. For example, a difference of 290 and 283 mm was estimated between daily and 1-hour time precipitation events occurring during peak evaporation hours for arid and dry sub-humid climatic conditions, respectively. Similarly, 24hr and 1hr precipitation events outside peak evaporation hours show cumulative *NI* differences of 646 and 660 mm for arid and dry sub-humid climatic conditions.
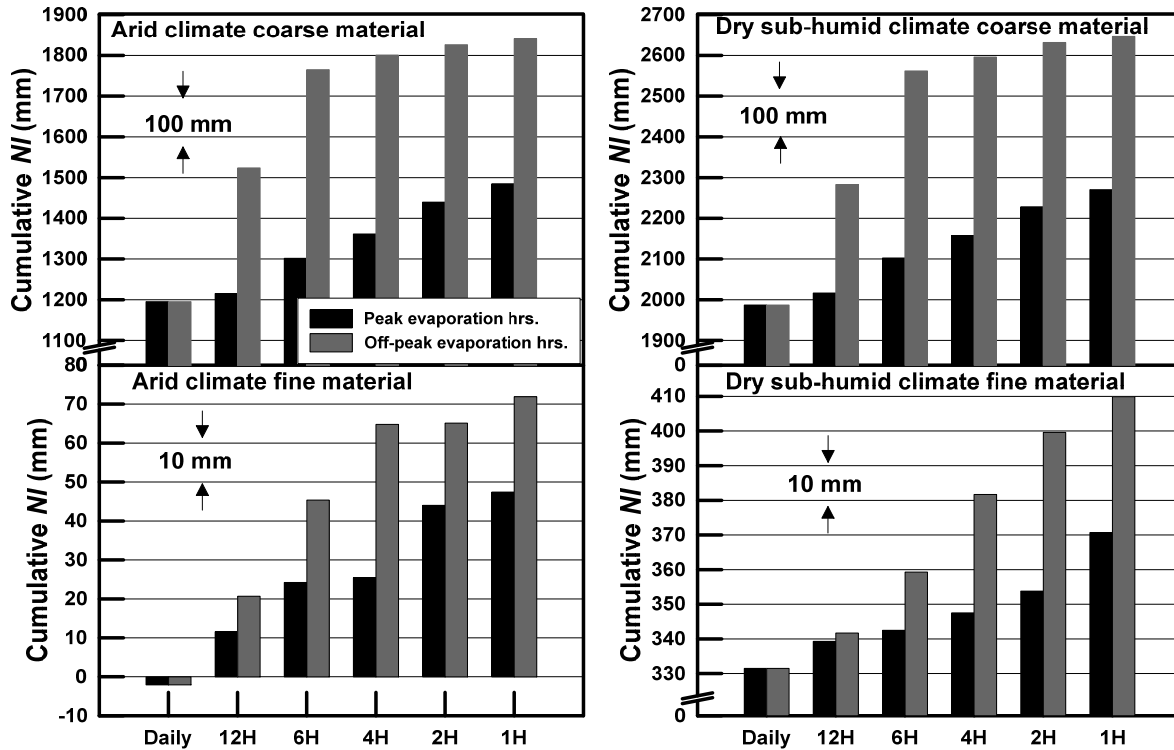
Fig. 4.19: Comparison of NI in arid and Dry sub-humid climatic conditions

As mentioned earlier for fine-grained material the increase in *NI* values as a result of increased precipitation intensities is one order of magnitude lower than the coarse-grained material. This is true for both climate types. It is also shown in Fig. 4.19 that for most instances the changes in *NI* for fine-grained materials are comparable for the two climates types. For example, differences in *NI* of 49 and 39 mm were estimated for arid and dry sub-humid climatic conditions. These differences are from simulations run with daily and 1-hour time precipitation events occurring during peak evaporation hours. Similarly the computed water gain (*NI* = 74 mm) for 1hr precipitation intensity outside the peak evaporation hours under the effect of arid climatic conditions is consistent with the water gain computed on dry sub-humid climatic conditions (*NI* = 78 mm).

4.2.2.2 Vertical solute displacement over time in coarse and fine-grained soil material

The solute displacement in coarse and fine-grained materials during peak and off-peak evaporation hours for dry sub-humid climatic conditions is presented in Fig. 4.20. It can be observed, that the increase in precipitation intensity resulted in faster downward movement of solute for both coarse and fine-grained materials. A similar observation can be made for the time of precipitation occurrence. Precipitation events occurring outside the peak evaporation hours further facilitate the downward movement of the solute. The results for dry sub-humid climatic conditions are similar to those presented earlier for arid climatic conditions.

In all simulations run with coarse-grained material hydraulic properties, the solute transport times due higher precipitation intensity events are not affected substantially. Plotted results (Figs. 4.20 (a), (b) and (c)) show that the time required for the solute to be completely flushed out of the soil domain varies over a narrow range of 9.5 to 10.5 months. Similarly, the time for any solute mass to reach the bottom boundary shows slightly wider range of 5.5 to 9.5 months. In comparison to the arid climatic conditions, it can be concluded that the effect of precipitation intensity and time of occurrence is less pronounced in wetter climates for coarse soils.

Solute movement in fine-grained soils shows a downward displacement under the effect of sub-humid climatic conditions. Significant differences regarding the solute displacement were observed between the daily and 1-hour resolution precipitation input data. For example, 1-hour resolution precipitation data results in complete flushing out of the solute from the soil domain in less than 17 years.
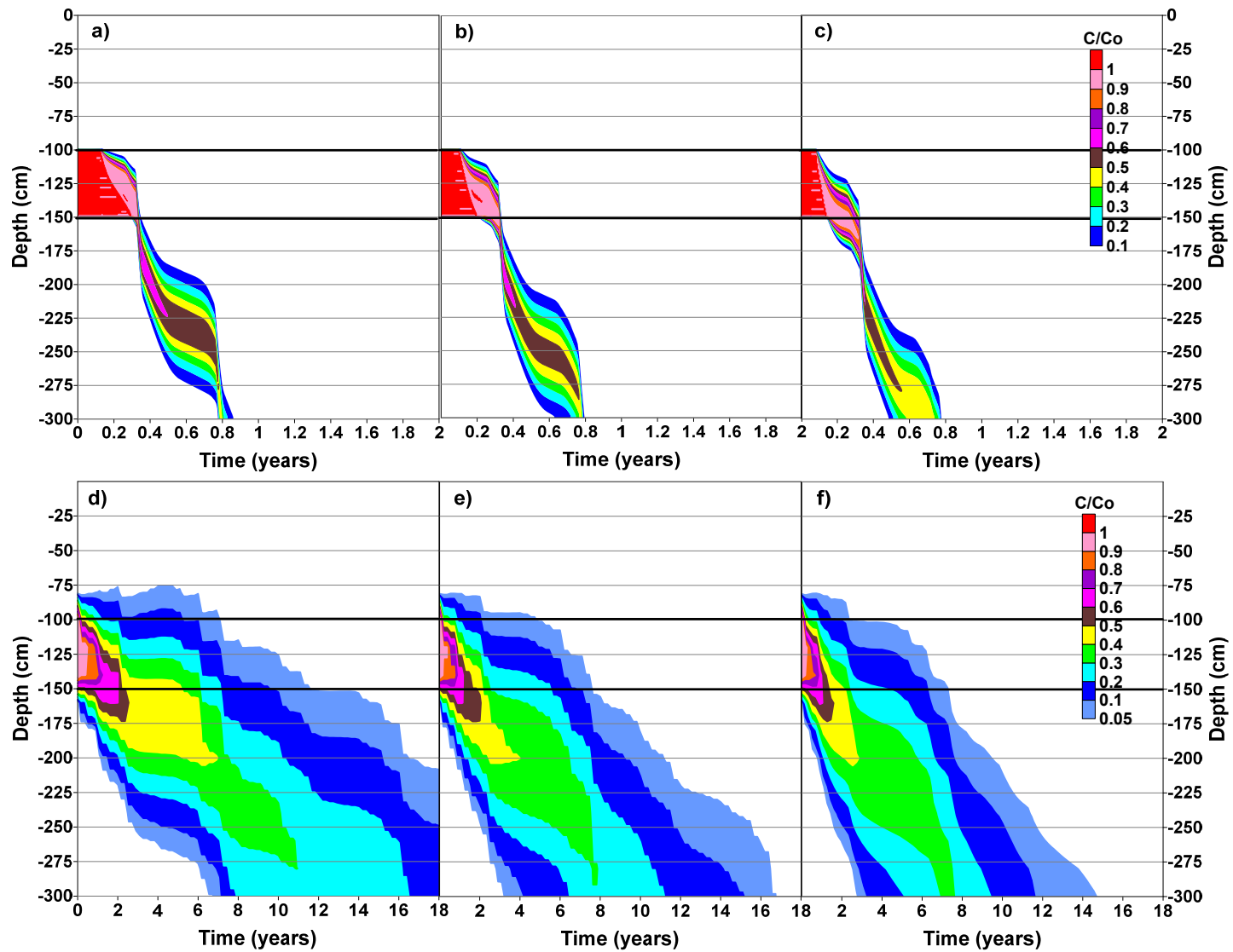
Fig. 4.20: Vertical solute displacement in dry sub-humid climatic conditions
Coarse-grained soils: **a)** daily resolution, **b)** 1-hour resolution and **c)** 1-hour resolution during off-peak evaporation hours
Fine-*grained* *soils:* **d) daily resolution, **e)** 1-hour resolution and **f)** 1-hour resolution during off-peak evaporation hours

This time reduces by 2 years if the 1-hour precipitation events are assumed to occur outside the peak evaporation hours. Both of these observations are in contrast to the solute transport predicted using the 24hr resolution precipitation data. It can be observed that if 24hr resolution precipitation input data is used, a part of solute still remains in the soil domain at the end of 18 years period. Similarly, precipitation intensities and time of occurrence of precipitation events also effect the time for any amount of solute to reach the bottom boundary. It can be observed that time to reach the bottom boundary varies from 3 years to 7 years. The longest time period is associated with the simulation run with 24hr resolution precipitation data, while the shortest time is associated with simulation run with 1hr resolution precipitation data and precipitation occurrences outside the peak evaporation period. Therefore, it can be concluded that the effect of precipitation intensity and time of occurrence are significant for dry sub-humid climatic conditions for fine grained materials.

4.3 Effect of depth of groundwater table on water and salt dynamics

A third set of simulations were run with coarse and fine soil hydraulic properties to assess the soil water and solute dynamics under the influence of shallow groundwater table. The simulations were run using daily and 1hr resolution precipitation data with the assumption that the precipitation events occurred during the peak evaporation hours. The water table was assumed to be at the depths of 1 and 3 m. No change was made to solute source depth. Results of the simulations with water table depths of 1 & 3m were compared to the simulations run with deep water table setting.

4.3.1 Arid climatic conditions - Calgary region

4.3.1.1 Water balance at the ground surface for coarse-grained soil material

Figure 4.21 shows the estimated water balance at the ground surface for coarse-grained-material for different water table depths. Water balance results for deep water table condition are also shown in the same figure. The results for the daily resolution of precipitation data are shown in Fig. 4.21 (a), while for hourly resolution in Fig. 4.21 (b). Graphical results show no significant difference in water balance for any of the water table depths. This observation is consistent for daily and hourly climate data resolution. This is not an unexpected result. The air entry value of coarse-grained material is only a few cm of head. For such a small air entry value, capillary rise would be minimal and little to no interaction between groundwater table and atmosphere is expected.

It should be noted that, although flow part of the simulation shows no interaction between the groundwater table and atmosphere, however, the vertical transport is expected to be affected due to the depth of groundwater table depth. This is explained in the following section.
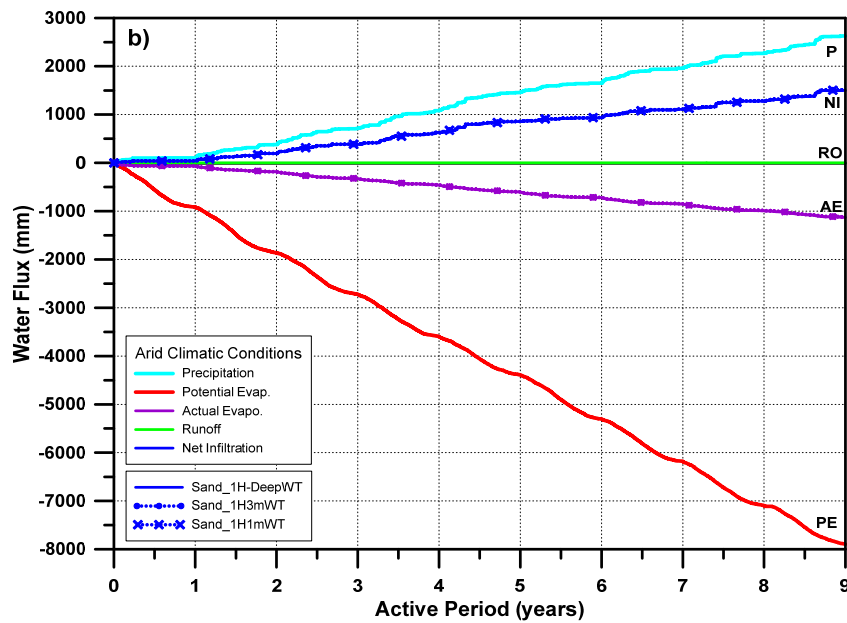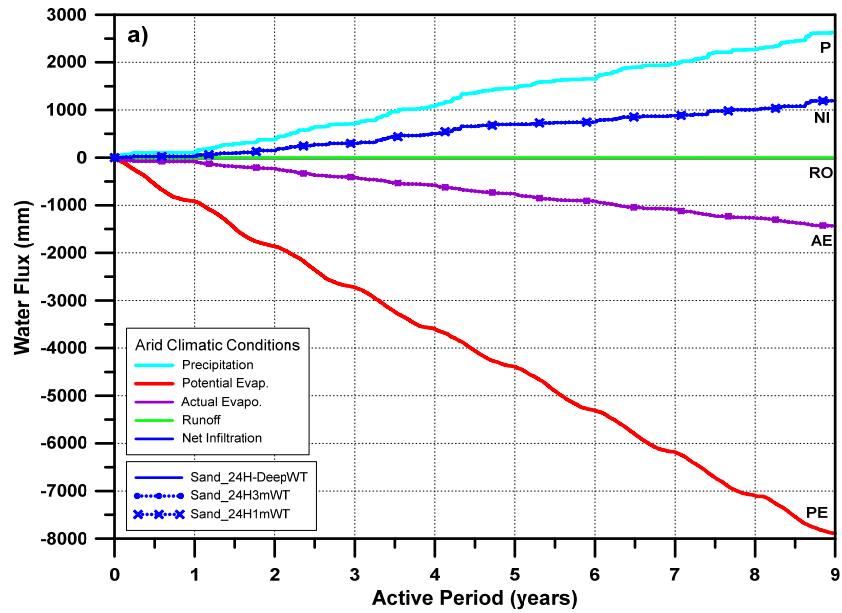
Fig. 4.21: Estimated water balance at the ground surface under the influence of different water table settings in coarse-grained soils - Arid climatic conditions

4.3.1.2 Vertical solute displacement over time for coarse-grained soil material

Figure 4.22 shows the vertical transport of solute from six different simulations. These simulations are representative of three different groundwater table depths and two different climate data resolutions. Water table depths are marked on individual profiles. Profiles to the right have lower water table depths as compared to a profile to their left. Similarly, top profiles are for simulations run with daily precipitation data while the bottom profiles were run with hourly precipitation data. Comparison of vertical solute transport for deep water table and water table depth at 1m depth shows huge differences. It can be observed that for 1m groundwater table depth, it would take 4-5 times as long for the solute to be completely flushed out of the bottom boundary, when compared to the deep water table condition. It can also be observed that time for vertical travel of solute for 3m water table depth is slightly more than the deep water table conditions. Another important observation from the comparison of the profiles of different water table depth is that for shallower water table depths there is lot more vertical spreading of the solute front.

The observations on slowing and more enhanced spreading of the solute for shallower groundwater depths can be explained based on the system saturations. For 1m depth, the entire depth of initial solute profile is within the groundwater table. In addition, at the bottom two third of the soil profile remains saturated. The higher saturation profile implies higher diffusive fluxes owing to the higher diffusion coefficients as the diffusion coefficient is a function of saturation. As diffusion is a Fickian process, therefore there would be diffusive fluxes in both upward and downward directions for shallow water table depths owing to concentration gradient in both directions. This will

delay the downward advection of the solute front and will also be responsible for some dispersion in the solute front. This conjecture is also supported by the comparison of solute movement for same water table depth but different precipitation intensity resolution. For example, the vertical transport for 1m water table depth for 24hr and 1hr precipitation data (Fig. 4.22 c & f) indicates that the time for solute to be flushed out of the system is lower for higher precipitation resolution. Moreover, it can also be observed that the solute front is less dispersed for higher precipitation resolution. It has been explained in the previous sections that higher precipitation resolution leads to higher advection. This higher advection balances out some of the diffusive fluxes resulting in slightly faster transport and less dispersed solute front for simulation run with higher resolution precipitation data.

4.3.1.3 Water balance at the ground surface for fine-grained soil materials

In fine-grained soils, the effect of water table setting shows a significant impact on the *NI* and *AE* values. Water balance at the ground surface for the fine-grained materials for two different precipitation intensities is shown in Fig. 4.23. Review of this figure indicates that with decrease in depth of groundwater table, there is an increasing trend in *AE*. This increasing trend is indicative of the interaction between the groundwater table and the atmosphere. Shallow water table depth results in upward movement of water from groundwater table towards the ground surface. This movement is a result of capillary action owing to the high air entry value of the fine-grained material.
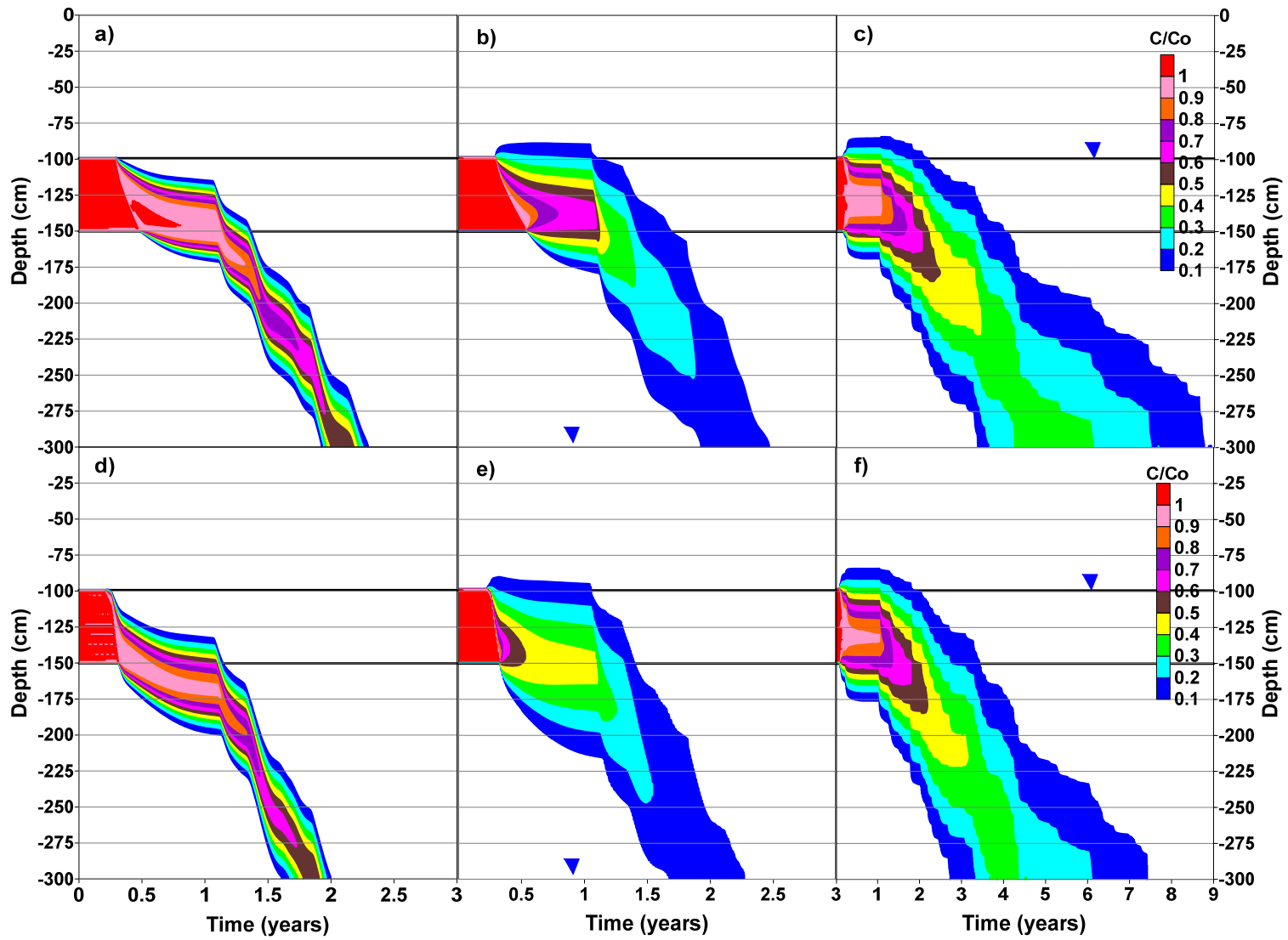
Fig. 4.22: Vertical solute displacement in coarse-grained soils - Arid climatic conditions
a)   Daily-DeepWT, b) Daily-3mWT, c) Daily-1mWT, d) 1H-DeepWT, e) 1H-1mWT, and f) 1H-1mWT

91

The upward movement of water results in higher saturation in the near surface soil layers, resulting in higher *AE* values. The higher *AE* values results in net water loss conditions at the ground surface. For example, for 24-hr precipitation data and deep water table, the water balance conditions at the ground surface appear to be net neutral, i.e. no appreciable water loss or gain (*NI ≈ 0*). This is in contrast to the results from the simulation run with the depth of water table at 1m, which shows a water loss of approximately -1617mm over the 9-year period. This water loss increases to more than double (3420 mm) if the intensity of precipitation data is changed to a 1hr resolution (Fig. 4.23 b) for the same water table depth of 1m. The increase in water loss with higher precipitation resolution might seem counter intuitive at first, since it was previously shown that the higher resolution results in more water gain. However, in shallow water table settings, more water might enter the system initially, but its further downward movement is impeded by upward gradient from the groundwater table due to capillary action. The net result is more water availability in the upper soil layers, further enhancing the *AE* and resulting in additional water loss.

It should be noted that the upwards water movement due to capillary action and evaporation losses at the ground surface poses a high potential of salinization near or at the ground surface. The results of solute transport are presented in the following section.
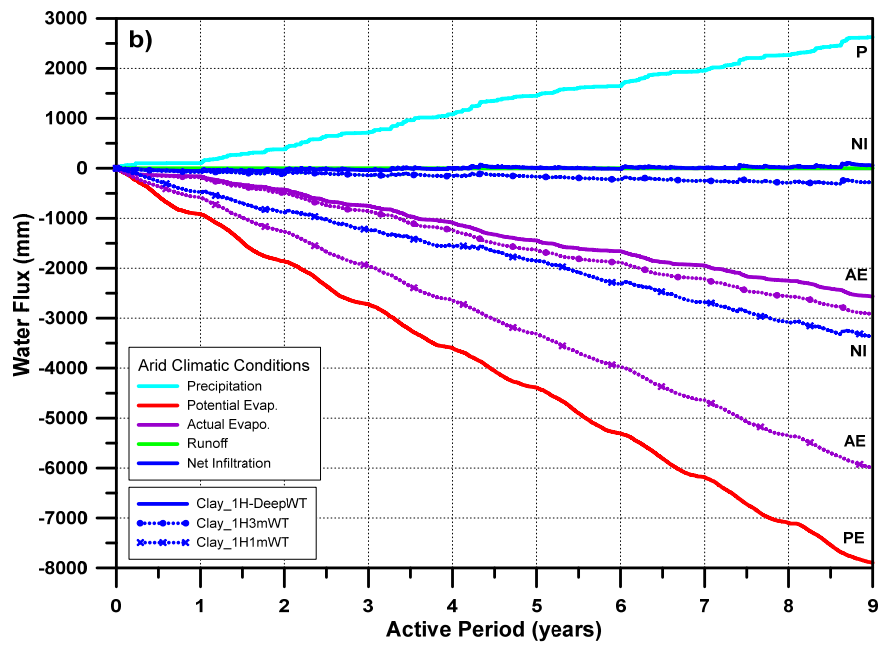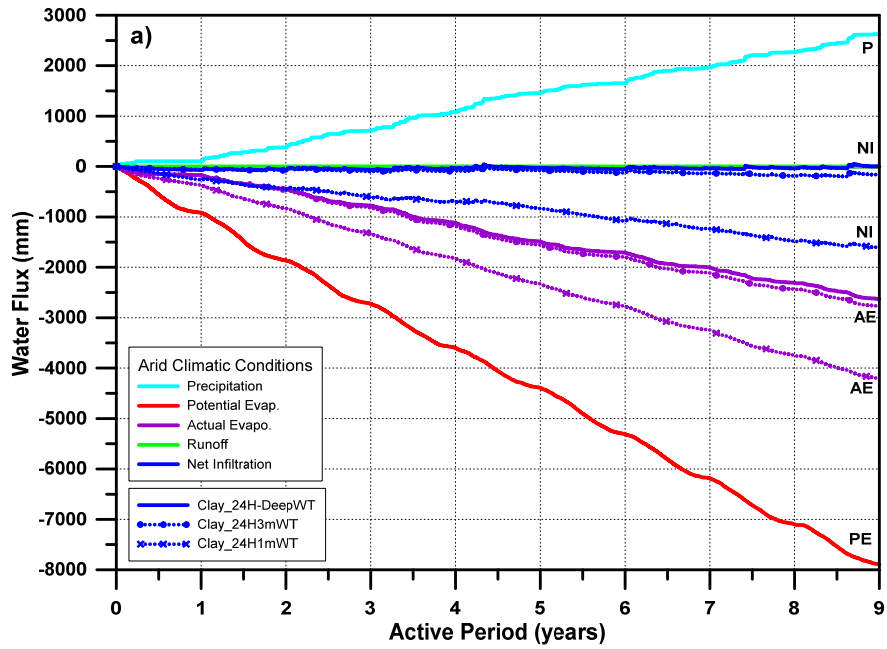
Fig. 4.23: Estimated water balance at the ground surface under the influence of different water table settings in fine-grained soils - Arid climatic conditions

4.3.1.4 Vertical solute displacement over time in fine-grained soil materials

Figure 4.24 shows the time history of the vertical solute transport in fine-grained material for various water table depths. These results are for arid climatic conditions. Results show that for fine-grained soils, the water table setting has an important influence on solute dynamics. It can be observed that for all simulations run with shallow groundwater table depths there is upward solute displacement. The results for deep water table setting and 24hr precipitation intensity (Fig. 4.24 a) show that there was some upward transport of solute with small amount of solute ending up in the near surface soil layers. For the same water table depth, the transport was observed to be predominantly downward if the hourly precipitation intensities were considered (Fig. 4.24 d). However, for shallow water table depths the combination of meteorological and soil conditions causes the solute to move upwards at a greater rate and in large quantities as can be seen in Fig. 4.24 b, c, e, and f.

The rate of upward solute transport appears to be consistent with the water balance results presented in the previous section. For example, the largest water loss was observed for 1m water table depth and for 1hr precipitation intensity resolution. It can be observed that the upward migration of solute was most rapid for this combination with some solute mass reaching the ground surface in a small fraction of a year. In general it is shown that upward solute transport increase with the decreasing groundwater table depth and higher resolution of precipitation input data.

Fig. 4.24: Vertical solute displacement in fine-grained soils during peak evaporation hours in arid climatic conditions.
a) Daily-DeepWT, b) Daily-3mWT, c) Daily-1mWT, d) 1H-DeepWT, e) 1H-1mWT, and f) 1H-1mWT

4.3.2 Dry sub-humid climatic conditions - Bighorn region

4.3.2.1 Water balance at the ground surface for coarse-grained material

Estimated water flux graphs for simulations run with coarse soil hydraulic properties under the influence of different water table depths for dry sub humid climatic conditions are shown in Fig. 4.25. Similar to arid climatic conditions, the contribution of shallow groundwater tables in the estimation of water balance appears to be negligible. Results also indicate that changes in the precipitation intensity resolution show no significant difference in the cumulative *NI* and *AE* for different water table depths.

4.3.2.2 Vertical solute displacement for coarse grained material

Graphical results shown in Fig. 4.26 indicate widening of the solute contour curves consistent with the shallower depth of the water table in coarse-grained materials. This trend is more noticeable in simulations run with daily data. Generally, the downwards solute displacement is consistent with the rapid response of coarse-grained soils to drain infiltrating water out of domain due to the high hydraulic conductivity value and lower water retention properties. As also observed for arid climatic conditions, plotted results show a noticeable time lag in the solute displacement under shallow water table settings. This lag is more pronounced in simulations run with daily data and water table depth at 1 m. As explained, earlier this process is associated with molecular diffusion of contaminants in saturated soil conditions. However, the transport is noticeably faster when compared to results for arid climatic region (Fig. 4.22). Comparison of solute contours for dry sub-humid and arid climatic conditions indicate that for 1m groundwater table depth the transport is at least three times faster in dry sub-humid climate.
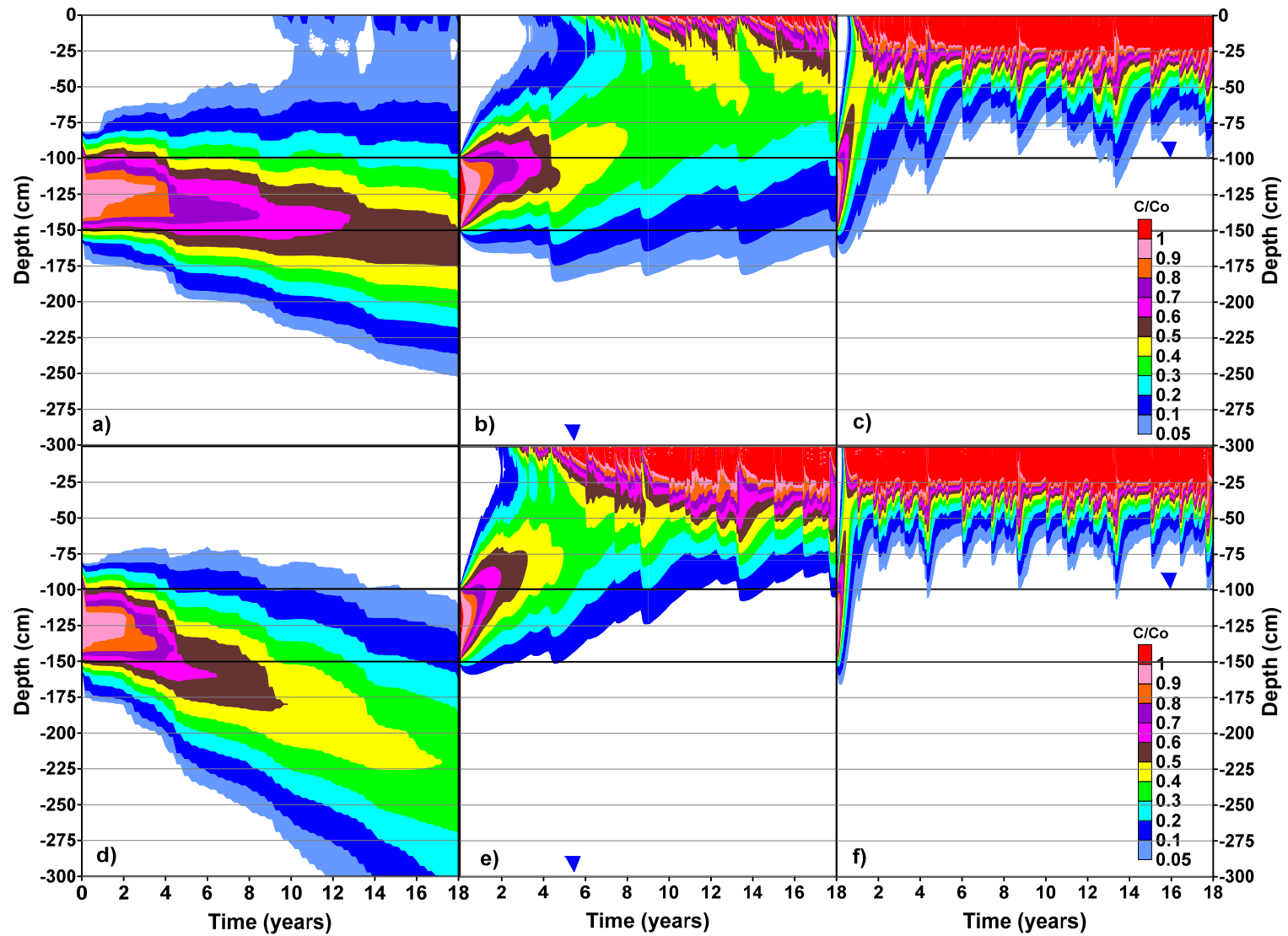
Fig. 4.25: Estimated water balance at the ground surface under the influence of different water table settings in coarse-grained soils – Dry sub-humid climatic conditions
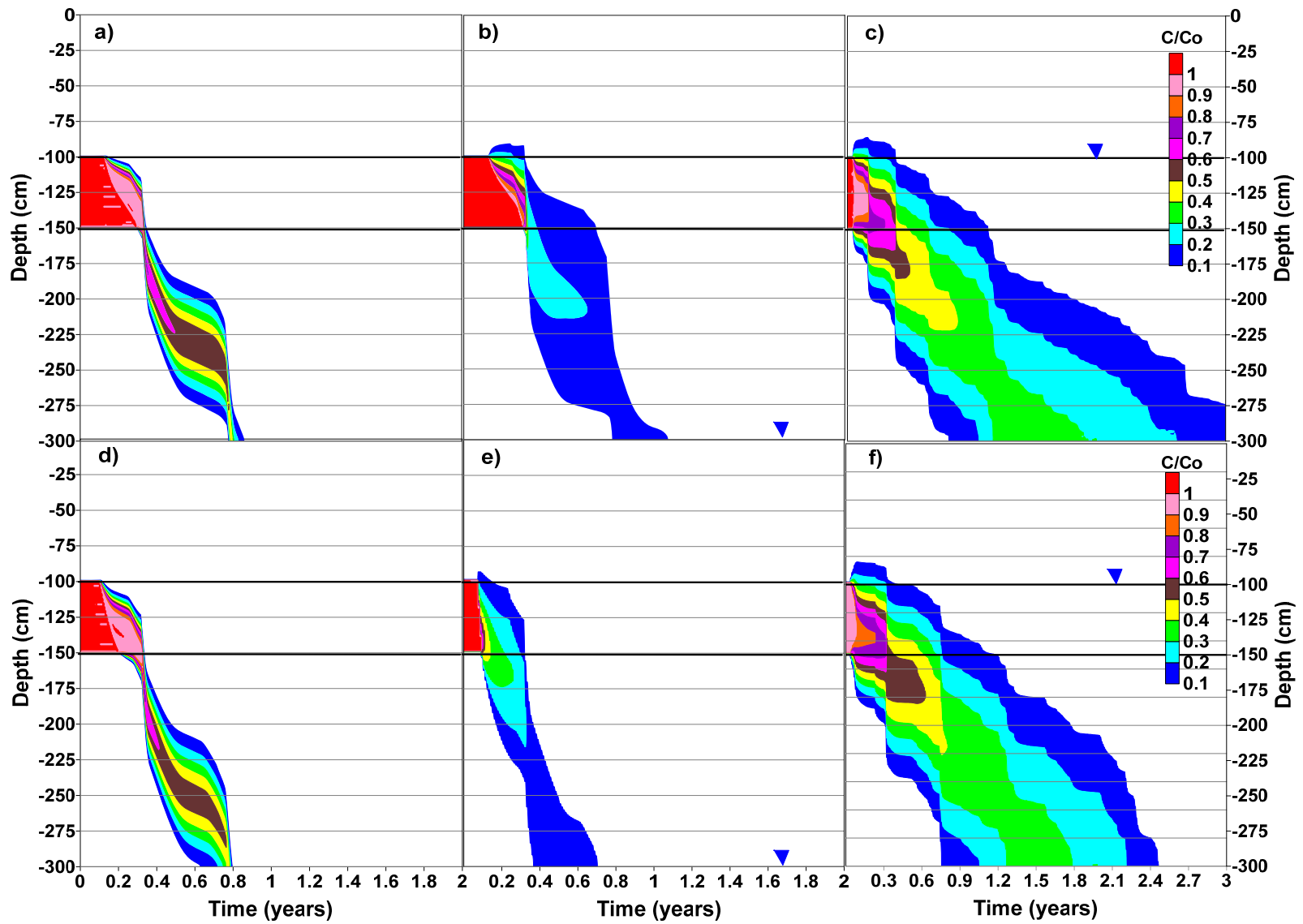
Fig. 4.26: Vertical solute displacement in coarse-grained soils during peak evaporation hours in dry sub-humid climatic conditions
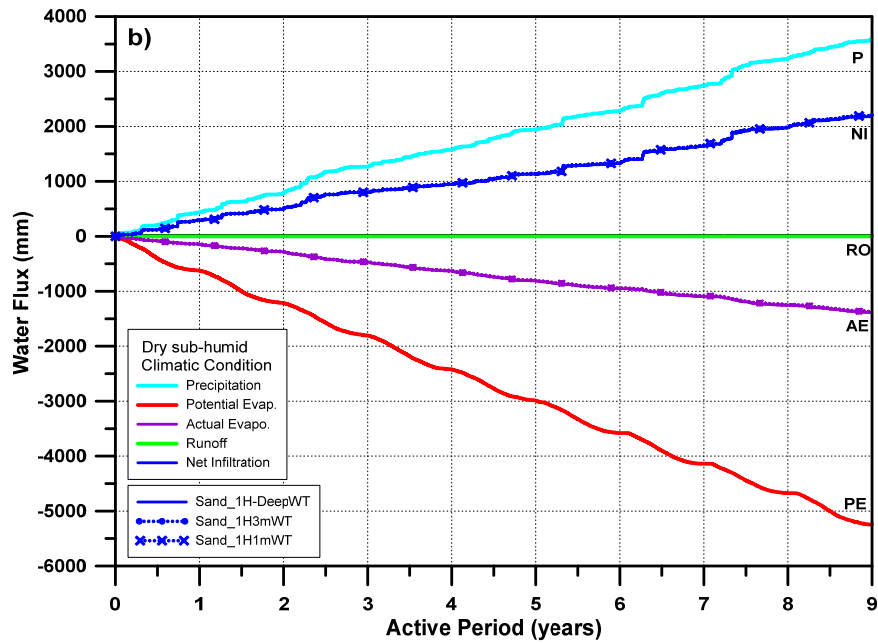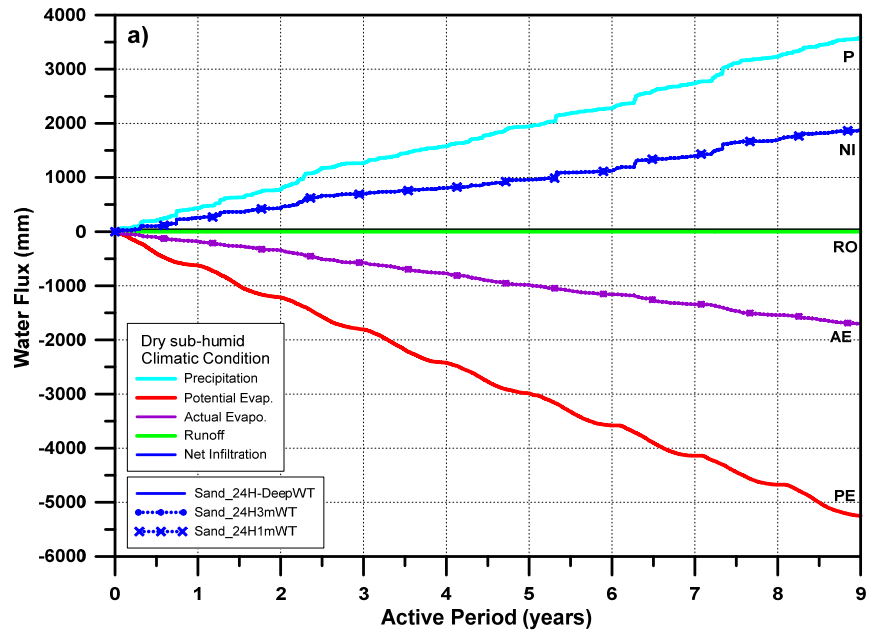a) Daily-DeepWT, b) Daily-3mWT, c) Daily-1mWT, d) 1H-DeepWT, e) 1H-1mWT, and f) 1H-1mWT

4.3.2.3 Water balance at the ground surface for fine-grained material

The effect of water table setting in fine-grained soils is more accentuated in terms of evaporation losses in comparison with arid climatic conditions. Review of Fig. 4.27 shows *AE* curves drawing closer to the *PE* curve. This is indicative of the fact that for the dry sub-humid climatic conditions, shallower groundwater table in fine-grained material ensures the availability of water in the near soils surface to be much closer to the total evaporative demand of that area.

The downward translation of the *AE* curves shown in Fig. 4.27 is indicative of the water loss at the ground surface and implies reduction in *NI* values. In the water balance graphs presented in this figure it can be observed that the *NI* curves show a downwards trend to negative values indicating net water loss conditions as the groundwater table is raised. It should be noted that although for dry sub-humid climatic conditions, evaporation losses at the ground surface are much closer to the evaporative demand of the area, it does not necessarily translates to net higher water loss at the ground surface when compared to arid climate.

Fig. 4.27: Estimated water balance at the ground surface under the influence of different water table settings in fine-grained soils – Dry sub-humid climatic conditions
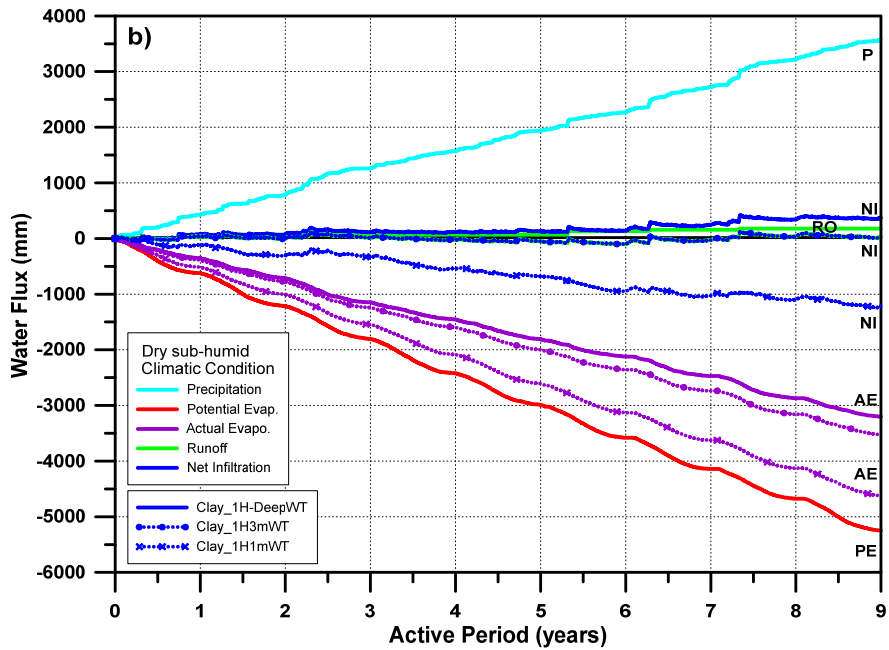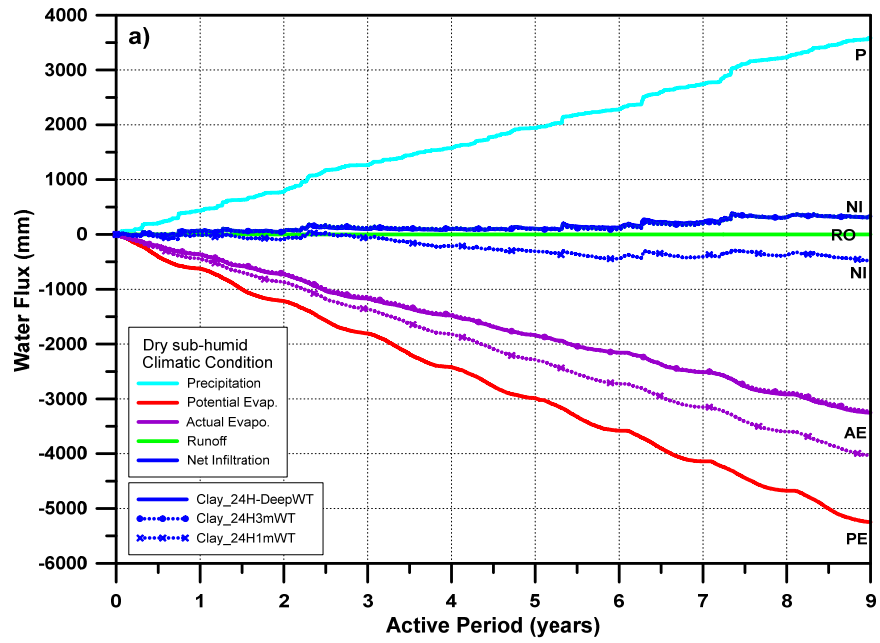
Figure 4.28 compares the *AE* and *NI* values for the arid and dry sub-humid climatic condition. The values are cumulative at the end of the 9-year period. A number of observations can be made from this figure. The most important observation is that for dry sub-humid climate, net water loss is only observed for 1m water table depth. This is in contrast to the arid climate, where water loss was observed for 3m groundwater depth as well and net neutral water conditions were observed for deep groundwater table. Higher water loss at the ground surface for arid climatic conditions is consistent with the estimated *AE* values, which are higher than those for dry sub-humid climate. Based on these observations, a number of important conclusions can be drawn.

For dry sub-humid climatic conditions, evaporation losses at the ground surface being close to the evaporative demand is due to lower potential evaporation and higher precipitation, when compared to arid climate. This does not necessarily translate to higher net water loss or higher upward gradients in the soil. For the ground water table depth of 3m, for dry sub-humid climatic condition, the water balance at the ground surface is neutral to water gain conditions. This is in contrast to arid climatic conditions where for same water table depth net water loss conditions are predicted. It is expected that owing to the water balance differences at the ground surface for the two climates, sub surface solute transport would be different as well.
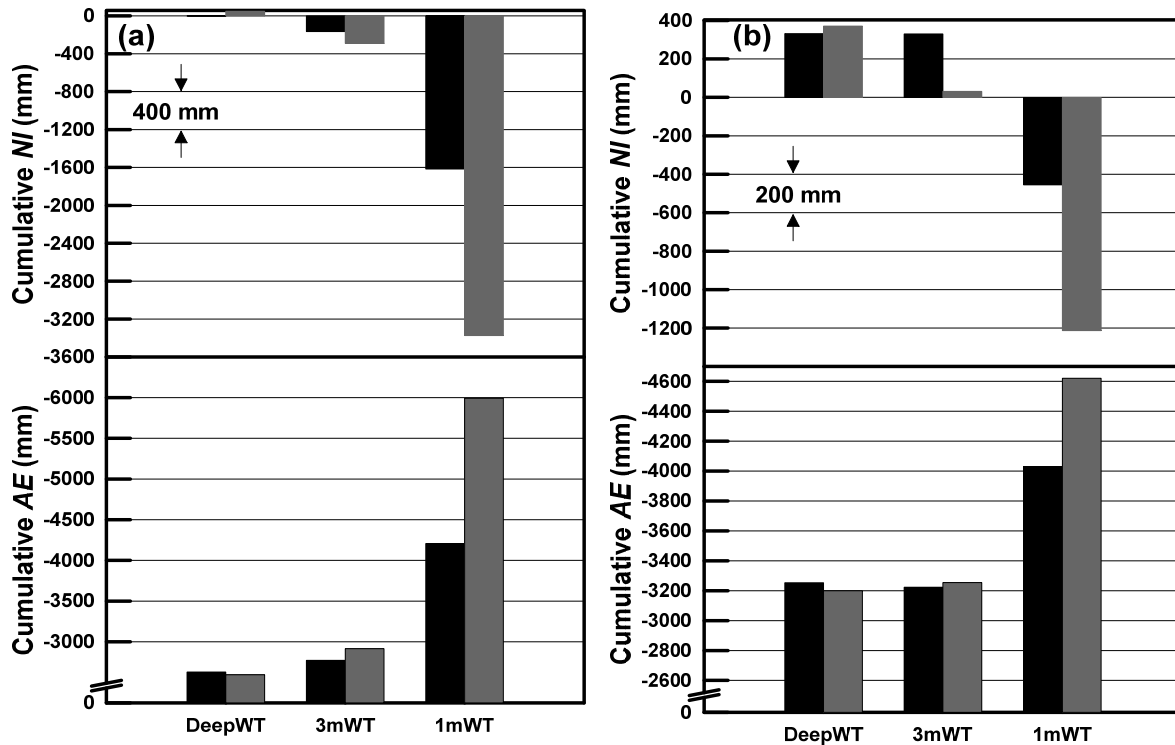
Fig. 4.28: Effect of temporal variability on water balance at the ground surface in fine-grained soils **a)** arid and **b)** Dry sub-humid climatic conditions

4.4.2.4 Vertical solute displacement in fine-grained soil materials

The vertical solute displacement contours for dry sub-humid climactic condition and fine-grained soils are shown in Fig. 4.29. In general, the solute contours are different from those reported for arid climate as they show both upward and downward solute displacements. The solute displacement contours align consistently with the water balance results presented in the previous section. For example, net water gain conditions at the ground surface were predicted for 3m water table depth using daily resolution precipitation data. The corresponding solute contour profile in Fig. 4.29 b indicates that the solute transport is predominantly downwards. However, some mass of

solute has made its way into the near surface soil layers, indicating some solute transport in the upward direction. For the same water table depth of 3m, using 1hr resolution precipitation data, close to net neutral water balance conditions were predicted. The corresponding solute profile in 4.29 (e), indicates that although the solute transports still appears to be predominantly in the downward direction, the concentration of the solute in the near surface layers has increased. This is indicative of more upward transport of solute. Similarly, for water table depth of 1m and daily resolution of precipitation input data, net water loss conditions were predicted. The vertical solute transport profile for these conditions shown in in 4.29 (c) clearly indicates that now the transport is predominantly in the upward direction. However, some downward migration of the solute can also be observed in the same figure. The downward movement of the solute can be attributed to the fact that at the bottom two thirds of the domain is saturated, and concentration gradient can induce diffusive fluxes in the downward direction. The solute transport contours for 1m groundwater depth and 1hr precipitation intensity data shown in Fig. 4.29 (f) clearly indicate that majority if not all of the transport is in the upward direction. This is also consistent with the water balance prediction as higher net water loss for 1m groundwater table depth was predicted when the resolution of precipitation data was change from daily to hourly. The observation of the absence of downward solute migration can be explained by the fact that higher advection in the upward direction overcomes the downward diffusive fluxes.
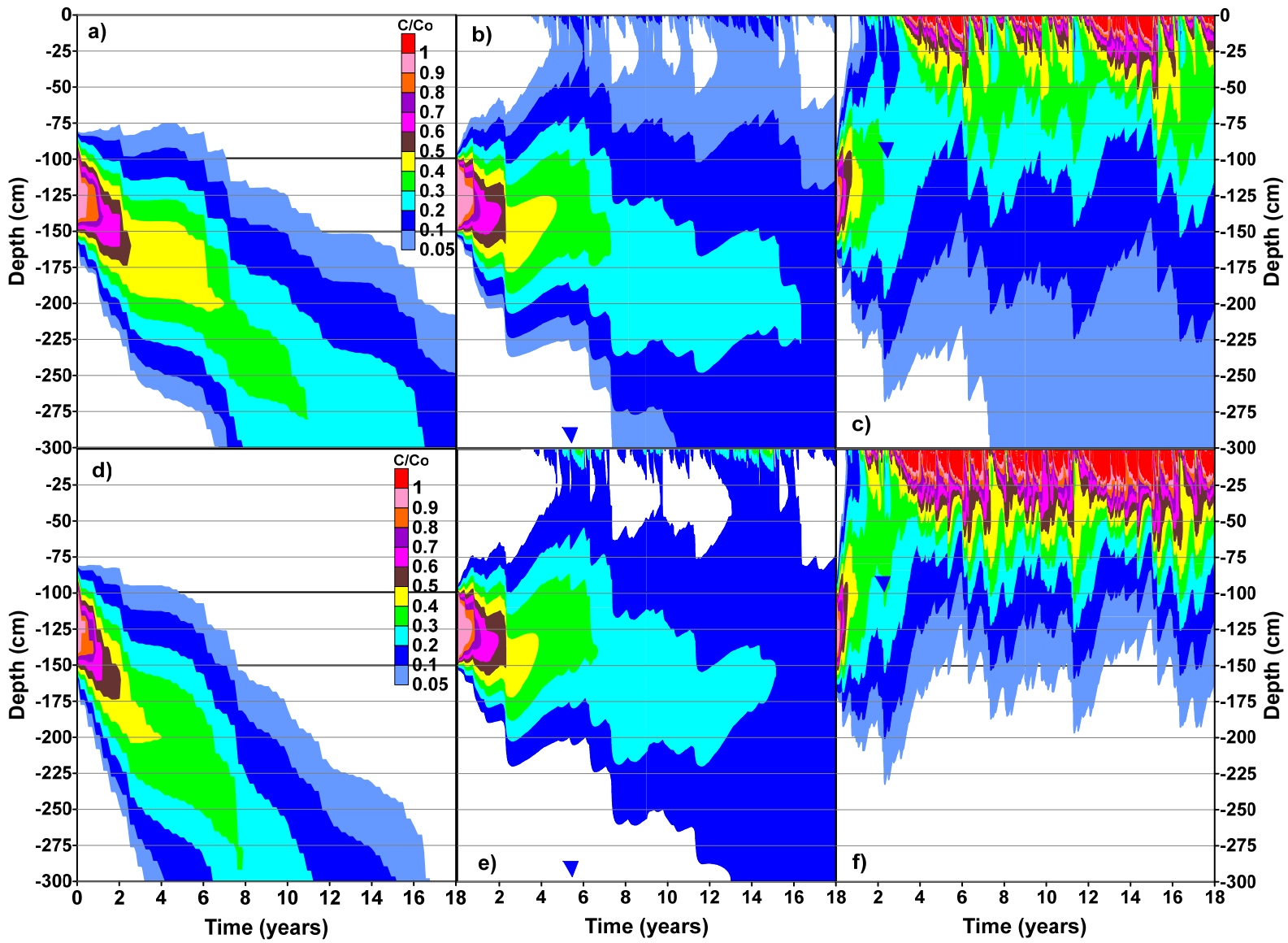
Fig. 4.29: Vertical solute displacement in fine-grained soils during peak evaporation hours in dry sub-humid climatic conditions a) Daily-DeepWT, b) Daily-3mWT, c) Daily-1mWT, d) 1H-DeepWT, e) 1H-1mWT, and f) 1H-1mWT

Chapter 5

Conclusions and Recommendations

5.1 Conclusions

The major objective of this thesis was to understand the effect of climate on vertical transport of salt in variably saturated environments using numerical modeling. Variably saturated flow and transport modeling with soil-atmosphere boundary was used to simulate water flow and transport of a conservative solute in variably saturated soils. The research comprised of four distinct phases. A brief description of each phase is provided below.

In the first phase of this research, climate data for various ecoclimatic regions of Alberta was compiled from the available sources. The compiled climate datasets were compared with Environment Canada reported climate normals to ensure that the compiled data is generally representative of the long-term climatic conditions of these regions. The climate data was only available at the daily resolution. A Matlab program was written to generate, sub-daily climate data from daily data using the procedure reported in the literature by Gladyeva and Saifadeen (2012). The phase one of the research resulted in 9-year climate datasets for 10 different geographical locations in Alberta. These datasets were available in 24, 12, 6, 4, 2 and 1hr resolution and were ready to be used in a number of different soil-atmosphere numerical modeling software.

The second phase of the research investigated the effect of different climate types on water and salt dynamics in variably saturated soils. Two different soils textures

namely coarse and fine were investigated. Variably saturated flow and transport modeling with soil atmosphere boundary was employed for this investigation. Daily records of climate data were used for the soil-atmosphere boundary. The groundwater table was assumed to be very deep and unit gradient boundary condition was as used as the bottom boundary.

The third phase of the research investigated the effect of temporal resolution of meteorological data on water and salt dynamics in variably saturated soils. The modeling scenarios from phase 2 were simulated again with sub-daily climate data. Water balance and solute transport assessments were compared for various temporal resolutions of meteorological input data. The effect of time of occurrence of precipitation events on subsurface water and salt dynamics was also investigated. Two different occurrence scenarios were considered. In the first scenario, sub-daily precipitation events were assumed to occur during the peak evaporation hours. In the second scenario, sub-daily precipitation events were considered to occur during the off-peak evaporation hours.

The fourth phase of the research investigated the interaction between the groundwater table and the atmosphere. The groundwater table depth was varied from deep conditions to 1m from the ground surface. The investigation was carried out for fine and coarse soil textures using daily and hourly resolution of climate data for arid and dry sub-humid climactic conditions.

In the following sections conclusion derived from each of these phases are described. Conclusions are followed by identifying some of the contributions of this research. The chapter ends with recommendations for future research.

5.2 Overall Conclusions

5.2.1 Climate data compilation and classification

The climate classification carried out for 10 different locations in Alberta indicated that the climate in Alberta varies from Arid to Dry sub-humid climatic conditions. This classification was based on the estimation of Thornwaite 1955 annual moisture index (I_m). An I_m value of zero signifies that the annual precipitation and potential evaporation are equal. The compiled data revealed that for the province of Alberta, annual potential evaporation values are higher than the annual precipitation values. As such, in general, moisture loss conditions can be expected across the province. However, it should be noted that the annual moisture index (I_m) and many other such indices such as Thornwaite moisture index (TMI, as cited by Thornwaite, C.W., 1948) are estimated based on the assumption that limitless supply of water is available to meet the evaporative demand dictated by prevailing atmospheric conditions. This assumption is only valid for water bodies or soil surfaces, which always remain saturated. The actual evaporation is not only the function of prevailing atmospheric conditions but also the transient soil moisture conditions. This is essentially the crux of this thesis as in the later sections it was shown that transient soil moisture conditions are a function of soil texture and play a crucial role not only in subsurface flow and transport but also the water balance at the ground surface. The accurate estimation of the actual evaporation requires a multi-year accurate climate dataset. Therefore, it can be concluded that the site-specific climate data is essential for accurate estimation of water balance at a particular site.

5.2.2 Climate type and water and salt dynamics in variably saturated soils

The numerical simulation results for water balance at the ground surface and vertical transport of the solute in variably saturated profiles indicated that the effect of climate type is also closely linked to the soil texture. Simulations were run with compiled climate data from six different ecoclimatic regions in Alberta. The climate at these sites varied from arid to dry sub-humid. Results indicate that even for driest climate condition (arid climate) the water gain conditions at the ground surface could be expected for coarse-grained materials. Based on the results it can concluded that the hydraulic properties of the soil, namely soil water characteristic curve and hydraulic conductivity play a very important role is water balance at the ground surface. Coarse-grained materials have low retention and high conduction, facilitating the downward movement of the meteoric water. This makes them good evaporation soil barriers resulting in positive water balance at the ground surface, regardless of the climate type. However, the quantity of water gain and associated advective fluxes are a function of climate. Coarse material in wetter climate is expected to have higher water gain at the ground surface and larger downward advective flux values. Net water gain conditions at the ground surface however would result in downward movement of salt and therefore pose a risk for contamination of deeper groundwater resources. The risk of contamination of deeper groundwater resources for coarse-grained environments will be higher for wetter climates.

Flow and transport in fine textured soils seem to be even more dependent on the climate type. For arid climatic conditions, net water loss conditions exist for fine-grained soils. This is the result of the meteoric water, being held in soil layers closer to the

ground surface due to higher retention and lower conduction of fine-grained soils. Although such soils restrict the downward migration of the solute, upward transport to the root zone is probable. Therefore, for fine-grained materials and arid climatic conditions, it can be concluded that the vertical upward solute displacement from a diffusion dominated transport process can contaminate near surface soil layers. For wetter climates, the upward migration of salt in fine-grained soils is less probable. The results indicate that even very small quantities of water gain at the ground surface can induce enough downward advection to limit any upward diffusion. Based on the results it can also be concluded that for fine-grained soils in wetter climates, there is a higher probability of the salt to remain in near vicinity of its original location for longer periods of time.

5.2.3 Temporal resolution of meteorological input data and water and salt dynamics in variably saturated soils

In many instances, the climate data is only available at a daily resolution. An attempt to quantify the effect of temporal resolution of meteorological input data on flow and transport in variably saturated environments yielded the following conclusions.

The increase in temporal resolution of precipitation data resulted in *NI* value increases. The increase in the *NI* values was consistent with the decrease of *AE* values. The decreases of *AE* values and associated increase in *NI* values were observed for all climate types and for both coarse and fine-grained soil profiles. The review of results also indicated that the increase in *NI* values is higher for simulations run with the assumption that precipitation events happened outside the peak evaporation hours.

Based on the observations it can be concluded that the solute transport is accelerated as the resolution of precipitation data increases. It can also be concluded that the solute transport could potentially be faster for a particular temporal resolution of precipitation event, if the event occurred outside the peak evaporation hours.

In comparison to the arid climatic conditions, it can be concluded that the effect of precipitation intensity and time of occurrence is less pronounced in wetter climates especially for coarse-grained soils. It can also be concluded that with higher temporal resolution of precipitation data, net water gain conditions at the ground surface are simulated. This is in contrast to the simulation run with daily precipitation data which estimate net water loss conditions at the ground surface.

It should be noted that for fine grained material, the change in *NI* and *AE* values are less than those observed for coarse grained material. The primary reason for this is the difference in the hydraulic properties of the two materials. In comparison with coarse-grained material, the fine-grained material has higher retention and lower conduction. Therefore, for fine-grained materials the meteoritic water is held in the near surface soil layers longer as compared to coarse-grained materials. This results in higher actual evaporation for fine-grained materials than for coarse-grained material for same precipitation intensities. This observation is valid for both soil materials. However, differences in *AE* and *NI* appear to be an order of magnitude higher for coarse-grained material than for fine-grained material.

It was observed that for very small change in *NI* resulted in significantly changed solute transport in the domain, especially in arid climatic conditions. The change in resolution of precipitation data results in change of direction of solute transport.

Noteworthy to point out is that the biggest difference was seen in fine-grained material where changing the precipitation intensity results in no solute transport to the root zone. Based on the observations it can be concluded that the resolution of precipitation data is more important for simulations for fine-grained materials.

Moreover, as it was also explained before, earlier differences in fine and coarse-grained materials are due to the difference in their hydraulic properties. Less retention and more conduction in coarse materials facilitate the downward movement of water resulting in larger differences in *AE* and *NI* for different precipitation intensities. On the other hand, fine-grained materials impede downward movement of water due to more retention and less conduction, resulting in smaller differences in *AE* and *NI* for different precipitation intensities. The changes in *NI* values for different precipitation intensities are similar for the two climate types.

5.2.4 Interaction between groundwater table and atmosphere and its effect on water and salt dynamics in variably saturated soils

Based on the results presented in this thesis, it can be concluded that interaction between the groundwater table and atmosphere is not just a function of depth of groundwater table and unsaturated hydraulic properties of the soils. Climate type also plays an important role in the interaction between the groundwater table and atmosphere. This conclusion is based on the observation that for fine grained material and water table depth of 3m some interaction between the atmosphere and the groundwater table was observed for arid climatic condition. However, for dry sub-humid climatic conditions minimal to no interaction was observed between groundwater table

and atmosphere. This is attributed to the higher precipitation and lower evaporative demand for dry sub-humid climatic conditions, which results in higher downward fluxes in the system muting any capillary rise effects.

5.3 Contributions of this research

The research presented in this thesis provides a very first study on the effect of different climates from a particular geographical location on water and salt dynamics in variably saturated environments. This study highlights and addresses many important issues related to soil-atmosphere modeling such as: use of appropriate and representative climate data, temporal resolution of climate data, and relation between soil texture and climate. To the best of Author's knowledge, this is the first systematic study to look at some of these issues. Considering that salt release to land is associated with many activities such as oil and gas production, salt/sand processing, and runoff from snow removal dumps, it is anticipated that this study will be of interest to both academia and industry.

5.4 Recommendations for future research

5.4.1 Dimensionality

The current study investigated the vertical transport of salt in variably saturated environments. There are many instances where the lateral transport of salt could lead to contamination of surface and groundwater resources. Simulating flow and transport in two or three-dimensional variably saturated domains with soil-atmosphere boundary can

be computationally challenging. The simulations can become even more challenging if multi-year climate data sets are to be used. The use of multi-year climate datasets is essential to capture the effect of year to year variation in climate on results. Future research work should consider multi-dimensional models.

5.4.2 Effects of soil layer configuration

Layered soil profiles can be routinely found in the field. Layering can be result of any number of processes such as eluviation–illuviation, bioturbation and surface removal, erosion, deposition or inheritance (Phillips, 2001). Layering can affect both upward and downward movement of water and solute transport. For example, a fine textured soil overlying a coarse soil can act as capillary barrier and restrict the downward flow and transport. Additionally such layering configuration could also potentially affect the capillary rise owing to low air entry value of the coarse material. Future work should include a comprehensive study on the layering effects of soils on water and salt dynamics in variably saturated soils.

5.4.3 Comparison with existing risk assessment methods

Alberta Environment requires the use of a specific risk assessment tool SST (Alberta Environment, 2011) for developing Tier 2 soil remediation guidelines for chloride-based salt contamination below the root zone. Assessments by the recommended tool are very conservative and lack a rigorous approach for: (i) unsaturated flow and transport modeling (ii) soil-atmosphere boundary consistent with

various natural regions of Alberta (Bashir, R. 2014). As part of the future work, consideration should be given to making comparison between assessments using SST and site-specific modelling using the methodology employed in this research.

5.4.4 Effect of climate change

There is irrefutable scientific evidence that climate change is real. As shown in this research, transport in the upper soil layers is controlled by the atmospheric interactions via infiltration of meteoritic water. In lower layers, it is controlled by change in groundwater table depth, which can also be linked to atmospheric interactions via groundwater recharge. Therefore, the climate change is an important factor in water and salt dynamics in variably saturated environments. The effect of climate change for various regions of Alberta can be taken into consideration using Alberta Climate Model (Alberta Environment, 2005) and climate change scenarios for Alberta (Barrow, E. and Yu, G., 2005) as part of future work.

References

Chapter 1 – References

– Alberta Government. 2014. Subsoil salinity tool help file (version 2.5.3). Prepared by: Equilibrium Environmental Inc.

– Alberta Environment and Sustainable Resource Development (ESRD). 2014. Alberta Tier 2 and groundwater remediation guidelines. Land and Forestry Policy Branch. 151

– Alberta Environment (AENV). 2014. Water Act. Revised Status of Alberta 2000, Chapter W-3 with amendments current as December, 17, 2014

– Alberta Environment (AENV). 2001. Salt contamination assessment & remediation guidelines. Environmental Sciences Division. Environmental Services. ISBN: 0-7785-1717-9

– Anderson, M.P., and Woessner, W.M., 1992. Applied groundwater modeling. Academic Press, California, 381 pages.

– Donado, L. 2009. On multicomponent reactive transport in porous media: from the natural complexity to analytical solutions. University of Catalonia

– Feddes, R.A., Kabat, P., Van Bakel, P.J.T., Bronswijk, J.J.B., and Halbertsma, J. 1988. Modeling soil water dynamics in the unsaturated zone – State of the art. Journal of Hydrogeology, 100 (1988) 69-111

– Fredlund, D.G., Rahardjo, H. Fredlund, M.D. 2012. Unsaturated Soil Mechanics in Engineering Practice. John Willey & Sons Inc. New Yersey

– Gladyeva, R., and Saifadeen, A. 2012. Effect of hysteresis and temporal variability in meteorological input data in modeling of solute transport in the unsaturated soils using hydrus-1D. Journal of water management and research 68:285-293. Lund University.

– Government of Alberta. 2006. Environmental Protection Plan and Enhancement Act. Revised Status of Alberta 2000, Section E-12 with amendments in force as May, 24, 2006

– Hetrick, D. M., Travis, C.C., Kinerson, R.S. 1988. Comparison of an unsaturated soil zone model (SESOIL) predictions with a laboratory leaching experiment.

Proceedings of the 1988 Winter Simulation Conference M. Abrams, P. Haigh, and J. Comfort (eds). DOI: 10.1109/WSC.1988.716263

– Li, X. Chang, S. Salifu, K. 2013. Soil texture and layering effects on water and salt dynamics in the presence of a water table: a review. NRC Research Press. Env. Rev. 22: 41-50 pages

– Liu, S., Graham, W.D., Jacobs, J.M. 2004. Daily potential evaporation and diurnal climate forcings: influence on the numerical modelling of soil water dynamics and evaporation. Journal of Hydrology 309 (2005) 39-52

– Otton, J. 2006. Environmental aspects of produced-water salt releases in onshore and coastal petroleum-producing areas of the conterminous U.S. A Biography. U.S. Geological Survey, Reston, Virginia 2006. Open-file report 2006-1154

– Robertson, C., Ratiu, I., and Bures, G.H. 2015. In-situ remediation of brine impacted soils and groundwater using hydraulic fracturing, desalinization and recharge wells. Environmental Services Association of Alberta

– Ruttherford, S. 2004. Groundwater use in Canada. West Coast Environmental Law

– Rahman, S. 2014. Soil moisture measurements and modeling at a geomorphically reclaimed coal mine in New Mexico. Master of Science in Civil Engineering. University of New Mexico. Albuquerque, New Mexico

– Šimůnek, J. 2005. Models of water flow and solute transport in the unsaturated zone. Encyclopaedia of hydrological sciences. Edited by M.G. Anderson John Wiley & Sons, Ltd.

– Šimunek, J. van Genuchten, M. 2006. The Handbook of Groundwater Engineering. Chapter 22: Contaminant Transport in the Unsaturated Zone Theory and Modeling. Second Edition.CRC Press. Florida

– Zekser, I. and Everett, L. 2004. Groundwater resources of the world and their use. IHP-VI, Series of Groundwater No. 6. ISBN 92-9220-007-0

Chapter 2 – References

- Agriculture and Agri-Food Canada. 1998. The Canadian System of Soil Classification. Third edition. Soil Classification Working Group, Expert Committee on Soil Survey. Land Resource Research Centre, Ottawa.

- Alberta Government (GOA). 2014. Subsoil Salinity Tool Help File – Version 2.5.3. Prepared by Equilibrium Environmental Inc.

- Allen, R., Pereira, L., Raes, D., Smith, M. 1998. Cro Evapotranspiration – Guidelines for computing crop water requirements. United Nations Organization – Food and Agriculture Organization, FAO Irrigation and Drainage. Rome. M-56, ISBN 92-5-104219-5

- Bashir, R., Sharma, J., Stefaniak, H. 2015. Effect of hysteresis of soil-water characteristic curves on infiltration under different climatic conditions. NRC Research Press. Can. Geotech. J. 53:273-284 (2016) dx.doi.org/10.1139/cgj-2015-004

- Brook, R.H. and Corey, A.T. 1964. Hydraulic properties of porous media. Colorado State University. Hydrology paper, No. 3, Vol. 27

- Carsel, R., Parrish, R. 1988. Developing joint probability distributions of soil water retention characteristics. Water Resources Research, Vol. 24, No. 5, pages 755-769

- Deeb, M., Grimaldi, M., Lerch, T., Pando, A., Podwojewski, P., Blouin, M. 2016. Influence of organic matter content on hydro-structural properties of contrunstedtechnosols. Pedosphere 26(4): 486-498. Doi: 10.1016/S1002-0160(15)60059-5

- Delleur, J.W. 2007. The handbook of groundwater engineering. Second Edition. CRC Press. ISBN-13: 978-0-8493-4316-2

- Gladyeva, R., and Saifadeen, A. 2012.Effect of hysteresis and temporal variability in meteorological input data in modeling of solute transport in the unsaturated soils using hydrus-1D. Journal of water management and research 68:285-293. Lund University.

- Freeze, A., Cherry, J. 1979. Groundwater. Prentice Hall, Englewood Cliffs, NJ 07632

- Fredlund, D.G., Rahardjo, H. Fredlund, M.D. 1993. Soil mechanics for unsaturated soils. New York: Willey Publications, p. 517

- Fredlund, D.G., Rahardjo, H. Fredlund, M.D. 2012. Unsaturated soil mechanics in engineering practice. John Willey & Sons Inc. New Yersey

- Friske, P.W.B., Ford, K.L., Kettles, I.M., McCurdy, M.W., McNeil, R.J., and Harvey, B.A. 2010. North American soil geochemical landscapes project: Canadian field protocols for collecting mineral soils and measuring soil gas radon and natural radioactivity. Geological Survey of Canada, Open File 6282

- Heshmati, A.A., and Motahari, M.R., 2012. Identification of key parameters on soil water characteristic curve. Life Sci J 2012; 9(3): 1532-1537. ISSN: 1097-8135

- Huang. P. M., Li, Y., Sumner, M.E. 2012. Handbook of soil sciences – properties and processes. Second Edition. CRC Press – Taylor and Francis Group. 6000 Broken Sound Parkway NW, Suite 300. Boca Raton, FL. 33487-2742

- Li, X., Chang, S., Salifu, K. 2014. Soil Texture and layering effects on water and salt dynamics in the presence of a water table: a review. NRC Research Press. Env. Rev. 22: 41-50

- Maulem, Y., 1976. A new model for prediction of the hydraulic conductivity of unsaturated porous media. Water Resources Research 12(3), 513-522

- Narasimhan, T.N. 2005. Buckingham 1907: An Appreciation. Vadose Zone Journal, 4:434-441. DOI: 10.2136/vzj204-0126

- Neuman, S. P., Feddes, R.A., and Bresler, E. 1974. Finite element simulation of flow in saturated-unsaturated soils considering water uptake by plants. Third annual report. Project No. A10-SWC77, Hydraulic Engineering Lab., Technion, Haifa, Israel.

- Nielsen, D.R. 1958. Movement of water in unsaturated soils as related to soil physical properties. Ph.D. Thesis. Iowa State College

- Pan, L. And Wierenga, P. 1995. A transformed pressure head-based approach to solve Richard's equation for variably saturated soils. Water Resources Research 31: doi: 10.1029/94WR03291.issn: 0043-1397

- Patil, N.G. and Singh, S.K. 2016. Pedotransfer Functions for Estimating Soil Hydraulic Properties: A Review, Pedosphere, 26(4): 417-430.

- Richards, L.A. 1931. Capillary conduction of liquids through porous mediums. Journal of Applied Physics 1, 318; doi: 10.1063/1.17455010

- Ryle, M. and Vonberg, D.D. 1947. Solar Radiation at 175 Mc/s. Nature 158 (1946) 339

- Saxton, K.E. and Rawls, W.J. 2006. Soil Water Characteristic Estimates by Texture and Organic Matter for Hydrologic Solutions, Soil Sci. Soc. Am. J., 70: 1569-1578

- Schaap, M.,Leij, F., van Genuchten, M. 2001. Rosetta computer program for estimating soil hydraulic parameters with hierarchical pedotransfer functions. Journal of Hydrogeology 251 163-176

- Šimunek, J. van Genuchten, M. 1996. Estimating unsaturated soil hydraulic properties from tension disc infiltrometer data by numerical inversion. Water resources research. Vol. 32, No. 9, pages 2683-2696

- Šimunek, J. van Genuchten, M. 2006. The Handbook of Groundwater Engineering. Chapter 22: Contaminant Transport in the Unsaturated Zone Theory and Modeling. Second Edition. CRC Press. Florida

- Šimůnek, J. 2008. System-Dependent Boundary Conditions – Atmospheric Boundary Conditions. Department of Environmental Sciences, University of California Riverside

- Šimunek, J., Šejna, M, Saito, H., Sakai, M, van Genuchten, M. Th. 2013. The Hydrus-1D Software Package for Simulating the One-Dimensional Movement of Water, Heat, and Multiple Solutes in Variably-Saturated Media. Version 4.16. Department of Environmental Sciences. University of California Riverside, Riverside, California

- Tietje, O. And Hennings, V. 1996. Accuracy of the saturated hydraulic conductivity prediction by pedo-transfer functions compared to the variability within FAO textural classes. Elsevier Sciences. 0016-7061

- Van Genuchten, M.T., 1980. A closed-form equation for predicting the hydraulic conductivity of unsaturated soils. Soil Science Society of America Journal 44, 892-898

- Verreken, H., Weynants, M., Javaux, M., Pachepsky, Y., Schaap, M., van Genuchten, M. Th. 2010. Using pedotransfer functions to estimate the Genuchten-Maulem soil hydraulic properties: a review. Soil Science Society. Vadose Zone J. 9:795-820. doi: 10.236/vzj2010.0045

- United States Department of Agriculture. 1987. Module 3 – USDA textural soil classification – Study guide. National Employee Development Staff.Soil Conservation Service.

- Unguraşu, A.N., Anei, F.D., Stătescu, F. 2012. Estimation of soil hydraulic parameters with help of rosetta program. LucrăriŞtlinţifice. Vol. 55 Supliment/2012, seriaAgronomie

Chapter 3 – References

- Alberta Government (GOA). 2014. Subsoil Salinity Tool Help File – Version 2.5.3. Prepared by Equilibrium Environmental Inc.

- Brook, R.H. and Corey, A.T. (1964). Hydraulic properties of porous media. Colorado State University. Hydrology paper, No. 3, Vol. 27

- Carsel, R., Parrish, R. 1988. Developing joint probability distributions of soil water retention characteristics. Water Resources Research, Vol. 24, No. 5, pages 755-769

- Das, Y. 2015. Water balance and climatic classification of a tropical city Delhi - India. American Journal of Water Resources, vol. 3, no. 5: 124-146. doi: 10.12691

- Downing, D., Pettapiece, W. 2006. Natural regions and subregions of Alberta. Natural regions committee. Government of Alberta. Pub. No. T/852

- Environment Canada. 2017. Canadian climate normal 1981-2010. Retrieved from http://climate.weather.gc.ca/climate_normals/index_e.html

- Fredlund, D.G., Rahardjo, H. Fredlund, M.D. 2012. Unsaturated Soil Mechanics in Engineering Practice. John Willey & Sons Inc. New Yersey

- Gladyeva, R., and Saifadeen, A. 2012. Effect of hysteresis and temporal variability in meteorological input data in modeling of solute transport in the unsaturated soils using hydrus-1D. Journal of water management and research 68:285-293. Lund University.

– Shah, N., Nachabe, M. Ross, M. 2007. Extinction depth and evapotranspiration from groundwater under selected land covers. Ground water, Vol. 45, No 3 (pages 329-338)

– Šimunek, J., Šejna, M, Saito, H., Sakai, M, van Genuchten, M. Th. 2013. The Hydrus-1D Software Package for Simulating the One-Dimensional Movement of Water, Heat, and Multiple Solutes in Variably-Saturated Media.Version 4.16. Department of Environmental Sciences. University of California Riverside, Riverside, California

– Thornthwaite, C.W. and Hare, F.K. 1955. Climatic classification in forestry. Unasylva 9(2):51-59

Chapter 4 – References

– Alberta Environment and Sustainable Resource Development (ESRD). 2013. Evaporation and Evapotranspiration in Alberta.

– Den Hartog, G. and Ferguson, H.L. 1978. Mean Annual Lake Evaporation. Hydrological Atlas of Canada. Survey and Mapping Branch. Department of Fisheries and the Environment

– Downing, D., Pettapiece, W. 2006. Natural regions and subregions of Alberta. Natural regions committee. Government of Alberta. Pub. No. T/852

– Environment Canada. 2017. Canadian climate normal 1981-2010. Retrieved from http://climate.weather.gc.ca/climate_normals/index_e.html

Chapter 5 – References

– Alberta Environment. 2011. Reclamation criteria for wellsites and associated facilities application guidelines. Alberta Environment. Edmonton Alberta, 52 pp

- Alberta Environment. 2005. Alberta Climate Model (ACM) to provide climate estimates (1961-1990) for any location in Alberta from its geographic coordinates. Publ. No. T/749. Alberta Environment.

- Barrow E. & Yu, G. 2005: Climate scenarios for Alberta. A report prepared for the Prairie Adaptation. Research Collaborative (PARC) in co-operation with Alberta Environment

- Gladyeva, R., and Saifadeen, A. 2012. Effect of hysteresis and temporal variability in meteorological input data in modeling of solute transport in the unsaturated soils using hydrus-1D. Journal of water management and research 68:285-293. Lund University.

- Phillips, J.D. 2001. Contingency and generalization in pedology, as exemplified by texture-contrast soils. Geoderma. Volume 102, Issues 3-4, pages 347-370

- Bashir, R. 2014. Personal communication. December 15, 2014.

- Thornthwaite, C.W., 1948: An approach toward a rational classification of climate. Geographical Review 38, 55–94

APPENDICES

Appendix A.1
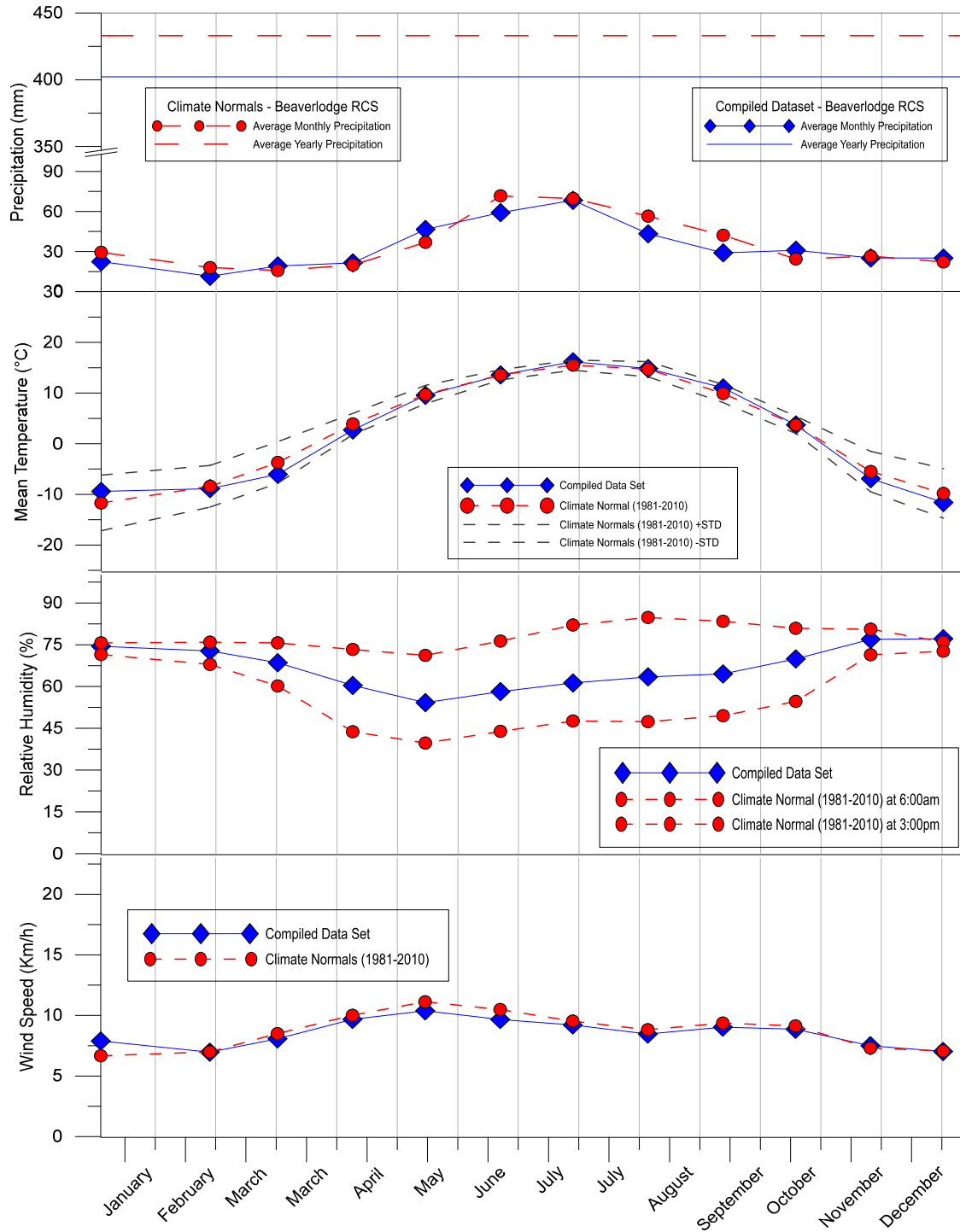
Fig. A.1: Compiled climate data vs Canadian climate normals of Beaverlodge Region

Appendix A.2
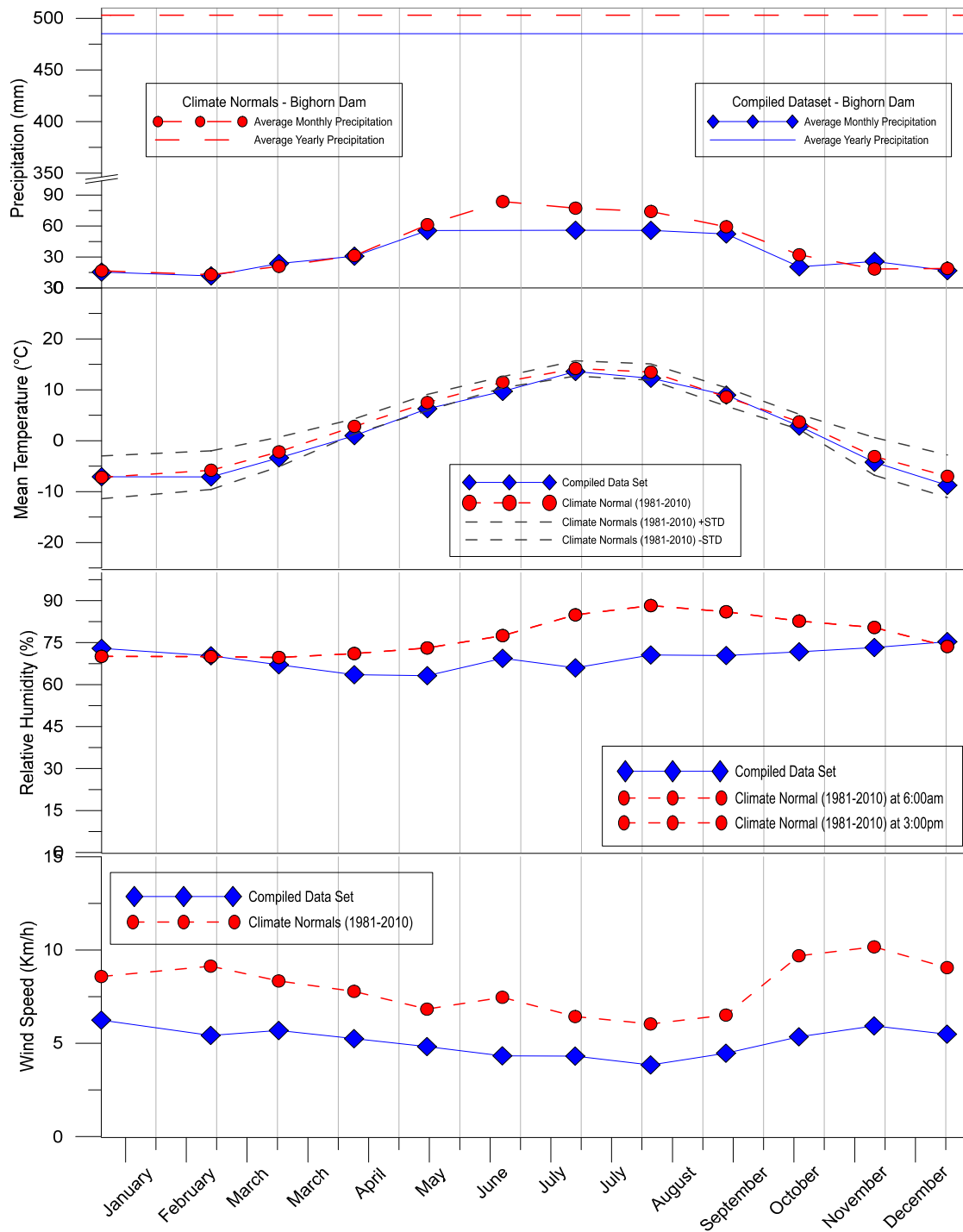
Fig. A.2: Compiled climate data vs Canadian climate normals of Bighorn Region

Appendix A.3
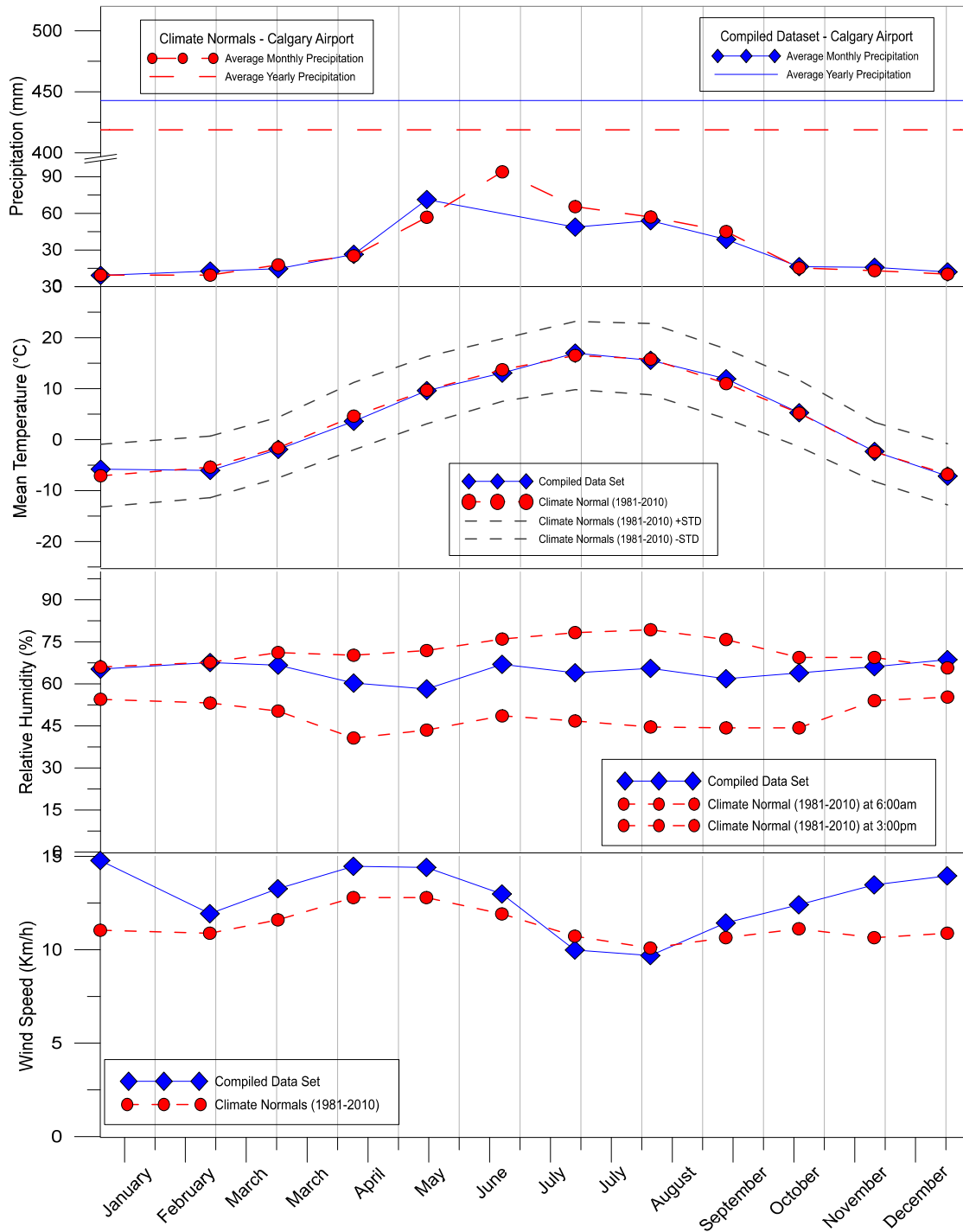
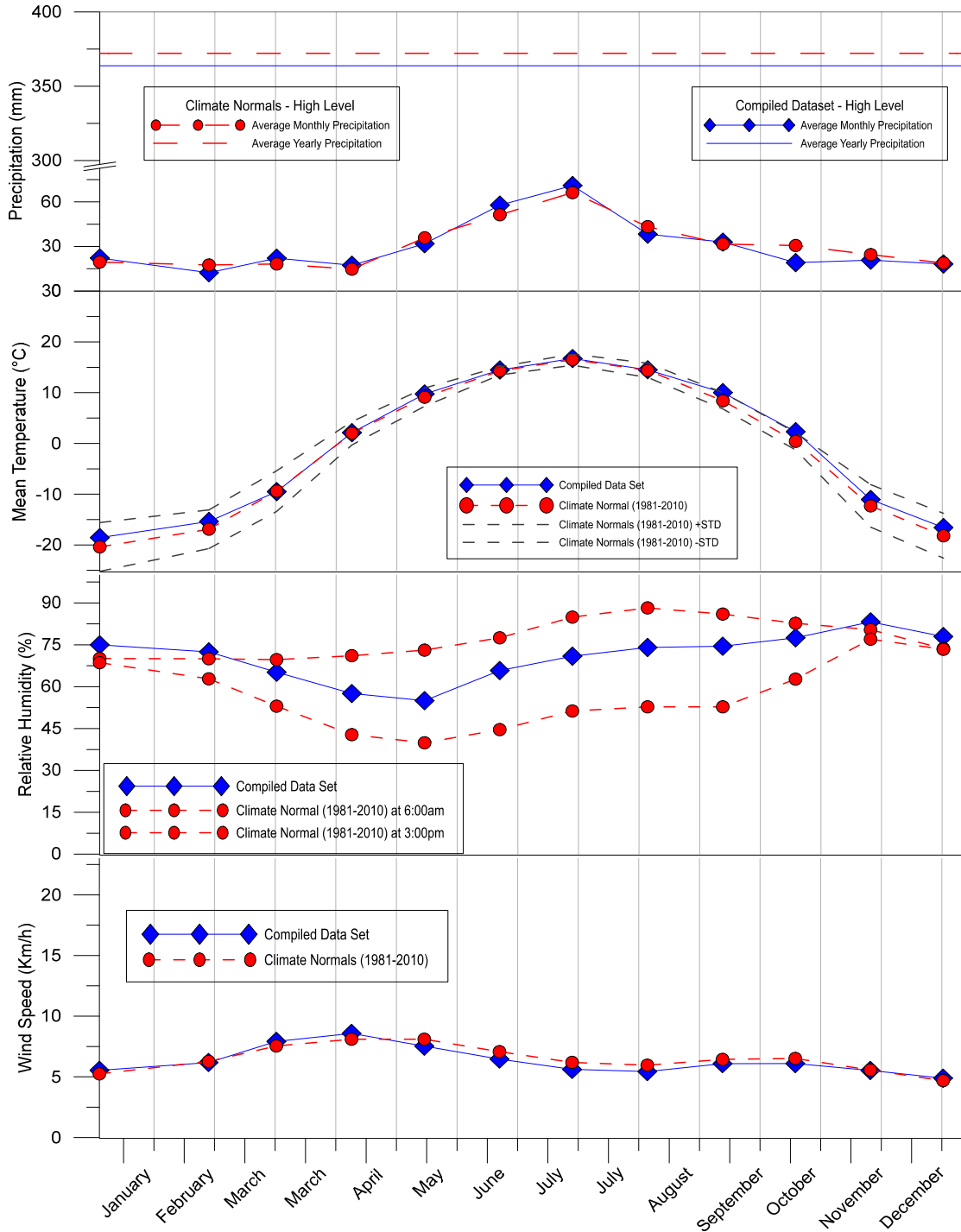**Fig. A.3:** Compiled climate data vs Canadian climate normals of Calgary Region

Appendix A.4
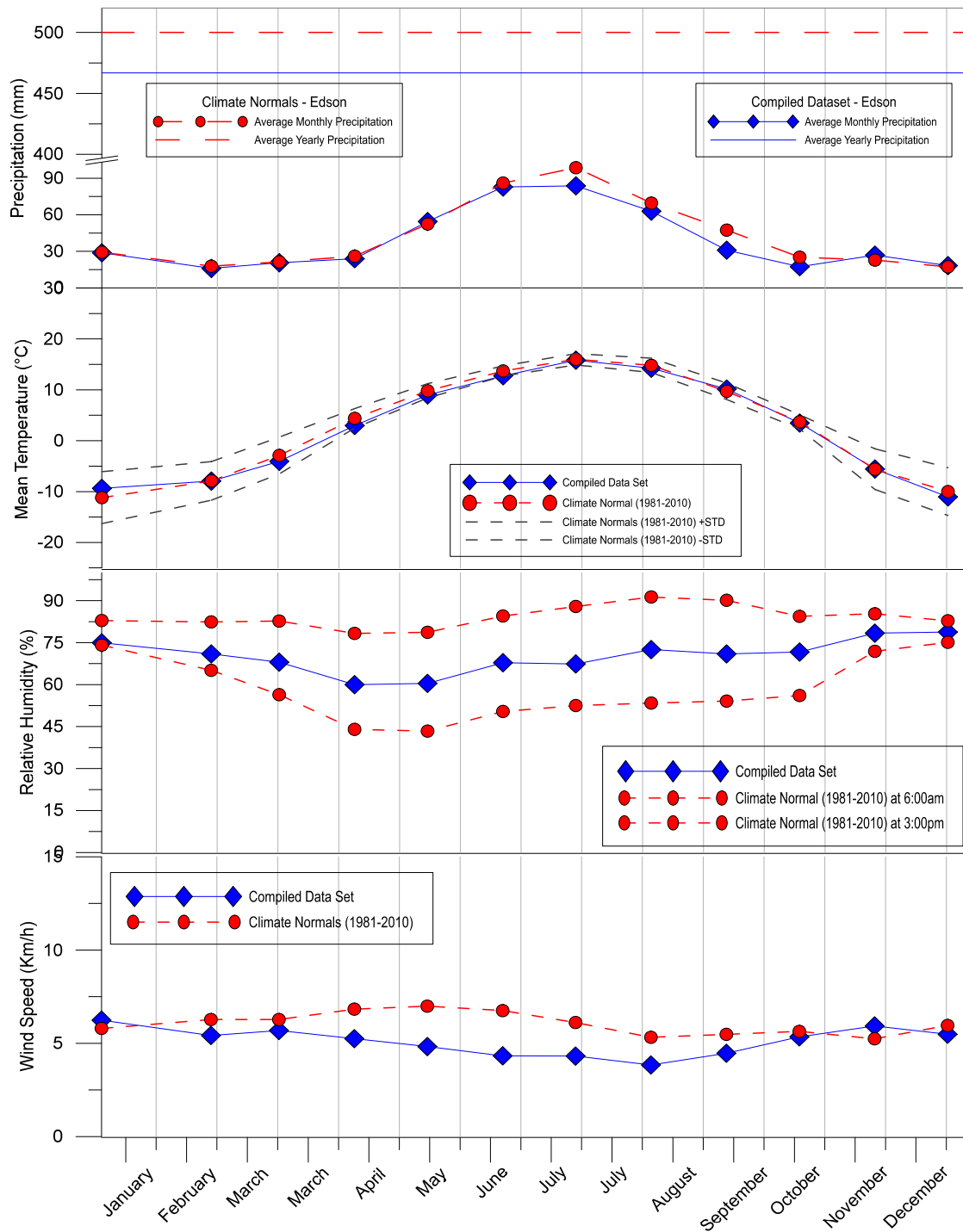
Fig. A.4: Compiled climate data vs Canadian climate normals of Edson Region
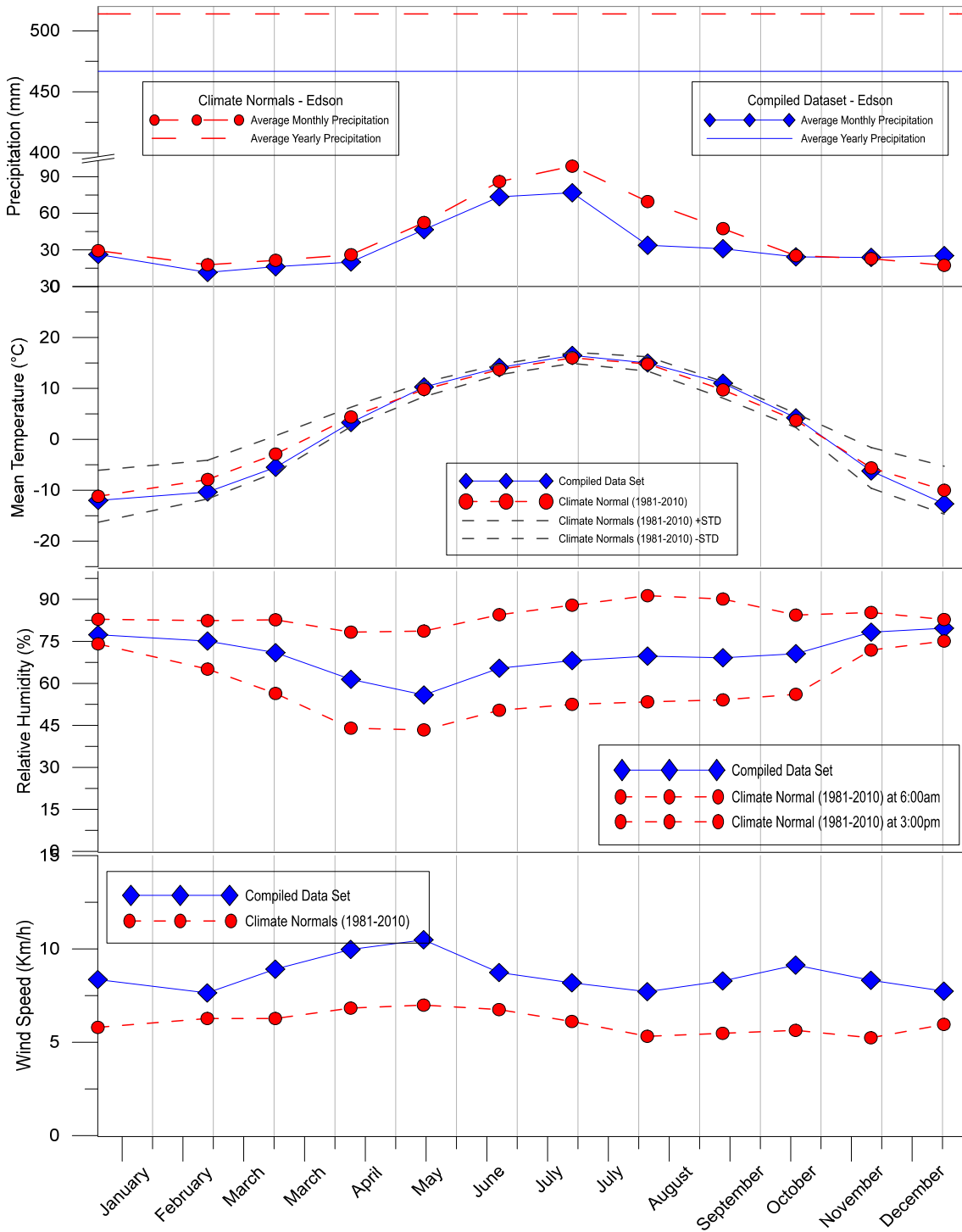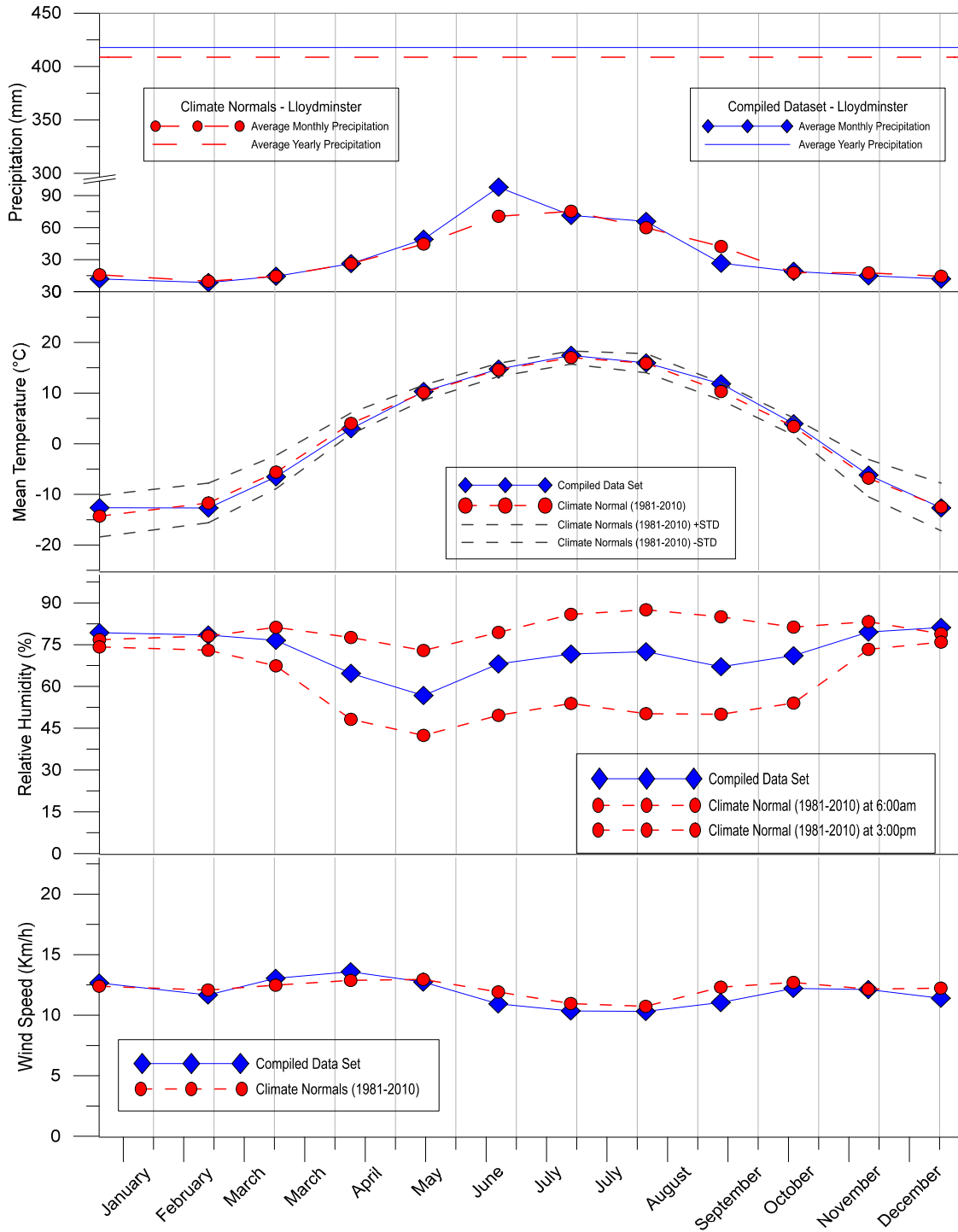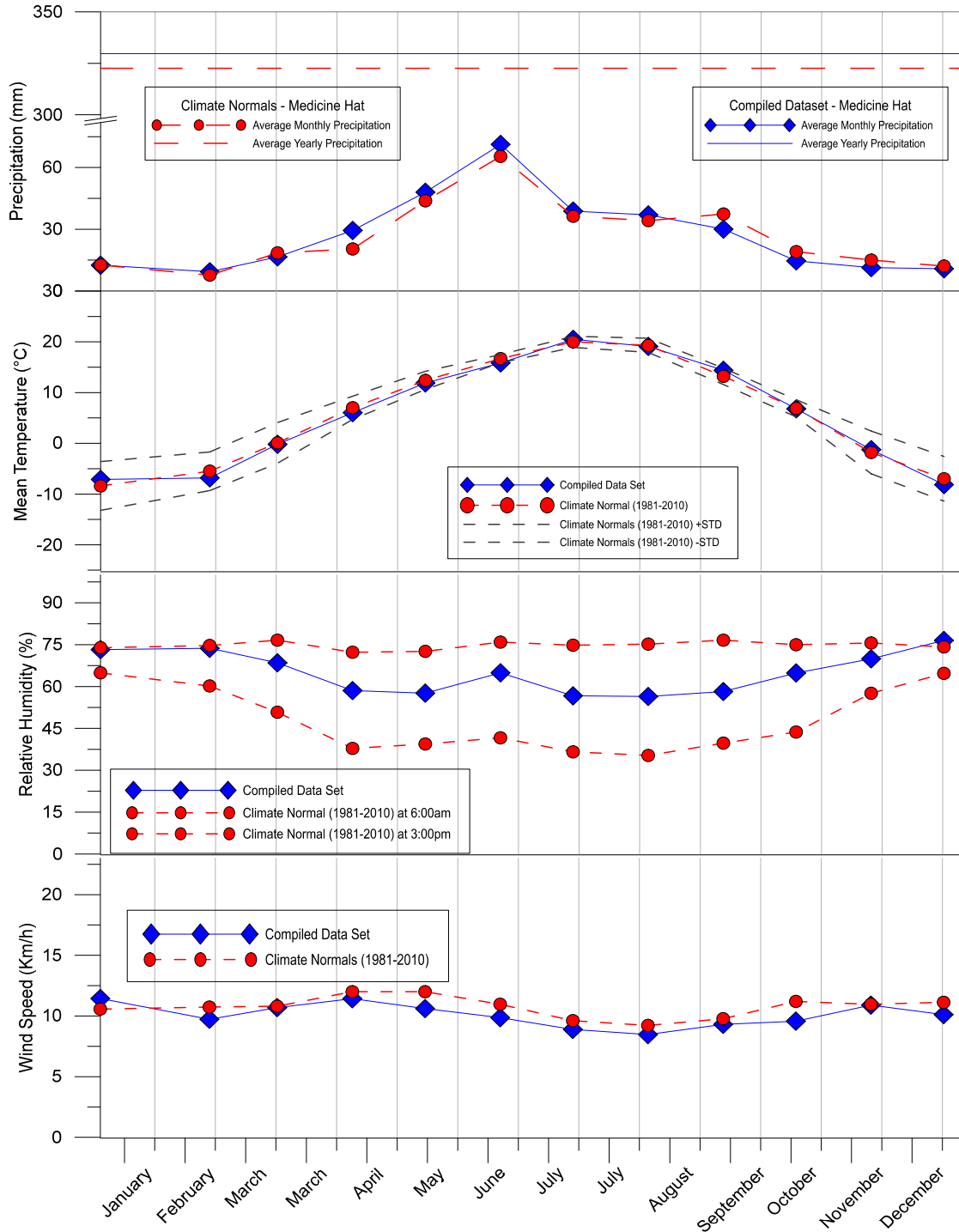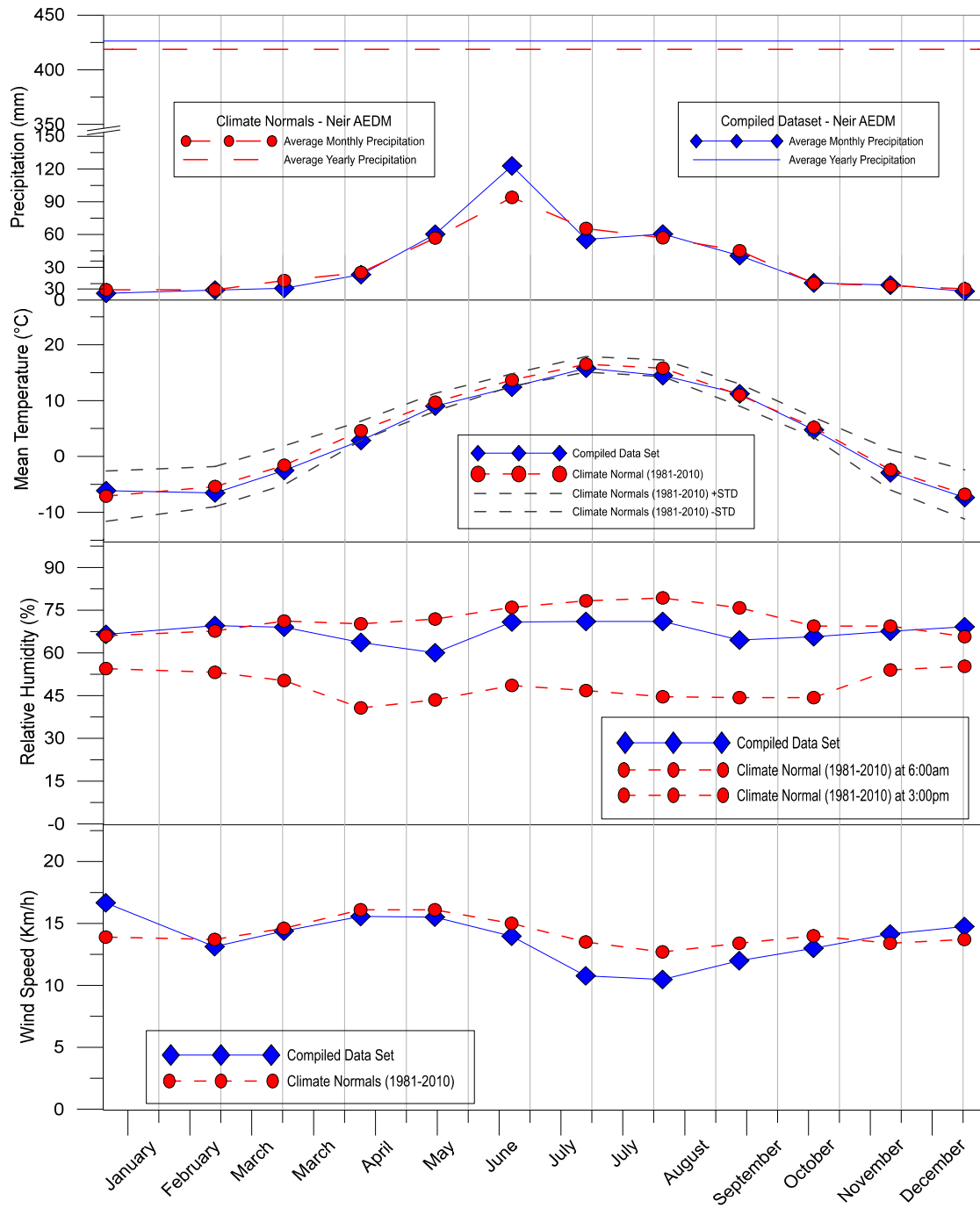
127
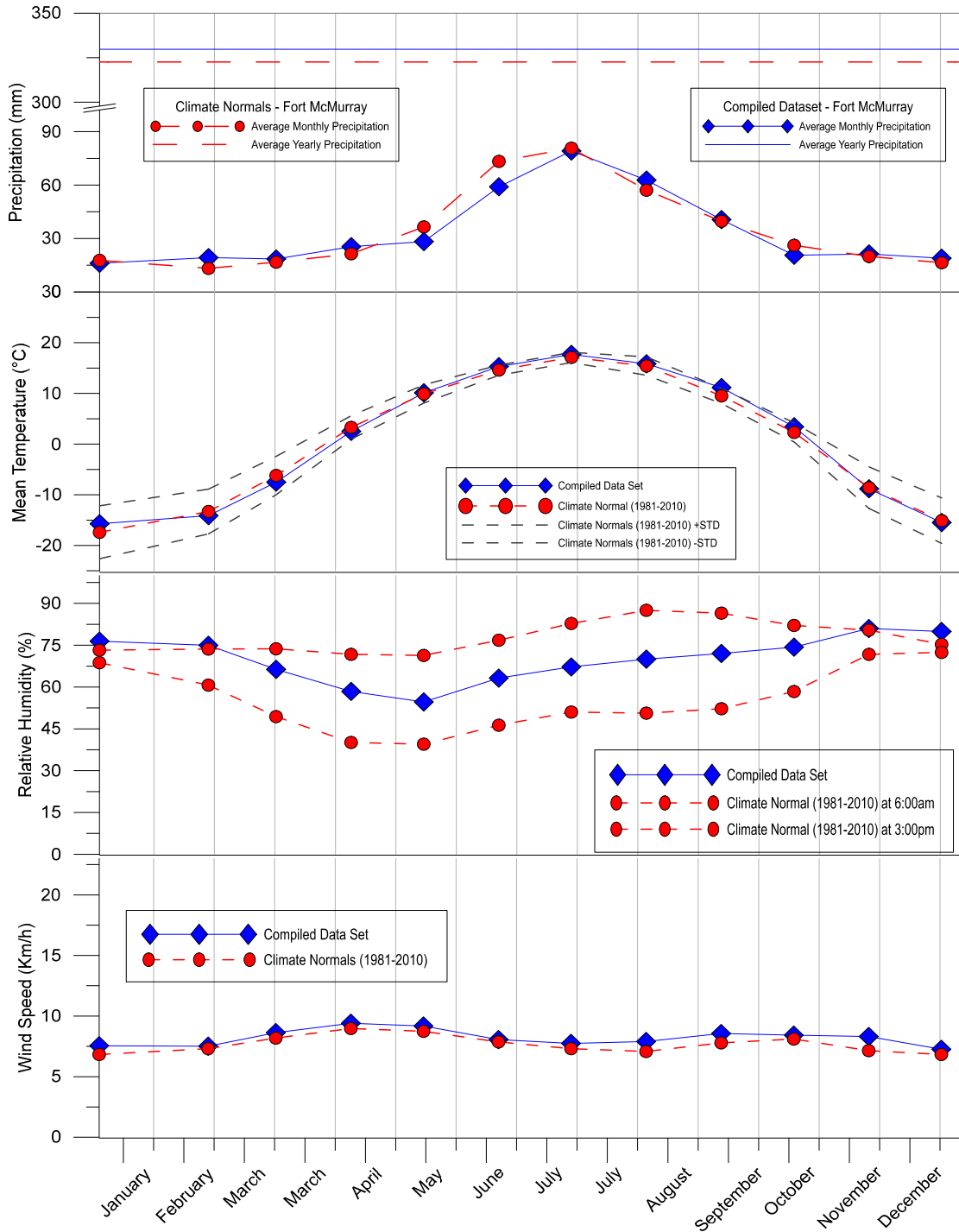
Appendix A.5

Fig. A.5: Compiled climate data vs Canadian climate normals of Fort Mcmurray Region

128

Appendix A.6

Fig. A.6: Compiled climate data vs Canadian climate normals of High Level Region

Appendix A.7

Fig. A.7: Compiled climate data vs Canadian climate normals of High Prairie Region

Appendix A.8

Fig. A.8: Compiled climate data vs Canadian climate normals of Lloydminster Region

Appendix A.9

Fig. A.9: Compiled climate data vs Canadian climate normals of Medicine Hat Region

Appendix A.10

**Fig. A.10:** Compiled climate data vs Canadian climate normals of Neir Region

Appendix B.1
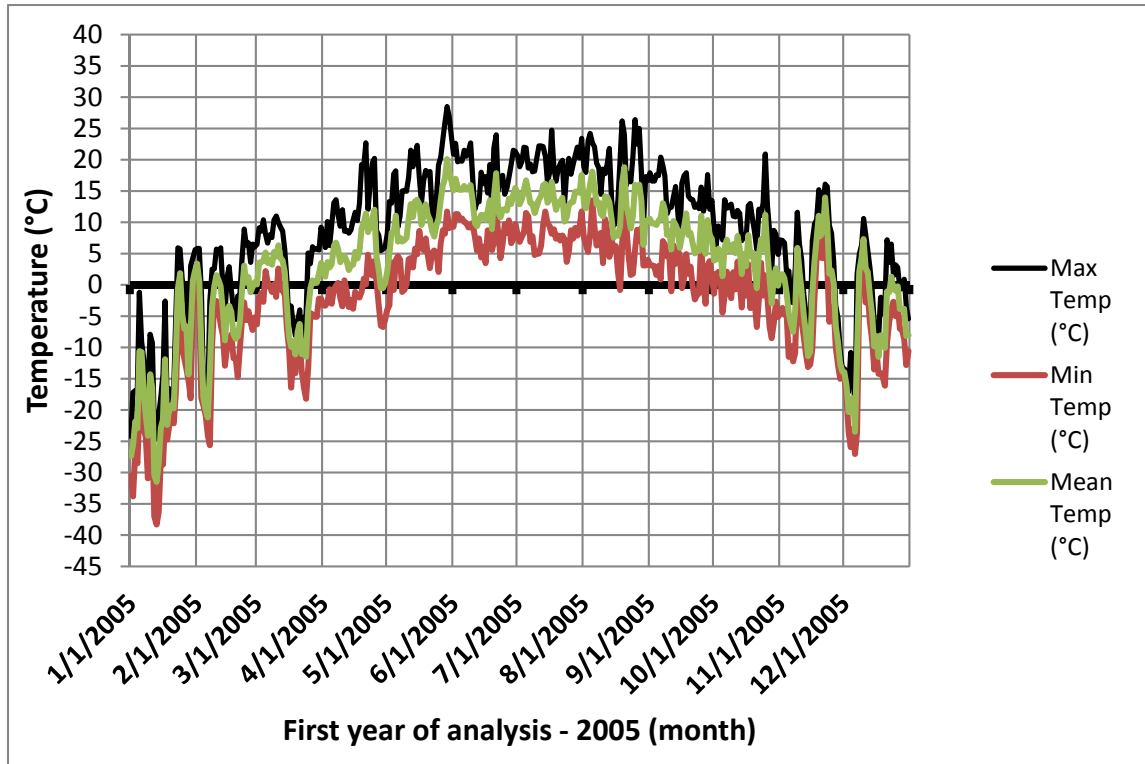
Table B.1: Calculation of the Active Season of the Beaverlodge Region

Year	Thaw	Freeze
2005	Friday, April 04, 2014	Tuesday, November 18, 2014
2006	Saturday, April 05, 2014	Tuesday, November 04, 2014
2007	Monday, April 14, 2014	Saturday, November 08, 2014
2008	Wednesday, April 09, 2014	Thursday, November 06, 2014
2009	Saturday, April 12, 2014	Tuesday, November 04, 2014
2010	Sunday, April 13, 2014	Saturday, November 15, 2014
2011	Wednesday, April 09, 2014	Tuesday, November 11, 2014
2012	Friday, April 04, 2014	Monday, October 27, 2014
2013	Tuesday, April 15, 2014	Tuesday, November 04, 2014
2014	Friday, April 18, 2014	Friday, November 07, 2014
Active Season	Thursday, April 10, 2014	Friday, November 07, 2014

Top: Compiled maximum, minimum, and mean temperature (°C) records corresponding with the first year of analysis (2005) at Beaverlodge Region.
Bottom: Calculation of the active season based on compiled nine-year continuous temperature records at Beaverlodge Region.

Appendix B.2
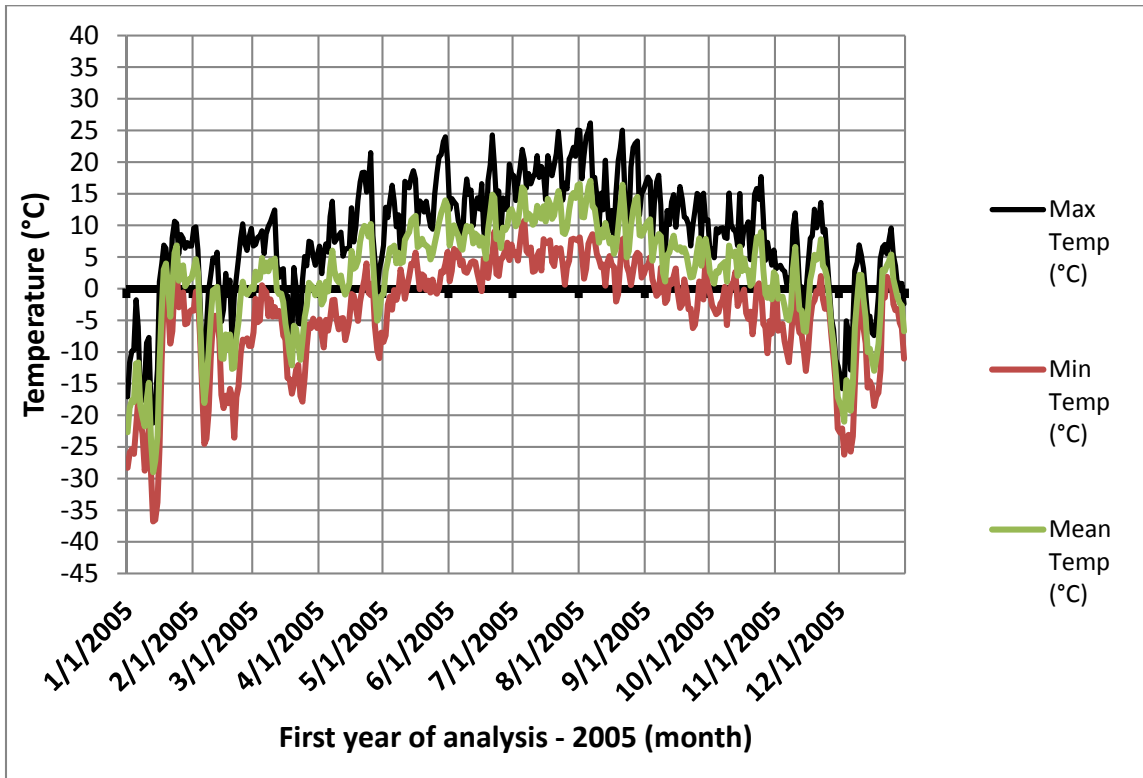
Year	Thaw	Freeze
Table B.2: Calculation of the Active Season of Bighorn Region		
2005	Saturday, April 12, 2014	Friday, November 14, 2014
2006	Monday, April 07, 2014	Monday, November 03, 2014
2007	Monday, April 14, 2014	Thursday, November 06, 2014
2008	Saturday, April 26, 2014	Wednesday, November 19, 2014
2009	Monday, April 14, 2014	Tuesday, November 11, 2014
2010	Wednesday, April 16, 2014	Friday, November 14, 2014
2011	Thursday, April 24, 2014	Saturday, November 01, 2014
2012	Thursday, April 17, 2014	Friday, November 07, 2014
2013	Friday, April 25, 2014	Tuesday, November 04, 2014
2014	Thursday, April 24, 2014	Monday, November 10, 2014
Active Season	Thursday, April 17, 2014	Saturday, November 08, 2014

Top: Compiled maximum, minimum, and mean temperature (°C) records corresponding with the first year of analysis (2005) at Bighorn Region.
Bottom: Calculation of the active season based on compiled nine-year continuous temperature records at Bighorn Region.

135

Appendix B.3

Top: Compiled maximum, minimum, and mean temperature (°C) records corresponding with the first year of analysis (2005) at *Calgary Region*.
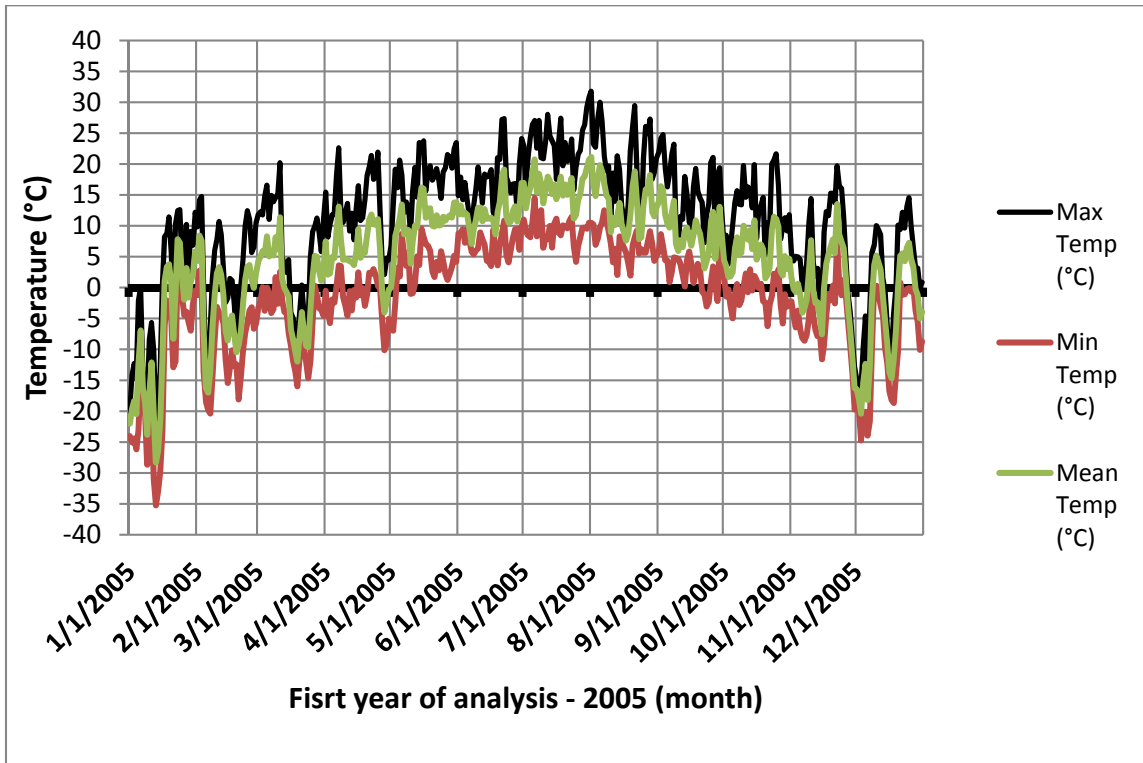
Table B.3: Calculation of the Active Season of the Calgary Region		
Year	**Thaw**	**Freeze**
2005	Friday, April 04, 2014	Thursday, November 27, 2014
2006	Sunday, March 30, 2014	Tuesday, November 04, 2014
2007	Monday, April 14, 2014	Tuesday, November 25, 2014
2008	Thursday, April 10, 2014	Wednesday, November 19, 2014
2009	Friday, April 11, 2014	Friday, November 21, 2014
2010	Tuesday, April 01, 2014	Sunday, November 16, 2014
2011	Tuesday, April 22, 2014	Saturday, November 08, 2014
2012	Friday, April 18, 2014	Friday, November 07, 2014
2013	Tuesday, April 22, 2014	Sunday, November 16, 2014
2014	Sunday, April 20, 2014	Sunday, November 09, 2014
Active Season	Saturday, April 12, 2014	Saturday, November 15, 2014

Top: Compiled maximum, minimum, and mean temperature (°C) records corresponding with the first year of analysis (2005) at *Calgary Region*.
Bottom: Calculation of the active season based on compiled nine-year continuous temperature records at Calgary Region.
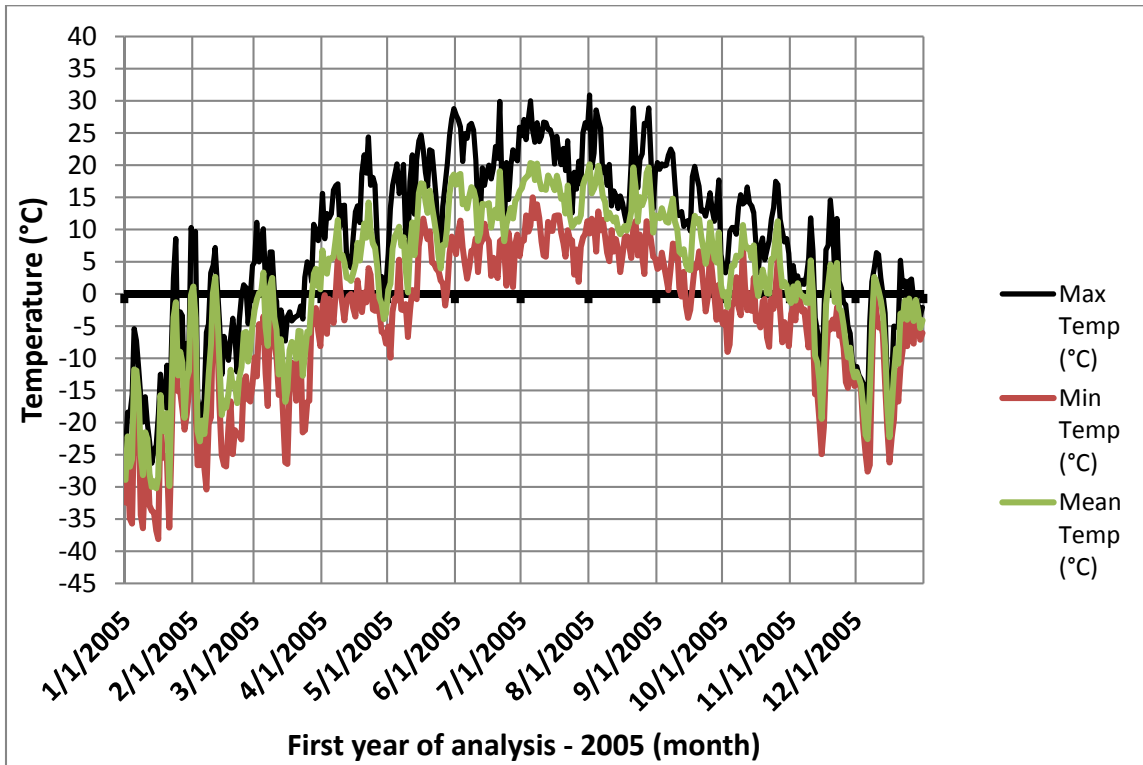
Appendix B.4
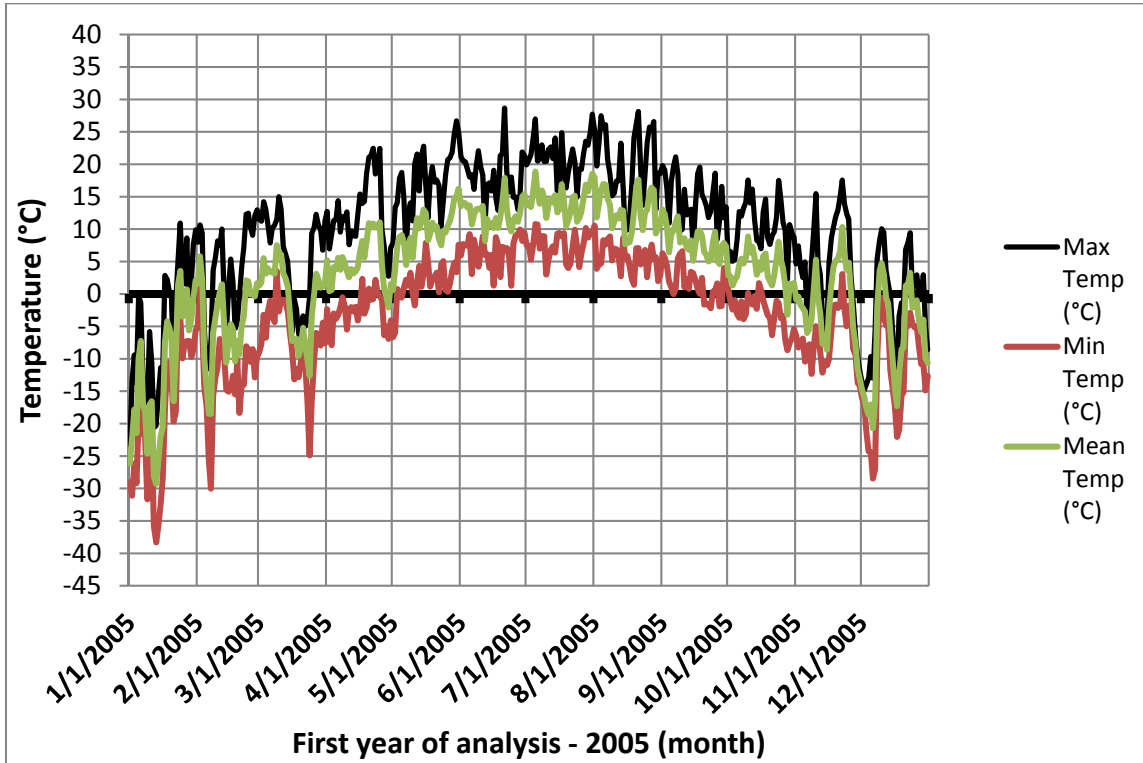
Table B.4: Calculation of the Active Season of the Edson Region		
Year	**Thaw**	**Freeze**
2005	Thursday, April 03, 2014	Tuesday, November 04, 2014
2006	Friday, April 04, 2014	Tuesday, November 04, 2014
2007	Tuesday, April 08, 2014	Tuesday, November 04, 2014
2008	Tuesday, April 08, 2014	Tuesday, November 11, 2014
2009	Friday, April 11, 2014	Sunday, November 09, 2014
2010	Sunday, April 13, 2014	Sunday, November 16, 2014
2011	Tuesday, April 22, 2014	Sunday, November 02, 2014
2012	Thursday, April 17, 2014	Monday, October 27, 2014
2013	Tuesday, April 22, 2014	Tuesday, November 04, 2014
2014	Saturday, April 19, 2014	Saturday, November 08, 2014
Active Season	Saturday, April 12, 2014	Wednesday, November 05, 2014

Top: Compiled maximum, minimum, and mean temperature (°C) records corresponding with the first year of analysis (2005) at Edson Region.
Bottom: Calculation of the active season based on compiled nine-year continuous temperature records at Edson Region.

Appendix B.5

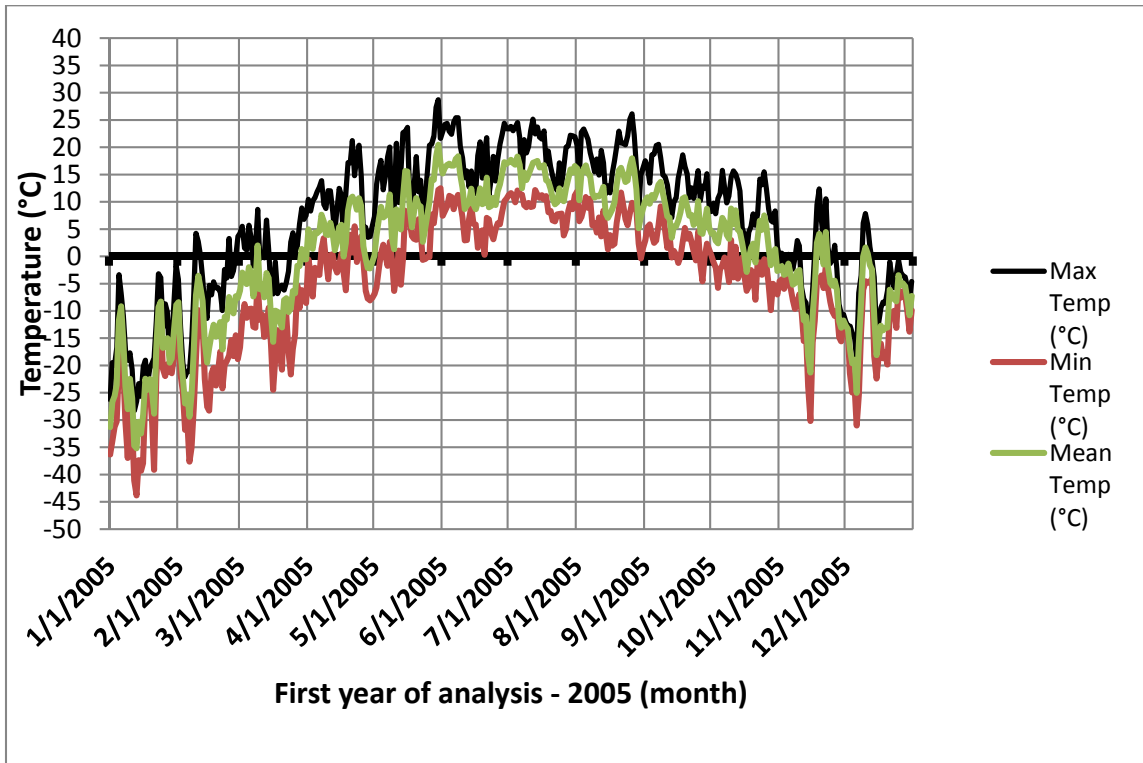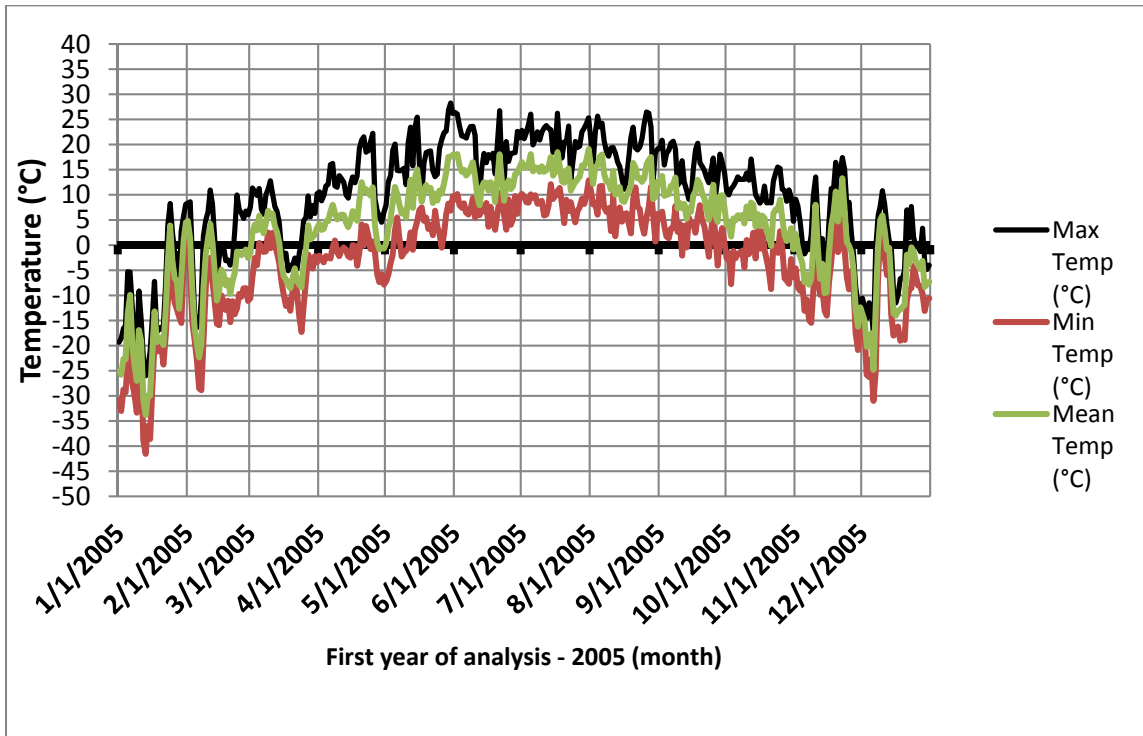| Table B.5: Calculation of the Active Season of the Fort Mcmurray Region		
Year	**Thaw**	**Freeze**
2005	Monday, April 07, 2014	Friday, November 07, 2014
2006	Sunday, April 06, 2014	Tuesday, November 04, 2014
2007	Monday, April 14, 2014	Wednesday, November 05, 2014
2008	Monday, April 14, 2014	Thursday, November 06, 2014
2009	Wednesday, April 09, 2014	Wednesday, November 12, 2014
2010	Thursday, April 03, 2014	Friday, November 07, 2014
2011	Tuesday, April 08, 2014	Monday, November 10, 2014
2012	Saturday, April 19, 2014	Tuesday, October 28, 2014
2013	Thursday, April 17, 2014	Monday, November 03, 2014
2014	Saturday, April 19, 2014	Monday, November 03, 2014
Active Season	Friday, April 11, 2014	Wednesday, November 05, 2014

Top: Compiled maximum, minimum, and mean temperature (°C) records corresponding with the first year of analysis (2005) at Fort Mcmurray Region.
Bottom: Calculation of the active season based on compiled nine-year continuous temperature records at Fort Mcmurray Region.

Appendix B.6

Top: Compiled maximum, minimum, and mean temperature (°C) records corresponding with the first year of analysis (2005) at High Level Region.

Table B.6: Calculation of the Active Season of the High Level Region		
Year	**Thaw**	**Freeze**
2005	Tuesday, April 01, 2014	Wednesday, November 05, 2014
2006	Thursday, April 03, 2014	Tuesday, November 04, 2014
2007	Monday, April 07, 2014	Monday, November 10, 2014
2008	Saturday, April 26, 2014	Thursday, November 06, 2014
2009	Thursday, April 10, 2014	Friday, November 07, 2014
2010	Sunday, April 13, 2014	Wednesday, November 12, 2014
2011	Tuesday, April 22, 2014	Sunday, November 09, 2014
2012	Friday, April 18, 2014	Saturday, November 01, 2014
2013	Tuesday, April 22, 2014	Friday, November 07, 2014
2014	Friday, April 18, 2014	Friday, November 07, 2014
Active Season	Monday, April 14, 2014	Thursday, November 06, 2014

Top: Compiled maximum, minimum, and mean temperature (°C) records corresponding with the first year of analysis (2005) at High Level Region.
Bottom: Calculation of the active season based on compiled nine-year continuous temperature records at High Level Region.

Appendix B.7

Top: Compiled maximum, minimum, and mean temperature (°C) records corresponding with the first year of analysis (2005) at High Prairie Region.

Table B.7: Calculation of the Active Season of the High Prairie Region		
Year	**Thaw**	**Freeze**
2005	Thursday, April 03, 2014	Friday, November 07, 2014
2006	Saturday, April 05, 2014	Tuesday, November 04, 2014
2007	Tuesday, April 15, 2014	Thursday, November 13, 2014
2008	Friday, April 25, 2014	Tuesday, November 11, 2014
2009	Saturday, April 12, 2014	Tuesday, November 18, 2014
2010	Thursday, April 03, 2014	Saturday, November 15, 2014
2011	Sunday, April 20, 2014	Tuesday, November 11, 2014
2012	Saturday, April 19, 2014	Monday, October 27, 2014
2013	Thursday, April 17, 2014	Monday, November 03, 2014
2014	Saturday, April 19, 2014	Thursday, November 13, 2014
Active Season	Sunday, April 13, 2014	Sunday, November 09, 2014

Top: Compiled maximum, minimum, and mean temperature (°C) records corresponding with the first year of analysis (2005) at High Prairie Region.
Bottom: Calculation of the active season based on compiled nine-year continuous temperature records at High Prairie Region.

Appendix B.8
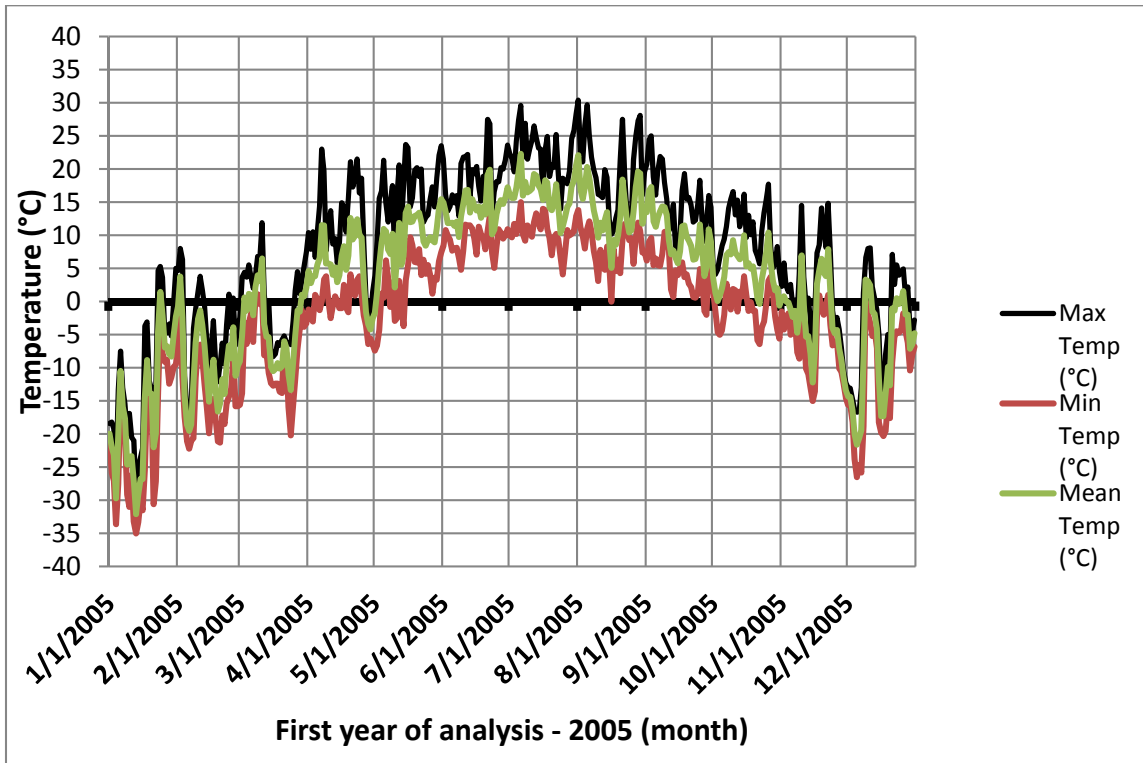
Table B.8: Calculation of the Active Season of the Lloydminster Region

Year	Thaw	Freeze
2005	Saturday, April 05, 2014	Friday, November 07, 2014
2006	Tuesday, April 08, 2014	Tuesday, November 04, 2014
2007	Monday, April 14, 2014	Wednesday, November 05, 2014
2008	Wednesday, April 16, 2014	Wednesday, November 12, 2014
2009	Saturday, April 12, 2014	Saturday, November 08, 2014
2010	Thursday, April 03, 2014	Saturday, November 15, 2014
2011	Wednesday, April 09, 2014	Tuesday, November 04, 2014
2012	Friday, April 18, 2014	Friday, October 31, 2014
2013	Thursday, April 24, 2014	Monday, November 03, 2014
2014	Saturday, April 19, 2014	Sunday, November 09, 2014
Active Season	Saturday, April 12, 2014	Thursday, November 06, 2014

Top: Compiled maximum, minimum, and mean temperature (°C) records corresponding with the first year of analysis (2005) at Lloydminster Region.
Bottom: Calculation of the active season based on compiled nine-year continuous temperature records at Lloydminster Region.

141

Appendix B.9

Top: Compiled maximum, minimum, and mean temperature (°C) records corresponding with the first year of analysis (2005) at Medicine Hat Region.
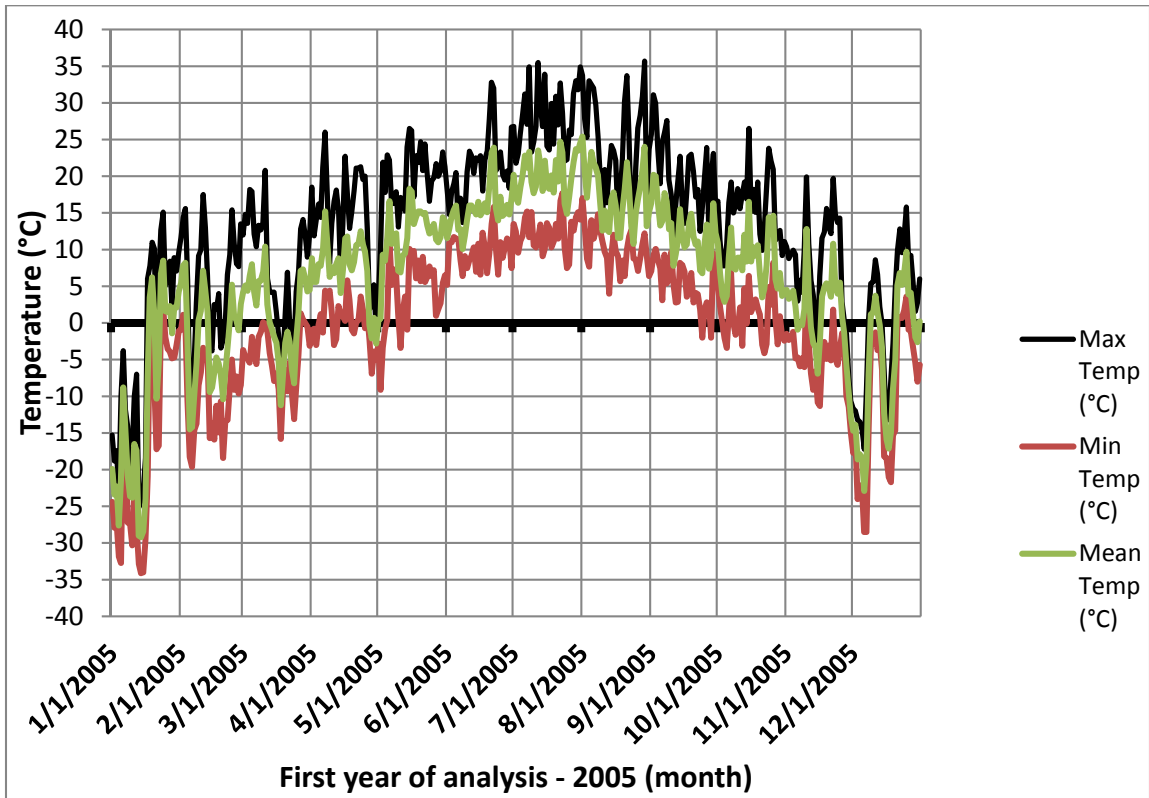
Table B.9: Calculation of the Active Season of the Medicine Hat Region

Year	Thaw	Freeze
2005	Tuesday, April 01, 2014	Tuesday, November 25, 2014
2006	Saturday, March 29, 2014	Saturday, November 22, 2014
2007	Tuesday, April 08, 2014	Monday, November 17, 2014
2008	Wednesday, April 02, 2014	Wednesday, November 19, 2014
2009	Thursday, April 03, 2014	Sunday, November 23, 2014
2010	Friday, April 11, 2014	Wednesday, November 12, 2014
2011	Saturday, April 19, 2014	Monday, November 17, 2014
2012	Sunday, April 13, 2014	Friday, November 21, 2014
2013	Tuesday, April 22, 2014	Saturday, November 15, 2014
2014	Sunday, April 13, 2014	Sunday, November 09, 2014
Active Season	Wednesday, April 09, 2014	Tuesday, November 18, 2014

Bottom: Calculation of the active season based on compiled nine-year continuous temperature records at Medicine Hat Region.

Appendix B.10
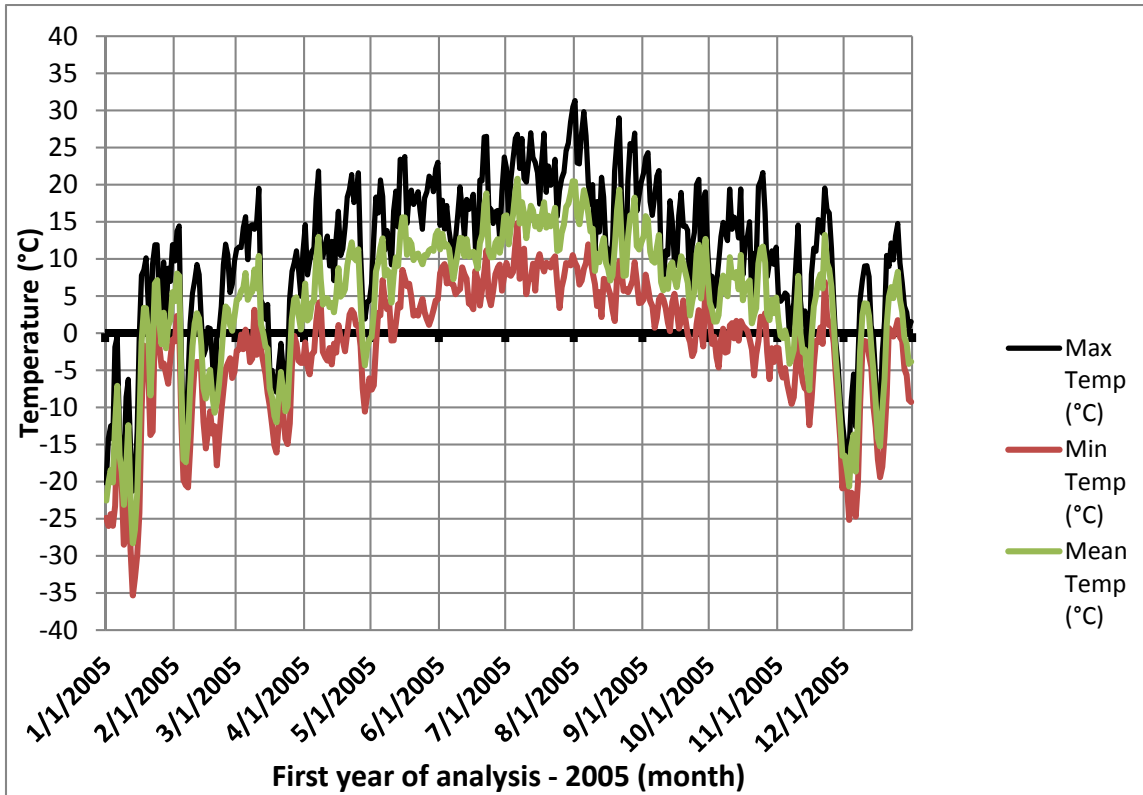
Table B.10: Calculation of the Active Season of the Neir Region

Year	Thaw	Freeze
2005	Friday, April 04, 2014	Tuesday, November 11, 2014
2006	Thursday, April 03, 2014	Thursday, November 06, 2014
2007	Friday, April 11, 2014	Sunday, November 09, 2014
2008	Monday, April 07, 2014	Thursday, November 13, 2014
2009	Thursday, April 10, 2014	Thursday, November 06, 2014
2010	Monday, April 14, 2014	Sunday, November 09, 2014
2011	Sunday, April 20, 2014	Tuesday, November 11, 2014
2012	Thursday, April 17, 2014	Saturday, November 01, 2014
2013	Friday, April 18, 2014	Sunday, November 02, 2014
2014	Friday, April 04, 2014	Sunday, November 09, 2014
Active Season	Thursday, April 10, 2014	Friday, November 07, 2014

Top: Compiled maximum, minimum, and mean temperature (°C) records corresponding with the first year of analysis (2005) at Neir Region.

Bottom: Calculation of the active season based on compiled nine-year continuous temperature records at Neir Region.

Appendix C.1

Matlab code used to convert compiled daily climate input data to an Overlapping precipitation (P) and potential evaporation (PE) event of 6-hour resolution

```matlab
% This code converts compiled daily climate input records to a higher time
% resolution data
% Calculation of an Overlap in precipitation and evaporation event from
% daily climate input to 6 hour resolution data

% First add reference of the specify excel file's name with daily
%Precipitation records
filename='I:\Eric Pastora Files\Climate Data Alberta2\10-Weather Station-
Calgary Airport\Calgary Airport-2005_2014 (2).xlsx';
% Select the sheet in the Excel fine
sheet = 'Hydrus';
% Select the range of records from Excel spreadsheet
xlRange = 'C2:C213';
prec = xlsread(filename, sheet, xlRange);
prec1 = prec';
p=0;
% In this example, the arrangement of the outout data has been programmed
% to reproduce 5 P records per each daily record. The output records
% will be distributed in the Hydrus-1D window: "Time variable boundary
% conditions" for the time interval for which the data records are provided
for j=1:1:212
    for i=p+1:1:p+1
        pd2006mmhM(1,i) = prec1(1,j)*0;
    end
    for i=p+2:1:p+2
        pd2006mmhM(1,i) = prec1(1,j)*(1/6);
    end
    for i=p+3:1:p+5
        pd2006mmhM(1,i) = prec1(1,j)*0;
    end
    p=i;
end
D={'2006'};
% Select the output Excel file's name
xlswrite('CA_Prec&Eva6h.xlsx',D,1,'A1');
xlswrite('CA_Prec&Eva6h.xlsx',pd2006mmhM,1,'A2');
disp((pd2006mmhM)')


% First add reference of the specify excel file's name with daily
%potential evaporation records
filename='I:\Eric Pastora Files\Climate Data Alberta2\10-Weather Station-
Calgary Airport\Calgary Airport-2005_2014 (2).xlsx';
sheet = 'Hydrus';
xlRange = 'D2:D213';
prec = xlsread(filename, sheet, xlRange);
prec1 = prec';
p=0;
for j=1:1:212
```

```matlab
    for i=p+1:1:p+1
        Evad2006mm6hM(1,i) = prec1(1,j)*0;
    end
    for i=p+2:1:p+2
        Evad2006mm6hM(1,i) = prec1(1,j)*(1/12);
    end
    for i=p+3:1:p+3
        Evad2006mm6hM(1,i) = prec1(1,j)*(1/12);
    end
    for i=p+4:1:p+5
        Evad2006mm6hM(1,i) = prec1(1,j)*0;
    end
    p=i;
end
M={'2006'};
xlswrite('CA_Prec&Eva6h.xlsx',M,1,'A30');
xlswrite('CA_Prec&Eva6h.xlsx',Evad2006mm6hM,1,'A31');
disp((Evad2006mm6hM)')
```
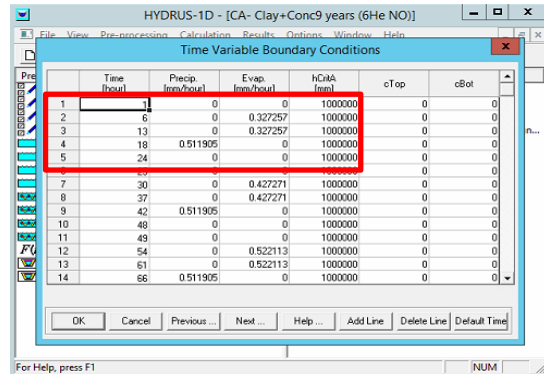
Output data from Matlab code used to convert compiled daily climate input data to overlapping P and PE event of 6-hour resolution

a)

| 2006		
Time	Precipitation (mm/hour) 6 Hours	Potential Evap (mm/hour) 6 Hours
(Hour)	Interval	Interval
1	0	0
2	0	0
3	0	0
4	0	0
5	0	0
6	0.511904762	0.327256851
7	0.511904762	0.327256851
8	0.511904762	0.327256851
9	0.511904762	0.327256851
10	0.511904762	0.327256851
11	0.511904762	0.327256851
12	0	0.327256851
13	0	0.327256851
14	0	0.327256851
15	0	0.327256851
16	0	0.327256851
17	0	0.327256851
18	0	0
19	0	0
20	0	0
21	0	0
22	0	0
23	0	0
24	0	0

b)
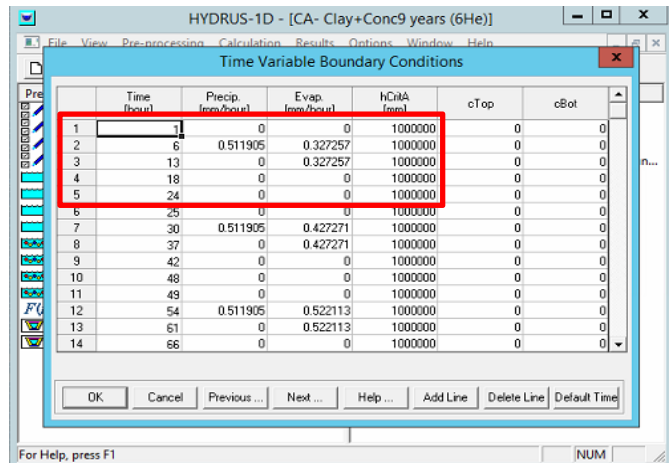
a) Output data arrangement of converted daily climate data to overlapping 6-hour resolution records for the Calgary modeling.

b) Calculated higher resolution values of precipitation (P) and potential evaporation (PE) for the atmospheric boundary conditions in Hydrus-1D.

Appendix C.2

Matlab code used to convert compiled daily climate input data to a Non-overlapping precipitation and potential evaporation event of 6-hour resolution

```matlab
% This code converts compiled daily climate input records to a higher time
% resolution data
% Calculation of a Non-overlappin precipitation and evaporation event from
% daily climate input to 6 hour resolution data

% First add reference of the specify excel file's name with daily
%Precipitation records
filename='I:\Eric Pastora Files\Climate Data Alberta2\10-Weather Station-
Calgary Airport\Calgary Airport-2005_2014 (2).xlsx';
% Select the sheet in the Excel fine
sheet = 'Hydrus';
% Select the range of records from Excel spreadsheet
xlRange = 'C2:C213';
prec = xlsread(filename, sheet, xlRange);
prec1 = prec';
p=0;
% In this example, the arrangement of the outout data has been programmed
% to reproduce 5 P records per each daily record. The output records
% will be distributed in the Hydrus-1D window: "Time variable boundary
% conditions" for the time interval for which the data records are provided
for j=1:1:212
    for i=p+1:1:p+2
        pd2006mmhM2(1,i) = prec1(1,j)*0;
    end
    for i=p+3:1:p+3
        pd2006mmhM2(1,i) = prec1(1,j)*0;
    end
    for i=p+4:1:p+4
        pd2006mmhM2(1,i) = prec1(1,j)*(1/6);
    end

    for i=p+5:1:p+5
        pd2006mmhM2(1,i) = prec1(1,j)*0;
    end
    p=i;
end
D={'2006'};
% Select the output Excel file's name
xlswrite('CA_Prec&Eva6hNO.xlsx',D,1,'A1');
xlswrite('CA_Prec&Eva6hNO.xlsx',pd2006mmhM2,1,'A2');
disp((pd2006mmhM2)')


% First add reference of the specify excel file's name with daily
%potential evaporation records
filename='I:\Eric Pastora Files\Climate Data Alberta2\10-Weather Station-
Calgary Airport\Calgary Airport-2005_2014 (2).xlsx';
sheet = 'Hydrus';
```

```matlab
xlRange = 'D2:D213';
prec = xlsread(filename, sheet, xlRange);
prec1 = prec';
p=0;
for j=1:1:212
    for i=p+1:1:p+1
        Evad2006mm6hM2(1,i) = prec1(1,j)*0;
    end
    for i=p+2:1:p+2
        Evad2006mm6hM2(1,i) = prec1(1,j)*(1/12);
    end
    for i=p+3:1:p+3
        Evad2006mm6hM2(1,i) = prec1(1,j)*(1/12);
    end
    for i=p+4:1:p+5
        Evad2006mm6hM2(1,i) = prec1(1,j)*0;
    end
    p=i;
end
M={'2006'};
xlswrite('CA_Prec&Eva6h.xlsx',M,1,'A30');
xlswrite('CA_Prec&Eva6h.xlsx',Evad2006mm6hM2,1,'A31');
disp((Evad2006mm6hM2)')
```

Output data from Matlab code used to convert compiled daily climate input data to non-overlapping P and PE event of 6-hour resolution

a)

b)

2006-2014		
Time (Hour)	Precipitation (mm/hour) 6 Hours Interval	Potential Evap (mm/hour) 6 Hours Interval
1	0	0
2	0	0
3	0	0
4	0	0
5	0	0
6	0	0.327256851
7	0	0.327256851
8	0	0.327256851
9	0	0.327256851
10	0	0.327256851
11	0	0.327256851
12	0	0.327256851
13	0	0.327256851
14	0	0.327256851
15	0	0.327256851
16	0	0.327256851
17	0	0.327256851
18	0.511904762	0
19	0.511904762	0
20	0.511904762	0
21	0.511904762	0
22	0.511904762	0
23	0.511904762	0
24	0	0

a) Output data arrangement of converted daily climate data to non-overlapping 6-hour resolution records for the Calgary modeling.

b) Calculated higher resolution values of precipitation (P) and potential evaporation (PE) for the atmospheric boundary conditions in Hydrus-1D.

Appendix D.1
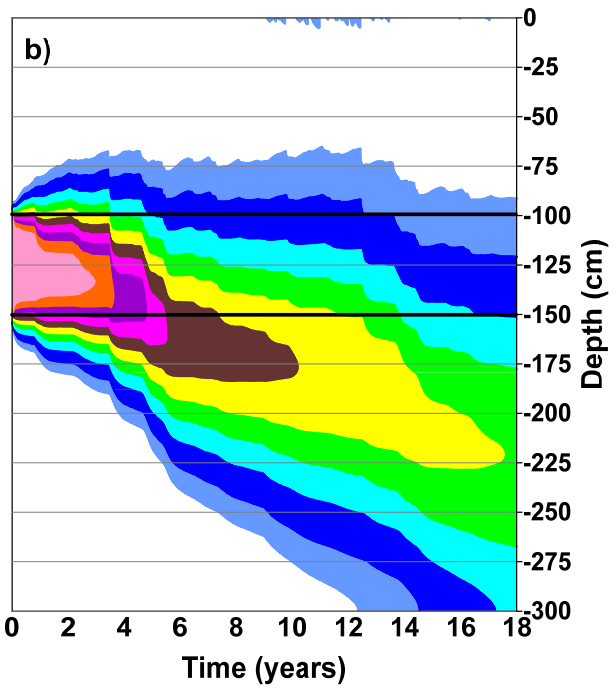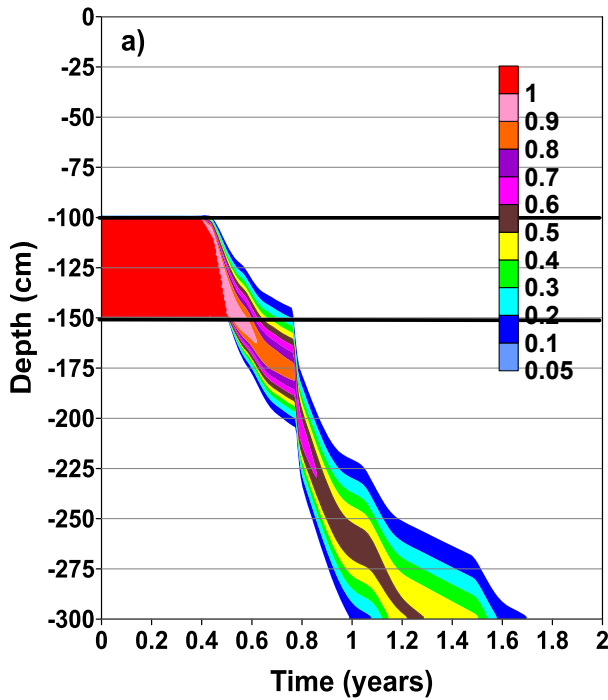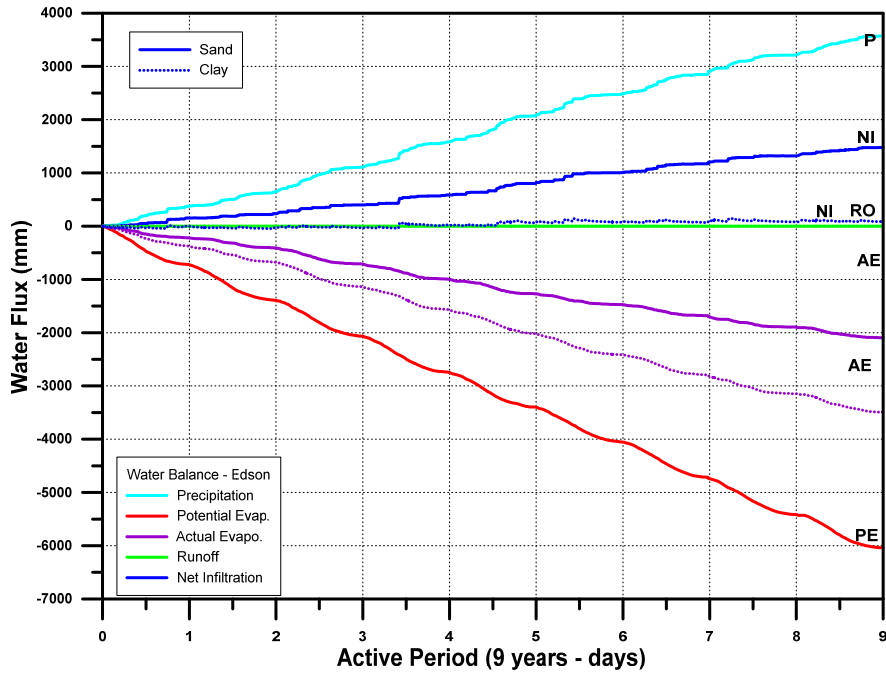
Top: Estimated daily water balance at ground surface under semi-humid climate conditions at *Edson Region*.

Bottom: Vertical displacement of the solute concentration contours in (a) coarse-grained material and (b) fine-grained soil materials

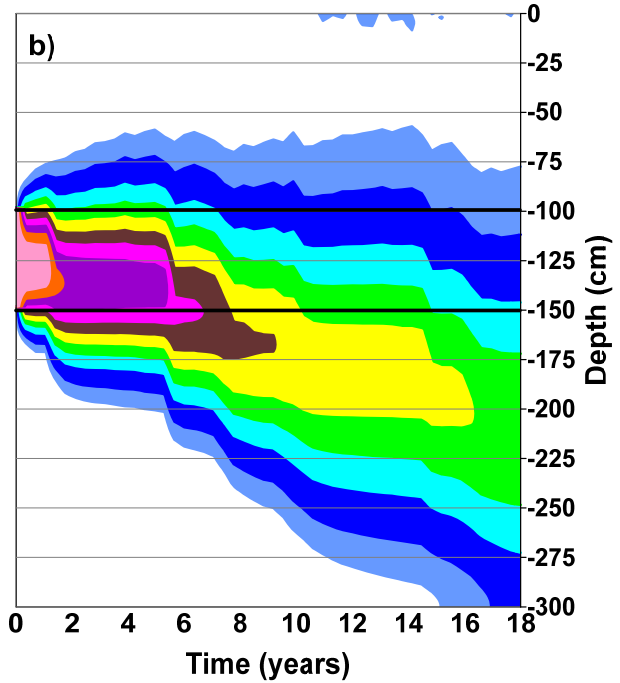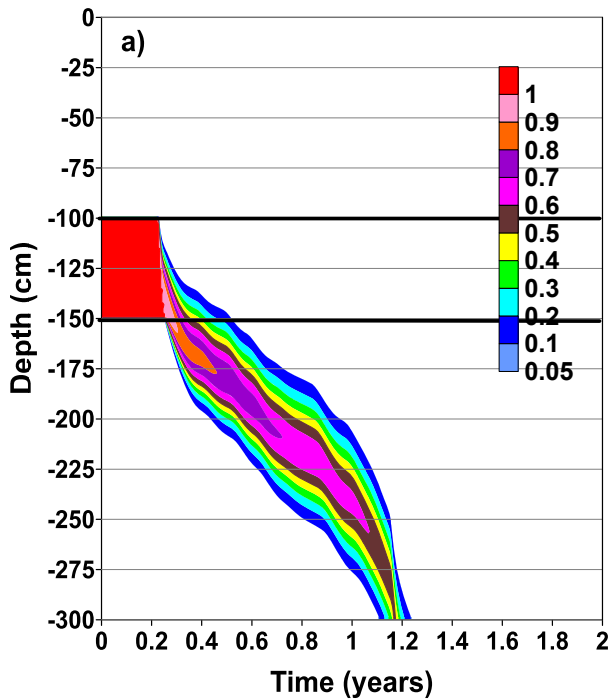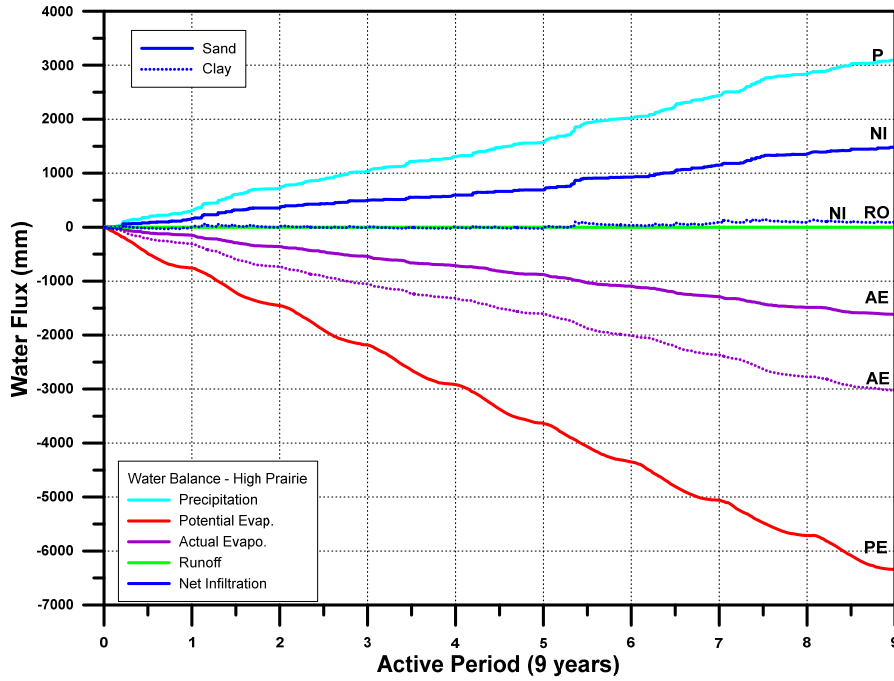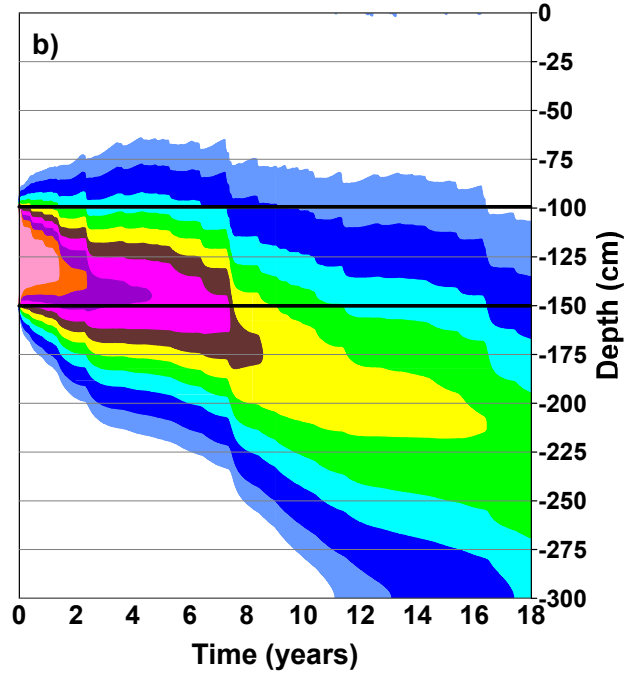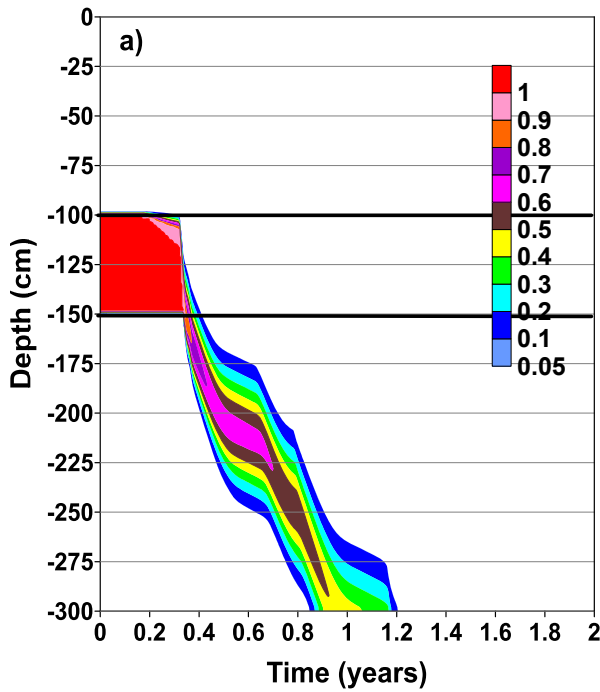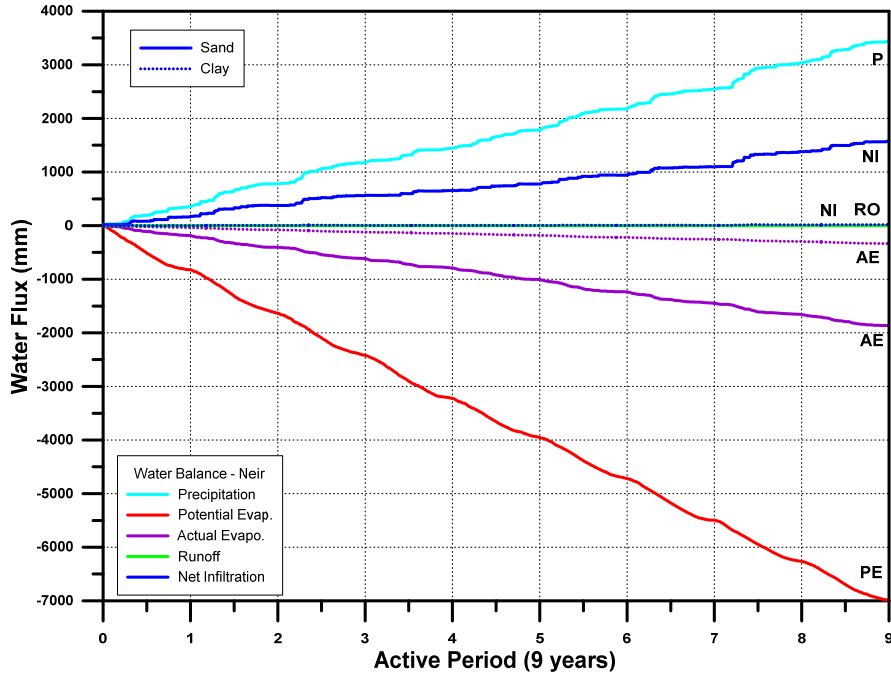# Appendix D.2
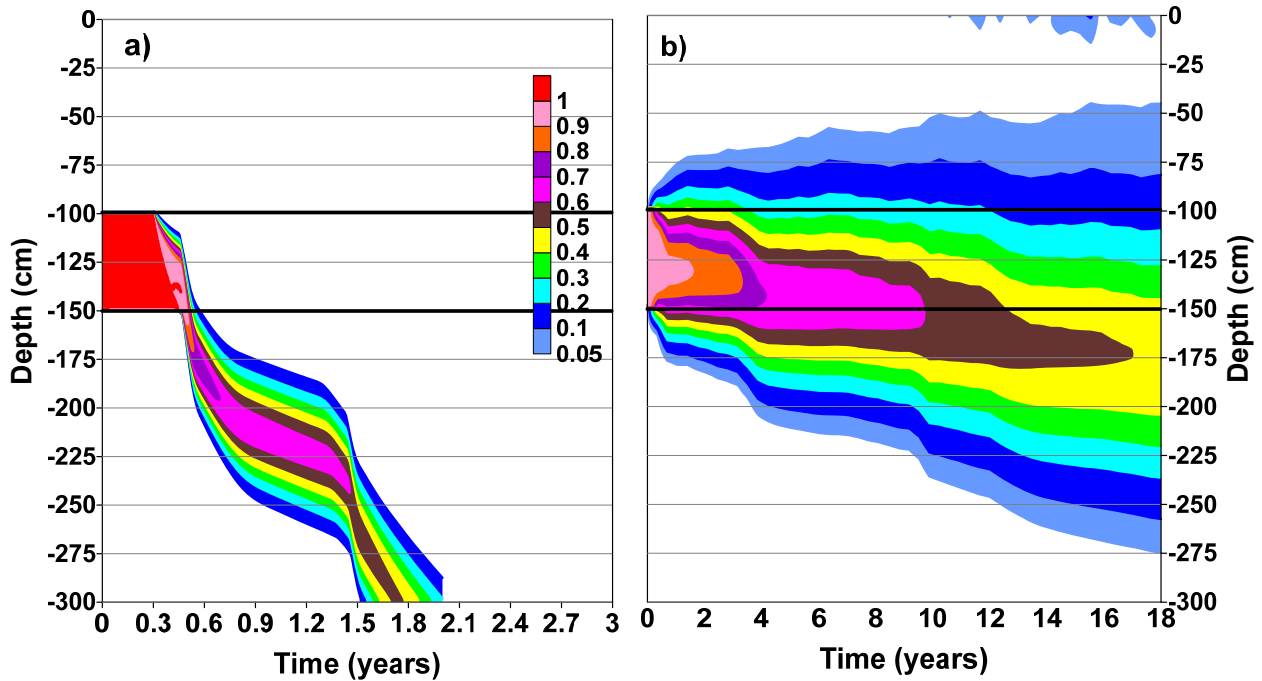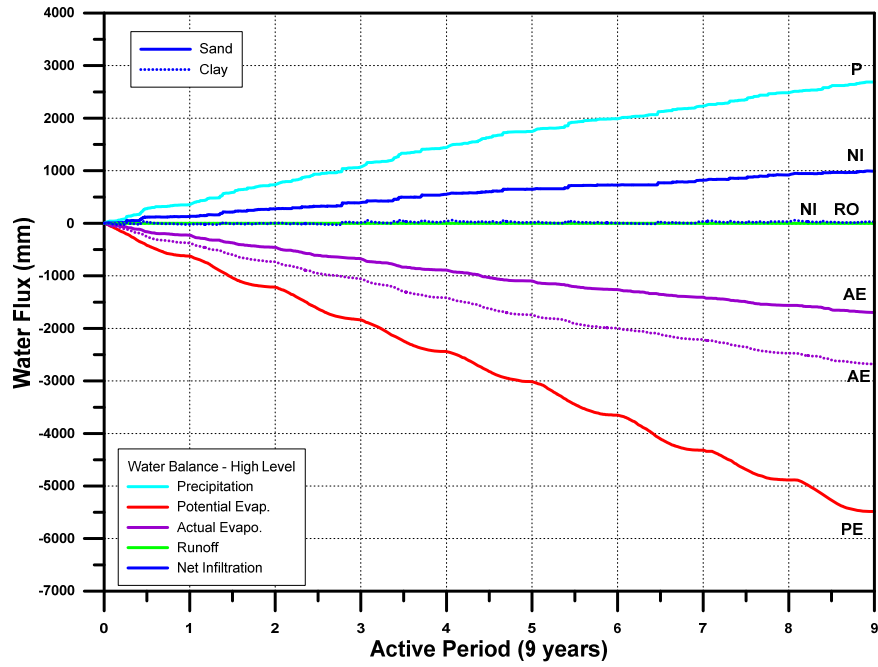
Top: Estimated daily water balance at ground surface under semi-arid climate conditions at *High Level Region*.

Bottom: Vertical displacement of the solute concentration contours in (a) coarse-grained material and (b) fine-grained soil materials
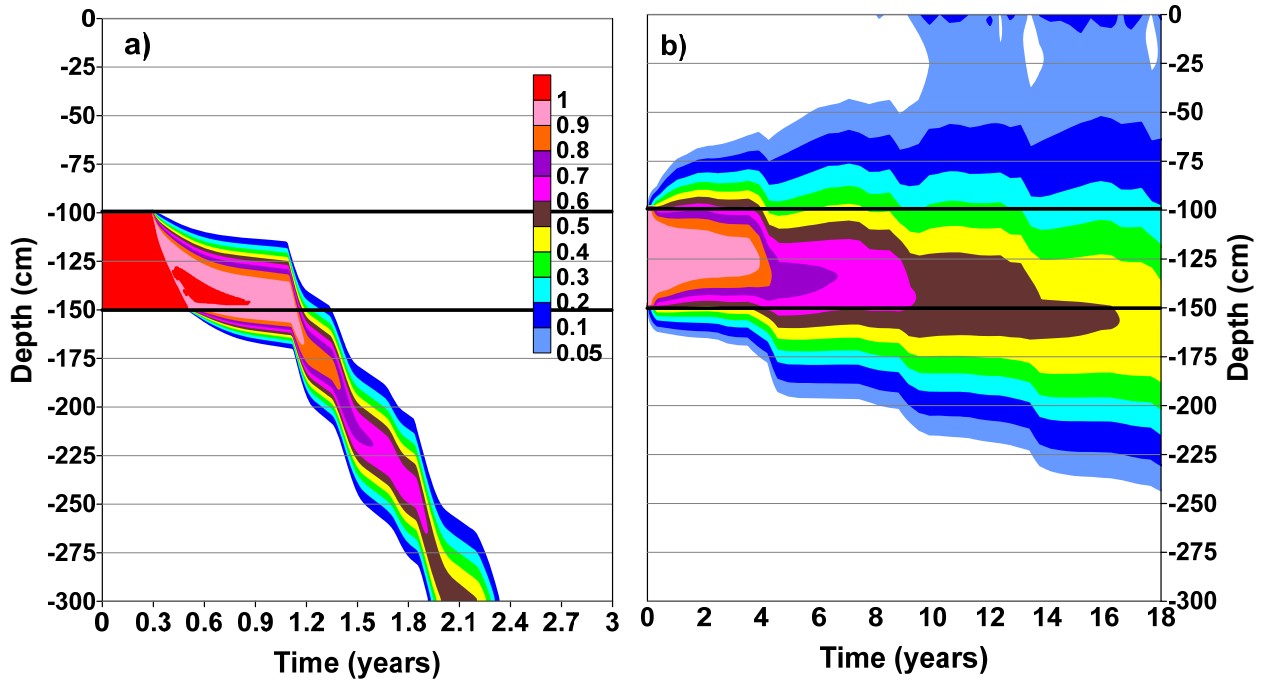
Appendix D.3
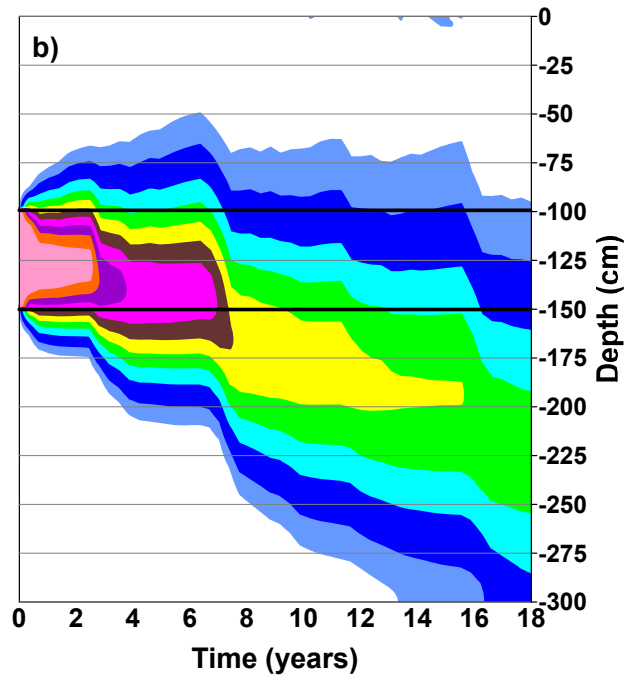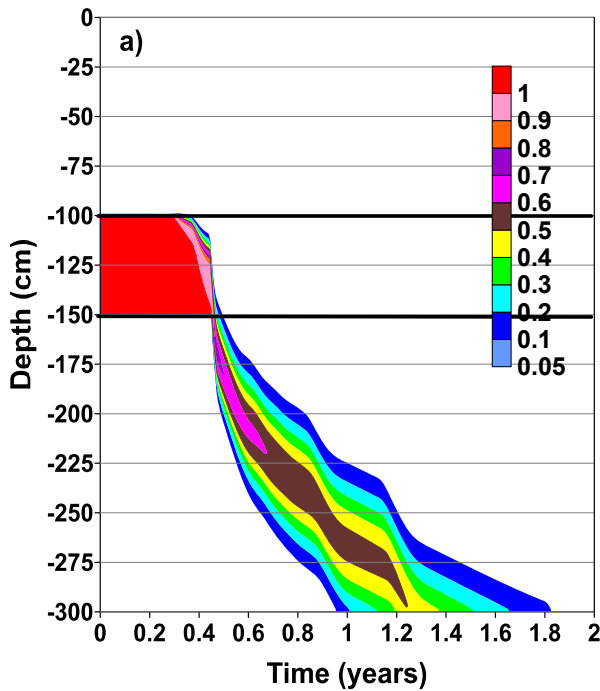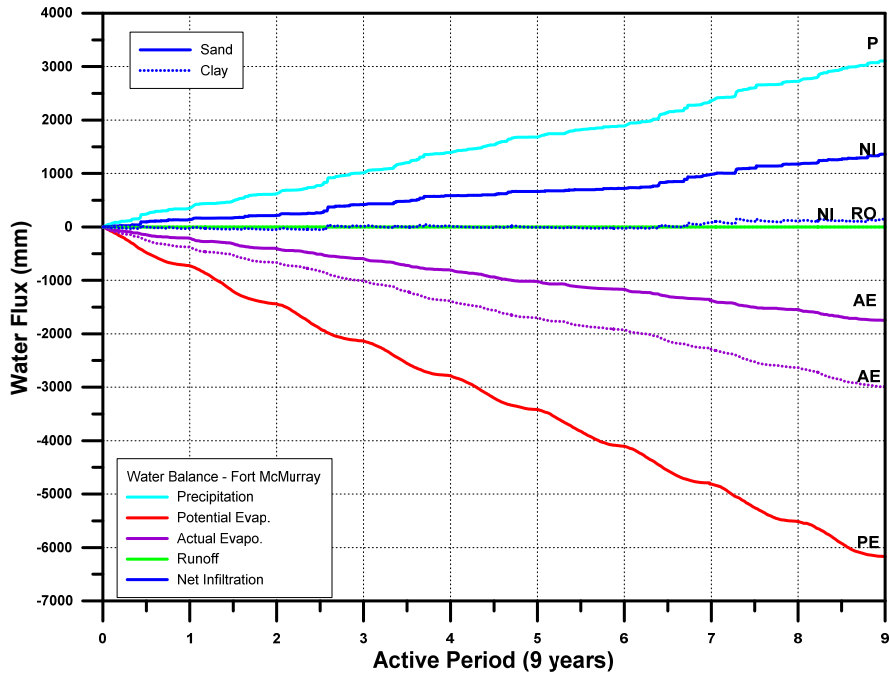
Top: Estimated daily water balance at ground surface under semi-arid climate conditions at *Fort Mcmurray Region*.

Bottom: Vertical displacement of the solute concentration contours in (a) coarse-grained material and (b) fine-grained soil materials
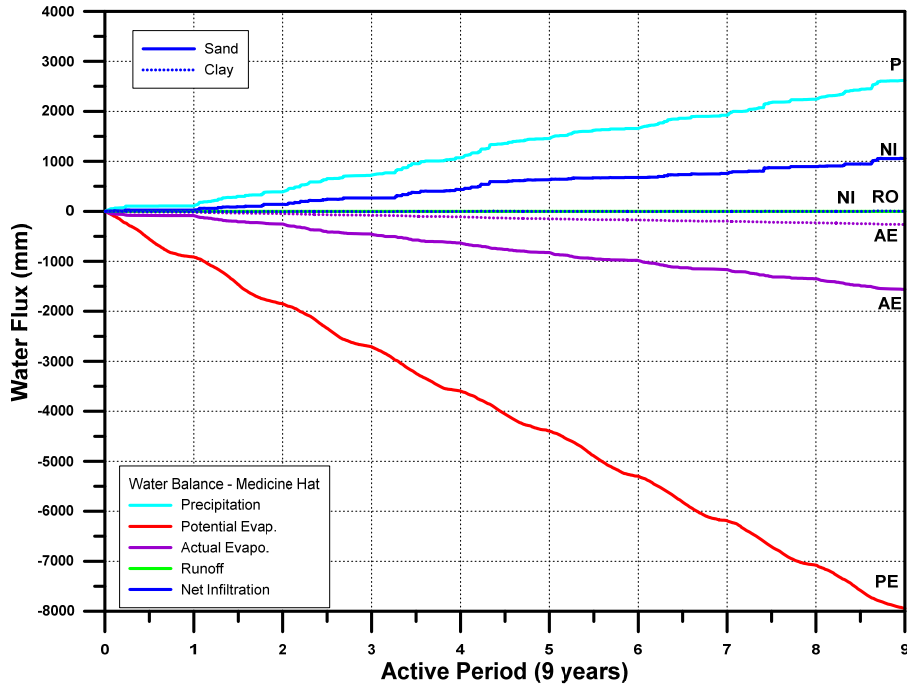
Appendix D.4
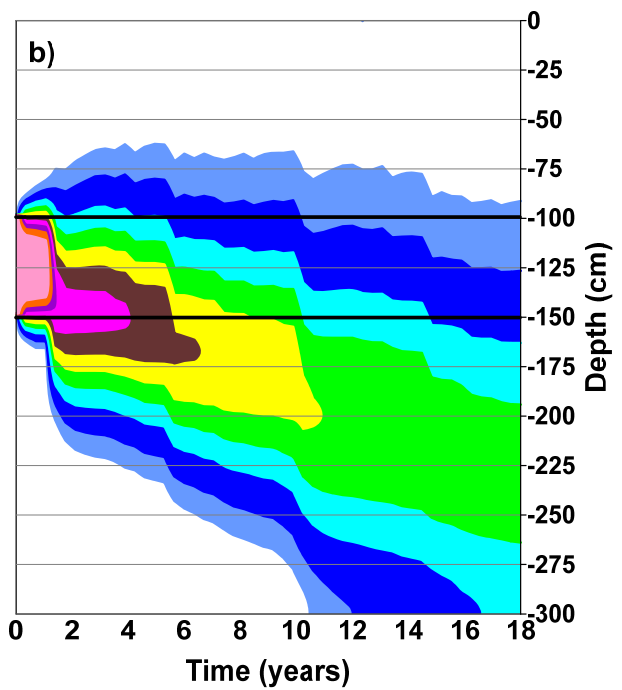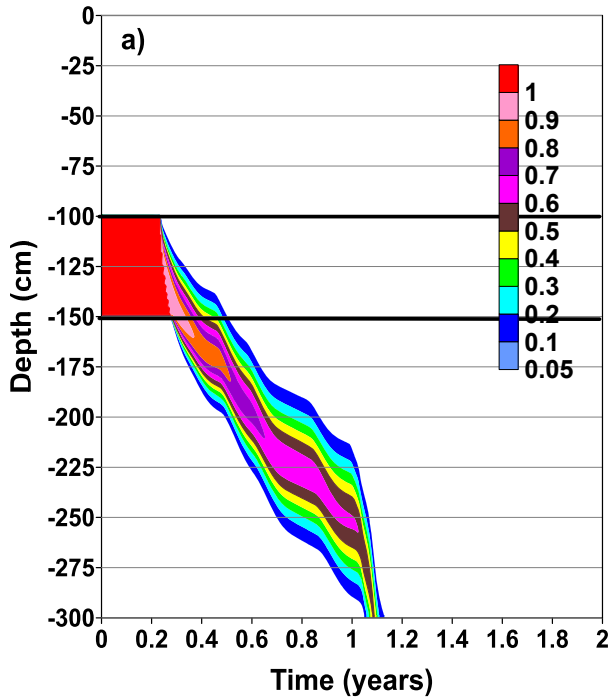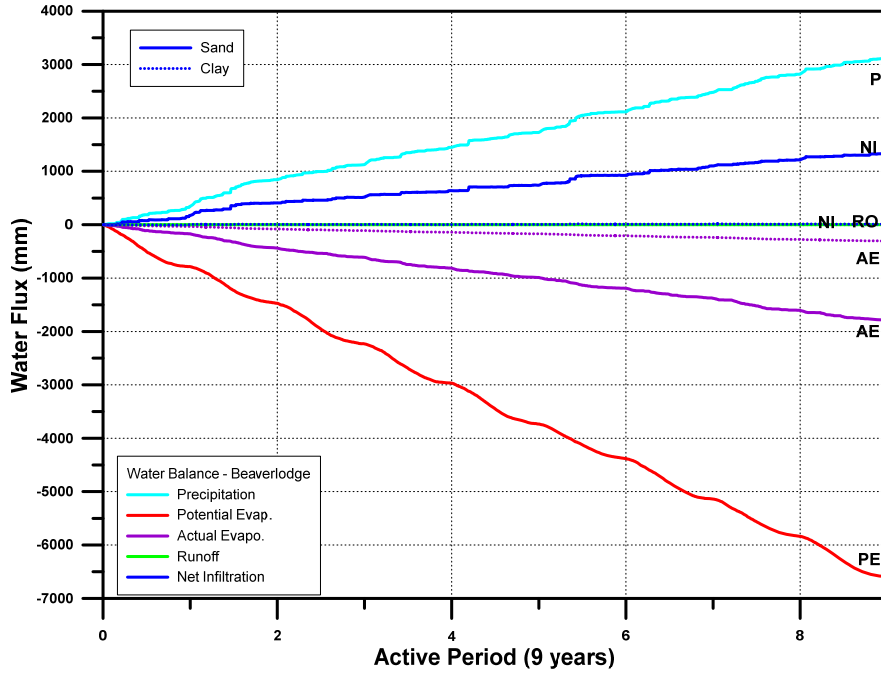
Top: Estimated daily water balance at ground surface under semi-arid climate conditions at *Beaverlodge Region*.

Bottom: Vertical displacement of the solute concentration contours in (a) coarse-grained material and (b) fine-grained soil materials

Appendix D.5

Top: Estimated daily water balance at ground surface under semi-arid climate conditions at *High Prairie Region*.
Bottom: Vertical displacement of the solute concentration contours in (a) coarse-grained material and (b) fine-grained soil materials

Appendix D.6

Top: Estimated daily water balance at ground surface under semi-arid climate conditions at *Neir Region*.
Bottom: Vertical displacement of the solute concentration contours in (a) coarse-grained material and (b) fine-grained soil materials

Appendix D.7

Top: Estimated daily water balance at ground surface under arid climate conditions at *Medicine Hat Region*.
Bottom: Vertical displacement of the solute concentration contours in (a) coarse-grained material and (b) fine-grained soil materials
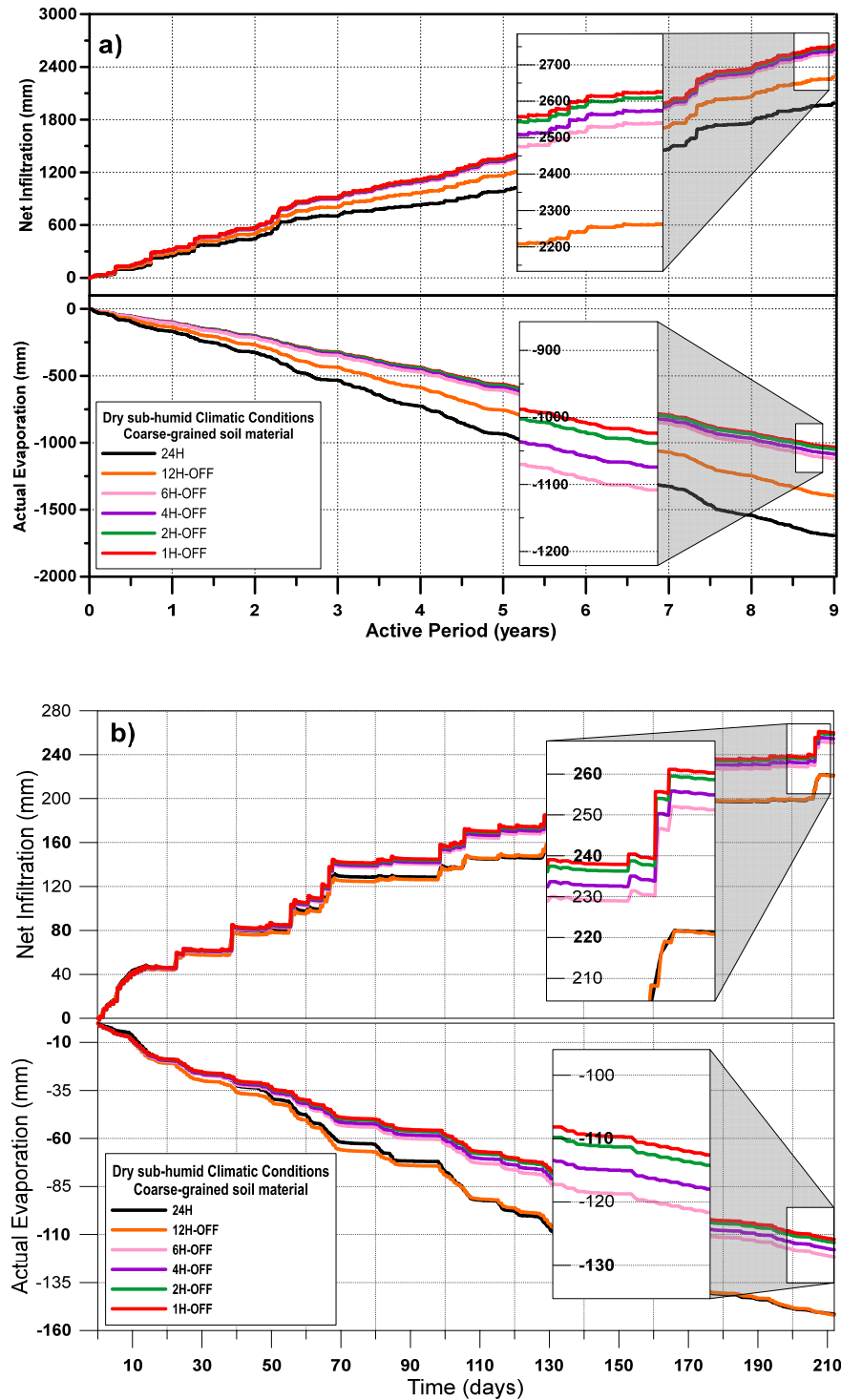
Appendix E.1
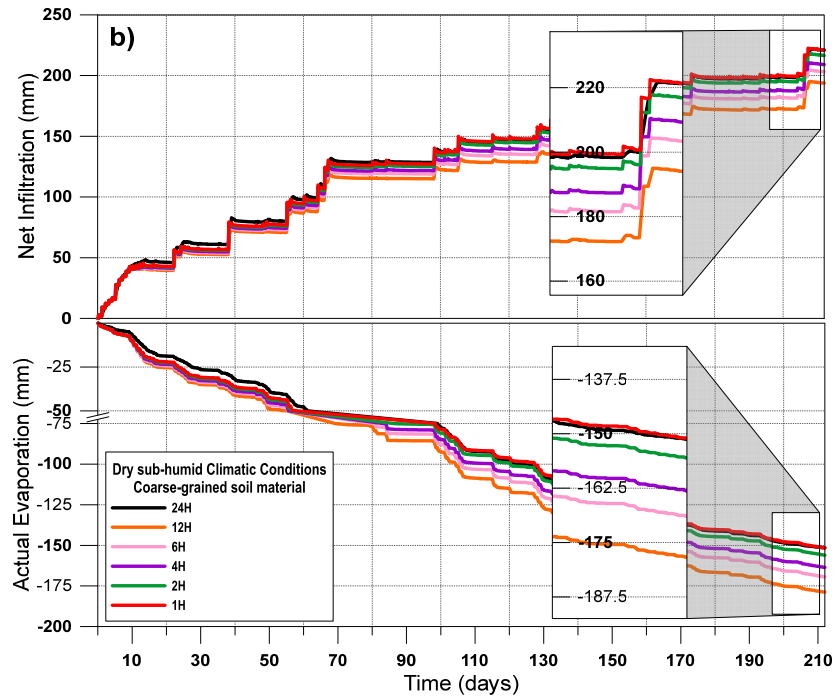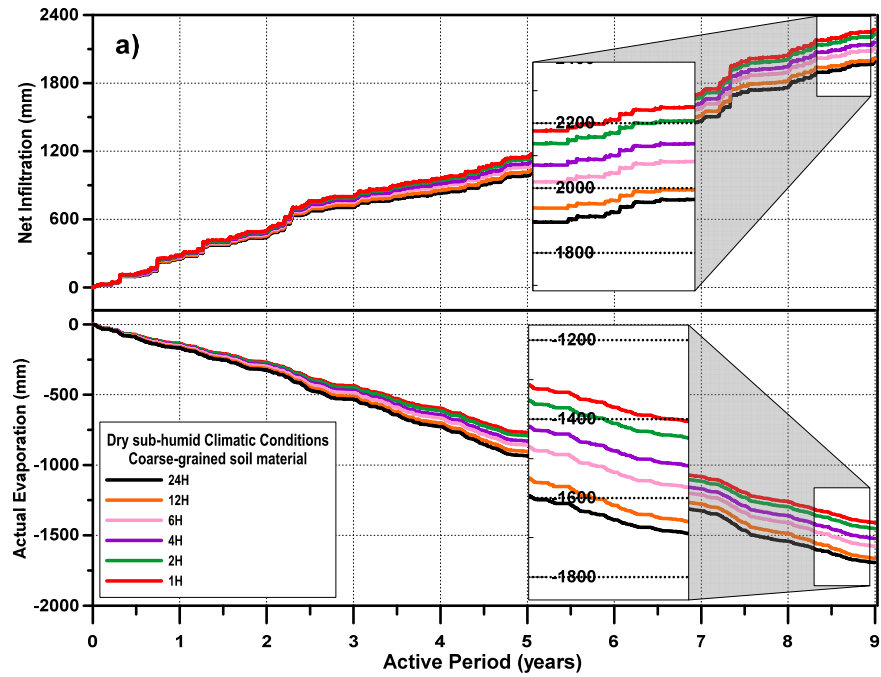
Estimated water balance in dry sub-humid climatic conditions assuming precipitation occurring during peak evaporation hours in coarse-grained soil materials
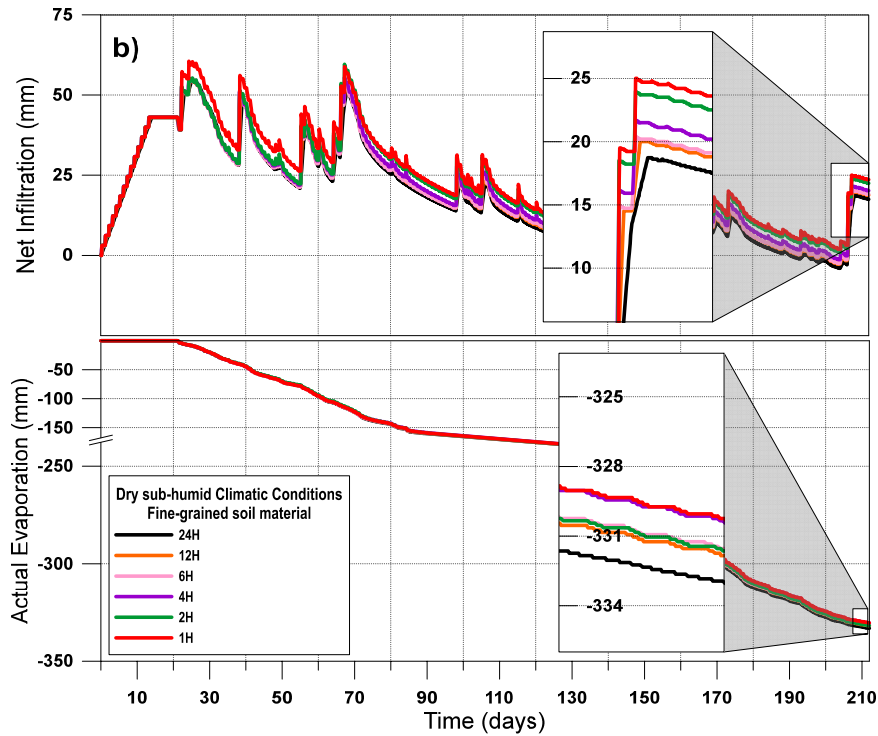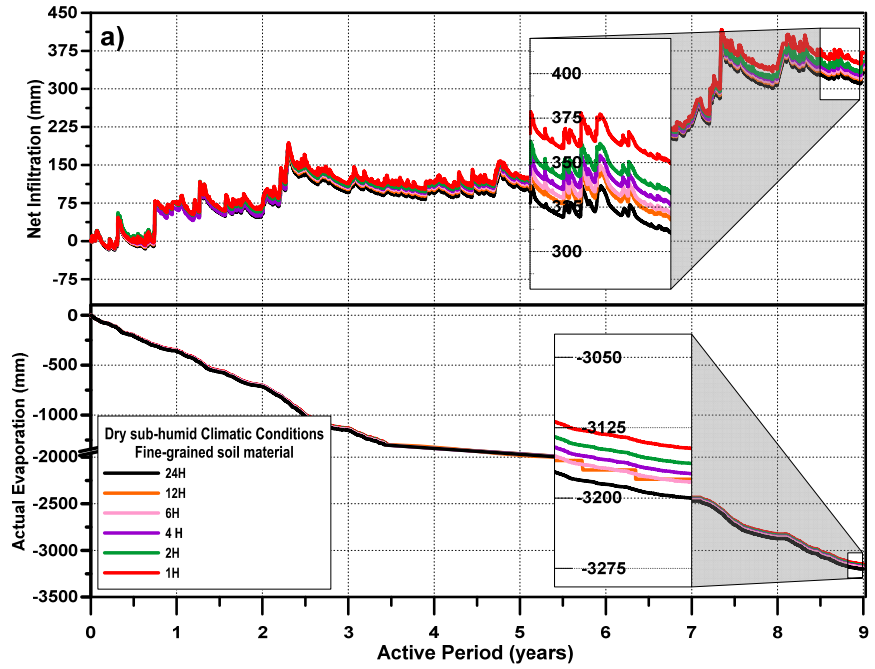**a)** Cumulative totals over the 9-year period, **b)** cumulative totals over the 9th water year

157

Appendix E.2

Fig. 4.19: Estimated water balance in dry sub-humid climatic conditions assuming precipitation occurring during off-peak evaporation hours in coarse-grained soil materials
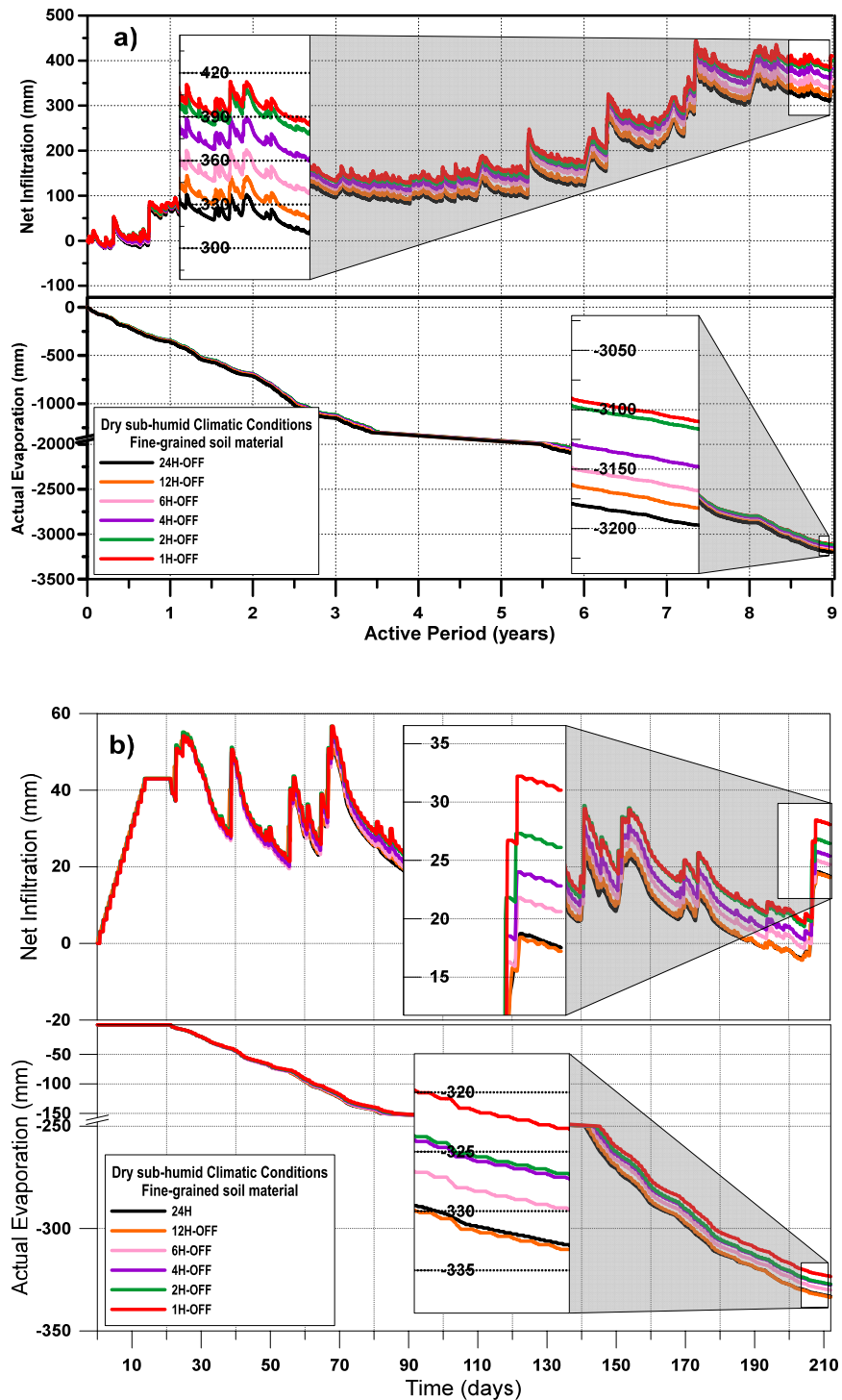*a)* Cumulative totals over the 9-year period, *b)* cumulative totals over the 9th water year

Appendix E.3

Estimated water balance in dry sub-humid climatic conditions assuming precipitation occurring during peak evaporation hours in fine-grained soil materials
a) Cumulative totals over the 9-year period, **b)** cumulative totals over the 9th water year

Appendix E.4

Estimated water balance in dry sub-humid climatic conditions assuming precipitation occurring during off-peak evaporation hours in fine-grained soil materials
a) Cumulative totals over the 9-year period, *b)* cumulative totals over the 9th water year